THE INDUSTRIAL APPLICATION OF A MULTIPLE TECHNIQUE PAPER DRYER SIMULATOR

by

Shaun Sidwall

A Thesis submitted to the Faculty of Graduate Studies and Research
in partial fulfillment of the requirements for the degree of
Master of Engineering

Department of Chemical Engineering
McGill University
Montreal

April 1999

0-612-50661-4

ABSTRACT

Drying Doctor, a multiple technique simulator of the paper drying process, has been developed at the Pulp and Paper Research Centre, McGill University. This thesis examines the different approaches to the modeling of this process, provides a rigorous validation of the simulation program and demonstrates its utility with four containerboard machines of Norampac Inc.

Several features differentiate this simulator from others. When heavy grades of paper are produced or when high intensity drying processes are used even with thin sheets, substantial thickness direction gradients of moisture content and temperature develop across the sheet, demonstrating the necessity of a fully microscale model such as employed by *Drying Doctor*.

Using industrial and laboratory data for a variety of paper grades and drying processes, 31 uncalibrated simulations for machine speed showed a standard deviation of only 3.4 % from known speeds. Through simulation of modified operating conditions such as steam pressure, spoiler bars, pocket air conditions and addition of the high intensity drying process, Yankee air impingement dryers, substantial production rate increases for the industrial partner's papermachines through use of the *Drying Doctor* simulator were shown possible.

RÉSUMÉ

Un simulateur combinant les différentes techniques de séchage du papier, 'Drying Doctor', a été développé au Centre de Recherche sur les Pâtes et Papiers de l'Université McGill.

Cette thèse traite des différentes approches utilisées pour la modélisation de ce procédé, apporte une validation rigoureuse du programme de simulation et met en évidence son utilité dans le cas de quatre machines cartons d'emballage de Norampac Inc.

Ce simulateur se démarque des autres de différentes manières. Dans le cas de la production de papiers de fort grammage ou lorsque des procédés de séchage haute intensité sont utilisés, même dans le cas de papiers de faible grammage, un gradient significatif de température et d'humidité se développe dans l'épaisseur de la feuille. Il est alors nécessaire d'utiliser un modèle à l'échelle microscopique tel qu'employé dans le Drying Doctor.

A partir de données recueillies dans l'industrie et au laboratoire sur des sortes de papier variées et divers procédés de séchage, trente et un simulations non calibrées de vitesse de machine ont été menées qui ont montré un coefficient de variation de seulement 3.4 % par rapport aux vitesses réelles.

Grâce au Drying Doctor, la simulation de conditions opératoires différentes tels que la pression de vapeur, les barres de turbulence, les poches d'air, l'introduction d'un procédé haute intensité, sécheur Yankee par contact direct de jets d'air, a montré que des augmentations significatives de production sont possibles sur les machines de partenaires industriels.

ACKNOWLEDGEMENTS

I would first like to thank my supervisor, Professor W. J. Murray Douglas. His guidance and time, perseverance and wisdom have made me the researcher I am today. His energy and encouragement seem endless and will always serve as motivation, his contribution to this thesis is immeasurable.

The financial support of PAPRICAN and Domtar throughout the duration of this study is gratefully acknowledged. Thanks to Bob Snow, J.J Davis, Paul Kalbun, and Tim Yang of Norampac Inc. who have provided information required for this work.

I would also like to thank Dr. Jean-François Bond for his patience and knowledge, much of my understanding of paper comes from his willingness to answer my questions. Thanks also to Mohsen Sadeghi, Manoj Dixit, Jean-Phillipe Bernie and Françoise Forel, my fellow researchers for the many discussions and help along the way.

A special thanks to my parents, Rita and Grant Sidwall, without their support and love I could not have achieved this, and of course, also to my brother, Kyle Sidwall.

Finally I would like to thank Iulia Negrea, without her I may never have embarked along this path. Her constant understanding and nurture may not have always been acknowledged, but it was always appreciated.

TABLE OF CONTENTS

LIST OF FIGURES

LIST OF TABLES

1 INTRODUCTION

In the paper industry, reduction of capital and operating costs of the dryer sections is and will remain a priority. This is especially so when rebuilding an existing dryer section to achieve increased production capacity or to accommodate changes of grade that increase the required dryer capacity. Another trend that increases dryer load is conversion from uncoated paper to the sized or coated product of higher value. These general statements apply also for containerboard, the grade that is the prime focus here. Containerboard, of basis weight in the range of 100 to over 300 g/m^2, includes two types of product. Corrugated medium, when converted, forms the fluted interior of boxboard. Linerboard provides the exterior layer of boxboard among many other functions. The 20-year growth rate of Canadian containerboard production, Figure 1-1, has been 5 % per year.

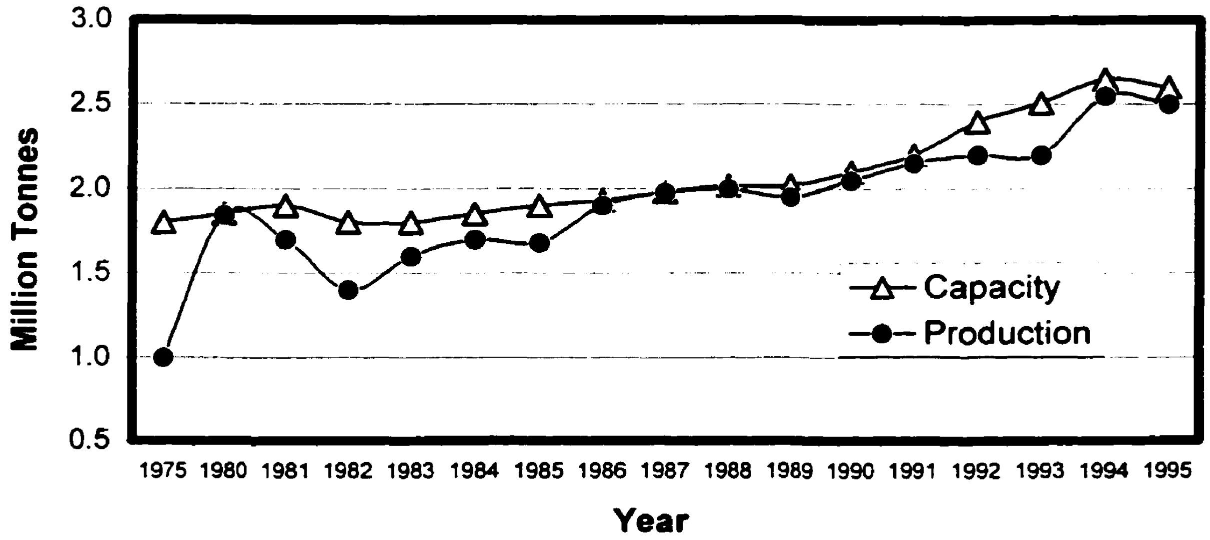

Figure 1-1: Canadian Annual Production and Capacity of Containerboard [CPPA, 1996]

Printing and heavier paper is now dried by an assembly of 40 to 90 steam heated cylinders. One accommodation to increased dryer load, simply addition of cylinders, is costly and is not always possible due to space constraints. A potential new strategy is to incorporate high intensity drying techniques such as air impingement, infrared and gasfired conduction drying at some location in the dryer section, thereby producing a "multiple technique" dryer section. The complexity of design and optimization of multiple technique dryer sections would be facilitated by a drying simulator able to treat the case where the moist paper passes through any number of different drying techniques, in any sequence, as the sheet goes from wet to dry.

The program *Drying Doctor*, developed recently at McGill University, simulates drying by solving the coupled differential equations for moisture, vapor and heat transport within the sheet. When drying involves two or more drying processes in series, *Drying Doctor* becomes a multiple technique simulator through use of different boundary conditions for the coupled transport equations they have in common. Thus the substantial gradients in moisture content, air humidity and temperature within the sheet at the exit from one drying process become the initial conditions for the drying process that follows.

In Chapter 4, validation testing of the *Drying Doctor* simulator is carried out with dryer section data from 7 papermachines producing a variety of grades from tissue through newsprint to linerboard, including the particularly demanding case of the high intensity conditions for air impingement drying in Yankee dryers. Heavier paper constitutes another critical test of dryer simulator validity because of the greater importance of heat and mass transport processes within the sheet. In Chapter 5, the *Drying Doctor* simulator is validated further with extensive data from the 4 containerboard papermachines of Domtar Inc. [now Norampac Inc.], then is applied to simulate a great variety of modifications to improve the productivity of these machines.

2 LITERATURE REVIEW

Printing and heavier paper is currently dried by steam heated cylinder dryers except for coated paper, where drying must start with a non-contact process, infra-red and/or air impingement flotation dryers. Cylinder dryer sections cost in the order of $50 million for a large modern machine and account for the largest portion of energy consumption of papermaking. A dryer simulator is a powerful tool for examining performance problems, process optimization and analysis of future equipment modifications for increasing production or changing grade. The first comprehensive literature review, Kirk (1984) covered simulation models from the 1950-1980 period.

2.1 Development of Cylinder Drying Phases

The landmark contribution to paper drying modeling was the Nissan and Kaye (1955) division of each cylinder-dryer pocket unit into 4 sections, Figure 2-1. This model allowed for evaporation from the sheet, conduction heat transfer from the cylinder and convection and radiation between the paper and the air. The original calculations for a dryer section took 120 man-hours with a desk calculator. Nissan et al. improved this model in 1960 and 1961. At first Nissan thought that, due to the felt, little water removal took place in phase II. In 1960 he modified this model to allow the felt to absorb liquid

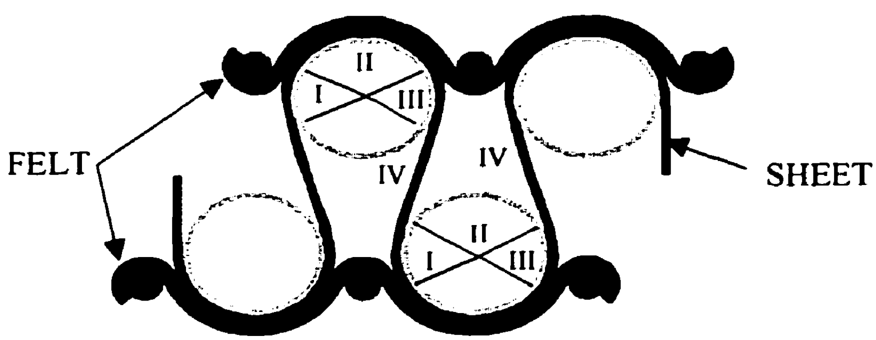

Figure 2-1: The Four Cylinder Drying Phases of Nissan

Phase I: Sheet in contact with the cylinder surface and air.
Phase II: Sheet contacted by the cylinder surface on one side and the felt on the other.
Phase III: Sheet again in contact with the cylinder surface and air.
Phase IV: Sheet in contact with air on both sides allowing evaporation from both sides.

water and in 1961 allowed for vapor diffusion into the felt and condensation there. Now with a digital computer, model complexity expanded while calculation time decreased to about 40 minutes, after about 70 h preparing the code of which only 25 h directly involved computer programming. The 1963 and 1964 work of Kirk et al. and Race disproved the earlier belief that the felt absorbed liquid water and revealed that felts remove moisture only as water vapor.

Lehtikoski (1970) extended Nissan's model by further dividing the dryer section into four zones: heating-up (increasing rate drying), constant rate drying, falling rate drying and fast-falling rate drying. Depoy (1972) expanded the Nissan four phase system to five phases, adding felt modeling, Table 2-A. His phase 4 is the cylinder area in contact with air, with phase 5 for the felt when not in contact with the sheet. Depoy determined heat and mass transfer coefficients from laboratory and industrial data.

Table 2-A: Cylinder Drying Phases of Nissan and Depoy

	Cylinder/ Paper	Cylinder/ Paper/Felt	Paper In Draw	Cylinder	Felt
Nissan	I & III	II	IV	-	-
Depoy	1	2	3	4	5

In Table 2-B, based on the extensive review of Wilhelmsson et al. (1993), the external systems include the steam (i.e. cascade, blowthrough) and condensate system, the cylinder dynamics (shell resistance, condensate layer) and the pocket ventilation system. The central feature of internal transport is the most difficult part of paper drying modeling. This aspect has evolved gradually, from evaporation only at the surface, to an evaporating front, towards a fully microscopic model encompassing all controlling transport phenomena. Some current models still employ the evaporating front assumption for the sheet drying model because they focus on other elements of the dryer, i.e. condensate flow, but computer power now enables simulation of all aspects without the major simplifications necessary earlier.

2.2 External System Focused Models

Knight and Kirk (1975) proposed a model emphasizing the operating conditions, including number of cylinders and their diameter, condensate flowrate and thickness,

Table 2-B Simulation Models for Cylinder Drying of Paper

Author(s)	Year(s)	Internal Transport			External Systems			Verified By:		Country
		Liquid	Vapor	Heat	Steam	Cyl.	P.V.[1]	Lab	Industry	
Nissan et al.	1955-61			✓				✓		USA
Lehtikoski	1970			✓		✓				Finland
Depoy	1972			✓		✓		✓	✓	USA
Powell & Strong	1974			✓					✓	Canada
Hartley & Richards	1975	✓	✓	✓				✓	✓	Australia
Knight & Kirk	1975-80					✓			✓	UK
Rhodius & Gottsching	1979			✓					✓	Germany
Snow	1980	✓	✓	✓		✓	✓		✓	USA
Donner & Renk	1982		✓	✓	✓	✓			✓	USA
Lemaitre et al.	1980				✓	✓	✓	✓	✓	France
Karlsson et al.	1982-92			✓	✓		✓			Finland
Lee et al.	1981-83	✓	✓	✓				✓	✓	USA
Lampinen & Toivenen	1984	✓	✓	✓				✓		Finland
Abbott et al.	1984				✓	✓	✓		✓	USA
Iida	1985								✓	Japan
Valmet (Eskilinen & Heikkilä)	1985-88	✓	✓	✓	✓	✓	✓		✓	Finland
Pearson	1986									USA
Ramaswamy	1990	✓	✓	✓					✓	USA
Asensio & Seyed-Yagoobi	1992	✓	✓	✓						USA
Deshpande & Pulkowski	1992					✓			✓	USA

1-Ventilation of dryer pockets

Table 2-B: Simulation Models for Cylinder Drying of Paper

machine speed and steam pressure. Their FORTRAN model assumed the sheet could not support internal gradients of temperature or moisture in the thickness direction, now known to be incorrect. Kirk (1980) used results to form power series correlations incorporating speed, basis weight, cylinder-paper contact heat transfer coefficient, cylinder diameter, draw length, felt evaporation reduction factor and critical moisture content. With these correlations, evaporation rate and number of cylinders could be predicted.

The Lemaitre et al.(1982) model dealt extensively with the external systems but ignored heat and mass transfer within the sheet. Coefficients for transfer of heat (between cylinder and sheet) and mass (between sheet and fabric, fabric and air) were obtained with non-linear parameter estimation from measured cylinder surface temperatures and literature values. The model produced acceptable results for dryer sections similar to those used to obtain the heat and mass transfer coefficients but, by ignoring internal transport, would be invalid for other applications, i.e. heavier grades.

The Abbott et al. (1984) model, using the GEMS general simulation system, is intricate in its external systems modeling but uses over-simplified sheet modeling with no internal transport. As GEMS is not specific to drying, let alone paper drying, building cylinder dryer sections is difficult and time consuming. Deshpande and Pulkowski (1992) of Beloit detailed operating conditions but used the simplest internal model, i.e. no thickness direction gradients. A simulation of general validity to include cylinder drying of heavier paper and for drying any grade by any high intensity process requires representation of the actual internal transport phenomena.

A 1995 pamphlet by Kiiskinen and Retulainen of the VTT Technical Research Centre, Finland, details BALAS (Balance Simulator), a Windows based program with a graphical user interface to calculate mass and energy balances, analyze heat recovery, optimize processes and develop unit operation models. Its use is claimed for analysis of the influence of new drying techniques on paper mill energy management.

In 1996 Wilhelmsson et al. applied their simulation to nine machines. The Windows program was done in Borland Pascal with a graphical user-interface for entering machine geometry and operating conditions. Elements included single and double tier drying and vacuum rolls. The output is written to three print files and one report file. A 40 cylinder dryer simulation running on an IBM 486-66 MHz computer required 5 minutes after the calculation coefficients were tuned. With two tuning parameters on each machine, the condensate coefficient and cylinder-to-paper contact heat transfer coefficient at 0 % moisture, the simulation results necessarily fit the experimental data. As their model also incorrectly assumes no internal mass transport phenomena its applicability is limited to light weight sheets dried under low intensity conditions.

Persson and Stenström (1996) apply this same simulator to a machine producing 211 g/m^2 paperboard, proposing its use to predict several operating condition changes for machine speed-up. The simulator may be tuned with its two calibrating parameters to measured dryer exit moisture content. However, through using a model without internal gradients, its predictions for changed conditions cannot be reliable as large gradients are known to exist with grades of this thickness. They also propose use of an IR dryer to preheat the sheet after the press section, but do so only by increasing the input sheet temperature as no capability of simulating IR drying is evident.

Stenström (1997) modeled separately the three dryer section aspects (multicylinder paper drying, condensate entrainment and condensate flow) but continued to assume all evaporation at the sheet surface and no internal moisture gradients, although allowing for temperature gradients. He claimed the model works well with low basis weight (<100 g/m^2) and reasonably with a 240 g/m^2 sheet. Although Stenström attributes this success to using a cylinder heat transfer contact coefficient dependant on basis weight, his measured data from 10 dryer sections show no such correlation. Simulation of a 60 cylinder machine requires about 5 minutes on a Pentium computer.

2.3 Internal Sheet Transport Focused Models

The Hartley and Richards (1974) model considered both liquid and vapor internal diffusion as well as heat transfer. Although it excluded external systems the model was verified both in the laboratory and on a full-scale machine. The model of Snow (1980), reportedly from 1966 work, allowed for internal heat, liquid and vapor transfer. Developed mainly for optimization and dryer design, this model included many operating conditions but made no allowance for the felt. For each furnish one entered a sheet thermal conductivity and heat capacity having no dependence on moisture content or temperature. Snow reported that the 1966 experimentation techniques should be improved but that the model, when compared to others of that time, provided excellent results and may have been the first to treat internal mass transport.

The Donner and Renk (1982) model took into account heat and vapor transfer along with cylinder operating conditions. They showed the utility of simulations for diagnosing the source of poor performance when trouble shooting dryers, claiming cylinder temperature measurements to be an inferior method. Their model assumed negligible cylinder to sheet contact heat transfer resistance and did not treat felting, over-simplifications leading to excessively high heat transfer rate prediction.

From 1980-1983 Hinds, Lee and Neogi published their model based on a notably comprehensive experimental study. With lab techniques they determined the coefficients for heat conduction and for liquid and vapor transport within the sheet, found to be specific to each grade used. Their model, defined by lab work, was then applied to industrial dryers with predictions within 2 % of measured average drying rates. These simulations were done by tuning the simulation to one machine for one grade, then applying the tuned model to several other papermachines with other grades from fine paper to corrugated medium, but without changing any model parameters. The normalized simulation results matched measured average drying rates well but energy consumption predictions deviated by up to 15 % with heavier grades. With simulations providing fair predictions for grades from fine paper to corrugated medium, this model demonstrates the importance of considering internal transport phenomena.

Iida (1985) expanded upon Lee and Hinds work, proposing for printing paper to assume no thickness direction gradients of temperature or moisture content, thereby greatly reducing computation time. Such an approximation, even if not greatly in error for cylinder drying of light weight grades, would make the model inapplicable for cylinder drying of heavier grades of paper or for drying even light-weight grades by any high intensity drying process.

Karlsson and Paltakari (1992) of VTT and Helsinki University of Technology respectively, claim that for the low intensity conditions of cylinder drying, the internal processes must be taken into account for basis weight over 120 g/m^2. However Bond et al. (1992) found significant internal gradients at much lower basis weight. With a model accounting for variable sheet porosity and thickness Karlsson and Paltakari made internal temperature and moisture measurements for sheets up to 480 g/m^2, but no validation was reported. Asensio and Seyed-Yagoobi reported their first model of single-tier cylinder drying in 1992.

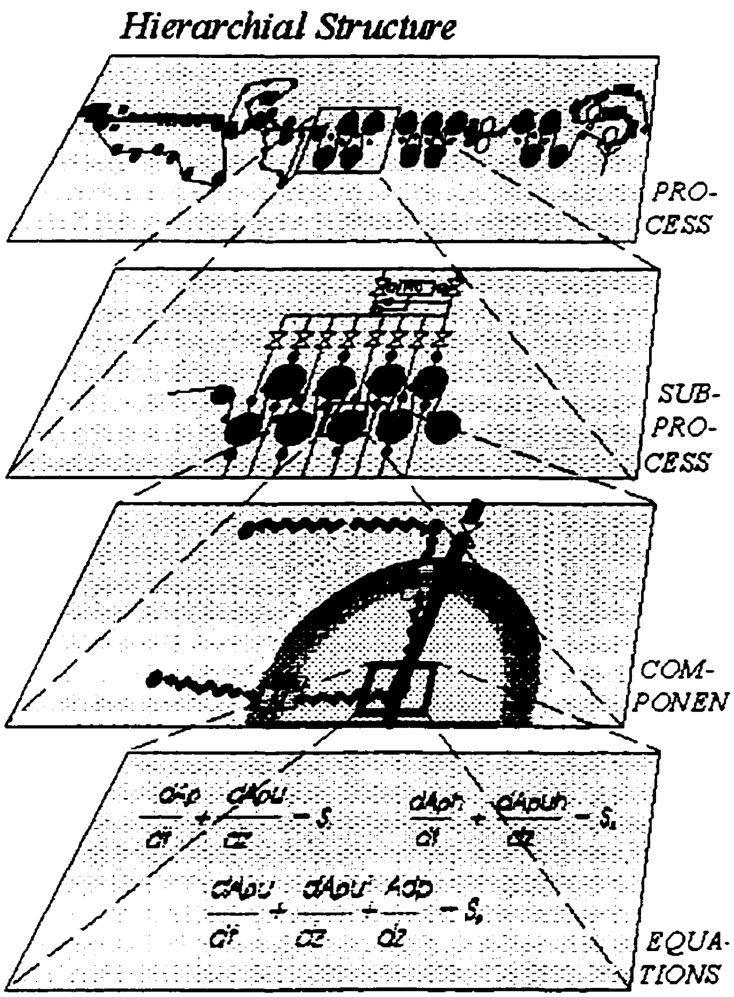

Figure 2-2: Hierarchy of APMS

Niemenmaa et al. (1996) of VTT and Finntech Ltd. introduced the Advanced Paper Mill Simulator (APMS), built on the Advanced PROcess Simulator (APROS). The VTT Internet homepage details these programs [Net2, Net3]. APROS, a general-purpose environment with a graphical user interface and tools for model development, is connected to an object-oriented real-time database. The user chooses graphical components from the model libraries, defining the variables in query forms for each component. Each element represents a component of a sub-process (Figure 2-2) defined by pre-programmed differential equations. This program can simulate the high intensity drying techniques of IR and airfoil dryers as well as cylinder dryers. Internal mass transfer differential equations are solved, but an important limitation is assumption of no internal temperature distribution, contrary to the substantial gradients determined at McGill for low intensity drying of heavier papers or high intensity drying of paper of any grammage. Niemenmaa et al. propose the program for use in design, plant analysis and employee training.

2.4 Non-Conventional Treatments of Internal Transport Processes

The Lampinen and Toivonen (1984) cylinder drying model treated mass transfer as vapor diffusion and capillary flow, and heat transfer by an apparent heat conductivity with a convection and a conduction term. For the capillary pressure required by their approach they developed a new paper structure based equation. The model showed excellent agreement for newsprint but, with no results for heavier paper, the approach cannot be considered valid for higher basis weights.

Eskelinen et al. (1985) gave few details of their addition of external systems to the Lampinen model, but showed several applications for trouble shooting dryer sections. As these authors are from a dryer manufacturer, Valmet Paper Machinery Co., it is not surprising they released few details. The world's major paper dryer manufacturers - Valmet, Beloit and Voith-Sulzer - require their own models but these proprietary simulators are neither in the public domain nor are they released to their paper company customers.

The Ramaswamy model (1990) for conventional and high intensity drying assumed a pressure build up within the sheet while on the cylinder, then instant pressure release with expansion of water vapor as the sheet leaves the cylinder. A detailed microscale model describing the internal sheet dynamics was used. The program did not use a graphical interface, consider felting or allow for the specification of varying cylinder or pocket conditions. As all cylinder and pocket conditions were identical and included in the code, this approach has limited potential. The high intensity dryers were simulated assuming an increased cylinder contact temperature and an applied mechanical pressure that are constant over the entire drying time. This model is not capable of simulating multiple technique drying as it can only simulate one type of dryer at a time and is limited to use of only one set of conditions for the entire dryer section.

2.5 Model Comparisons

In comparing three models that follow the four-phase drying definition of Nissan, Asensio et al. (1994) published the first comparison of paper drying simulators. The models were those of the Texas A&M University primary authors, of Lehtinen at Tampella Papertech Ltd., Finland and of Karlsson and Paltakari (1992). Although utilizing different assumptions, all predictions were relatively close, showing that for the low intensity drying conditions of cylinder drying various approaches can be used. All three had simulated a 49 g/m^2 newsprint and a 180 g/m^2 linerboard. Tuning or calibration may have been done, but was not noted for any of the models. The main model differences are heat transfer into the paper, internal transport mechanisms and evaporation from the web surface. For heat transfer to the web the Texas A & M model does not consider condensate flow, but correlates cylinder-to-paper heat transfer contact coefficient to the felt tension, basis weight and moisture content. The Tampella model uses experimental results of Karlsson for the cylinder heat transfer contact coefficient and literature values for condensate coefficients, thereby obtaining overall transfer coefficients of ~1620 and 1990 W/m^{2}K for single-tier and double tier cylinder drying. The VTT model uses a cylinder heat transfer contact coefficient that is a linear function of moisture content. These models treat internal transport quite differently. The Texas A & M model employs differential equations to describe heat, liquid and vapor transfer within the sheet, the VTT model assumes no z-direction gradients while the Tampella model uses uniformly shaped temperature and liquid moisture profiles throughout the dryer. For the Tampella model the z-direction sheet profiles are linear for temperature and parabolic for liquid moisture content, while for the cylinder shell a linear temperature profile is used. Evaporation rate is affected by felting; the Tampella model ignores felting, the others use evaporation reduction factors ranging from 20-40 %. Use of different definitions of heat transfer coefficient makes comparison of this aspect impossible. The closer collaboration among researchers that would improve the modeling of paper drying is constrained by the potential commercial value of a good model.

For three dryer sections specified, Stenström et al. (1994) presented valuable data for testing simulations, including at each cylinder the moisture content and temperature of the paper, cylinder surface, dryer pocket air and its dewpoint. Some operating conditions and design specifications are however missing.

2.6 Expert Systems

A Paper Drying Expert System (PDES) is described on the Internet [Net1]. This one-year project with Abitibi-Price, Stone-Consolidated, Domtar, EDS of Canada Ltd.

and KanEng Industries, Inc., was to design a prototype expert system to troubleshoot dryer sections and optimize the steam and condensate system. The Windows based program, applied in two mills, was claimed to be "...a fundamentally sound and useful tool for monitoring and recording the performance of a S & C {Steam and Condensate} system and for helping to diagnose the causes of poor performance." Later, Nault et al. (1997) discussed the application of this PDES in the Domtar Windsor mill. The system, installed in 1995, was subsequently improved.

The base program compares 50 press and dryer section inputs to entered benchmarks. The entered low and high levels of the latter come from actual and limiting operating conditions. When measurements reach either benchmark, machine operators receive an alarm and suggestions of corrective action based on previous operations. This diagnostic ability based on past experience is the central feature. With no predictive capability an expert system is not a simulator but a multi-variable system performance analyzer. A full record of operation can be maintained over time as an aid to good dryer operation. However for any change in paper specifications or operating conditions outside of previous experience, an expert system cannot predict what conditions will be required. An expert system, if used in combination with a dryer simulator, would provide a comprehensive basis for analysis of current operation and for simulation of performance with new operating conditions.

2.7 Comprehensive Model for Multiple Technique Drying: Drying Doctor

Three papers describe the *Drying Doctor* simulator. Bond, Gomes and Douglas (1996) introduced this simulation program applicable to single or multiple technique drying for cylinder, IR, Yankee and impingement air flotation drying. The program includes a graphical user interface for defining the dryer section, a database for storage of paper machine and paper product specifications and a graphical output of results. Its fully microscale model (Appendix B) differentiates this simulator from most in that evaporation is not limited to occur only at the surface of the paper or at a localized front but is allowed throughout the thickness of the sheet with continuous variation of sheet moisture content, as Lee and Hinds (1980) have shown is the case. Continuous variation of temperature and pore air humidity within the sheet is likewise allowed for, an essential characteristic for either high intensity drying processes with thin sheets or low intensity drying of thicker paper or cores. The boundary conditions may be varied during drying, thereby allowing simulation of any number of changes in drying process as a sheet goes from wet to dry. The combination of a fully microscale basis plus the unrestricted ability to change boundary conditions is what enables this model to simulate multiple technique drying. For cylinder drying the four phase model of Nissan is used. For air impingement drying the model is based on the work of Martin (1977).

Successful validation of this simulator by Bond et al. (1996) against reference cylinder drying data of Stenström et al. (1994) showed drying rate sensitivity to basis weight due to internal resistance to heat and mass transport. Exit moisture content simulation of a 50 cylinder dryer section required about 20 seconds on an IBM 486. As this simulator also accommodates the addition of water and solids to the sheet, as in coating, Bond et al. also demonstrated its ability to simulate the seven-technique processing of the sheet as it goes from a wet base sheet to dry paper coated on both sides. This on-line coated paper machine started with a three technique drying of the base sheet in successively a two tier cylinder section, a Yankee dryer, then another two-tier cylinder section. On-line coating consisted of a one-sided coater for the first side, an IR dryer and a one-sided air impingement dryer, then the identical sequence for the other side.

In the second paper concerning this software, Fralic et al. (1997) report its validation and application to three newsprint machines of Kruger, Inc.. In a 46 cylinder machine the condensate flow data appeared puzzling and an operating problem was suspected. The *Drying Doctor* simulation explained the condensate flow pattern, indicating no problem. Two methods for increasing speed of a 42 cylinder machine were simulated. Lowering the moisture content to the dryer by use of a shoe press was shown to increase production by 30 %, a speed increase that otherwise would have required addition of 10 cylinders. Another newsprint machine modification involved addition of a Sym-Sizer 2-sided coater and a soft-nip calender for a rebuild to on-line production of coated LWC paper, but with mill space constraints requiring unchanged paper machine length. By an iterative technique, a multiple technique dryer was designed to satisfy these constraints. The first 10 of the original 46 cylinders would be replaced by a Yankee dryer, cylinders 30-38 replaced by a Sym-Sizer two-sided coater, an IR dryer, an air turn and web stabilizers while the last two of the original cylinders were replaced with the soft-nip calender. Simulation of the final configuration of this seven technique drying-coating section, with no intervention by the user, required about 30 seconds on an IBM 486 computer. Their economic evaluation indicated a two-year payback for this design of a machine rebuild. In addition to the several validations, the usefulness of this simulator was thus demonstrated for analysis of dryer sections, speed-up modifications and design of major papermachine rebuilds requiring drying by multiple techniques. The 1997 publication also described additions to the simulator, which extended the capability to single/double felted cylinders and to single/double tier cylinders.

The most recent paper on this simulator, Farell et al. (1999), details the addition of equations for pressing, thereby expanding the model to a combined treatment of pressing and drying. They applied this integrated water removal simulator to a fine paper machine of Domtar Inc. with a four-nip press, one-tier and two-tier cylinder sections, size press and another two-tier cylinder section. With the simulator, 30 options were examined with the objective of a 25 % machine speed-up. Options evaluated were combinations of a steam box for various sheet temperature increases into the third press nip, addition of an extended third nip at various loads, various combinations of base sheet grammage and coat weight, and increasing cylinder steam pressure. Addition of an extended nip press loaded to 525 kN/m plus a steam box to bring the sheet from 40 to 60°C would achieve machine speed increases of 18-25 % for some base sheet grammage-coat weight combinations, with a 2 to 2 1/2 year payback. The utility of the *Drying Doctor* simulator to evaluate quickly, for many competitive scenarios, the effects of interacting changes to press and dryer sections was thereby demonstrated.

Drying Doctor now has simulation times under 1 minute on a P-166+ for most exit moisture content predictions and in the order of 5 minutes for the iterative solution of machine speed prediction. No user intervention is required during either type of simulation. Use of a PIII-500 could cut this time by a factor of about 3. The built-in machine speed prediction capability of *Drying Doctor* is unique, all other simulators requiring tedious adjustment of speed by trial to approach required exit moisture contents. As machine speed prediction is the commonly used mode when investigating the effects of varying operations, this advantage saves substantial user time and facilitates thorough examination of alternatives.

2.8 Summary

In the extensive modeling of cylinder drying of paper several models treat liquid, vapor and heat transport within the sheet, but all have fundamental flaws, be it reliance on numerous tuning parameters, lack of external system modeling or use of over-simplifications. *Drying Doctor* has full microscopic level modeling of all three transport phenomena, allowing evaporation and gradients of all three variables throughout the sheet and has a single tuning parameter for calibration if desired. The only known simulators of multiple technique drying are the *Drying Doctor* and APMS/APROS. The APMS/APROS simulator assumes no temperature gradient within the sheet, a simplification shown by the measurements of Lee and Hinds (1983) and Bond et al. (1998) as well as by *Drying Doctor* testing to be far from what occurs for high intensity drying processes with tissue or low intensity cylinder drying with heavier grades. Thus it appears that the simulator developed here is the only one not subject to any of these restrictions or approximations. Stenström (1997) stated:

> *"More work should be directed towards mass transfer phenomena in the sheet. This will be of importance not only for modeling the drying process but also understanding the close coupling between transport phenomena (mainly temperature and moisture content) and the different quality parameters of the sheet such as curl and strength."*

As the *Drying Doctor* simulator incorporates internal heat, moisture and vapor transport, including gradients of temperature, fiber moisture content and pore air humidity, Stenström's recommendation has been achieved with the McGill model.

3 *DRYING DOCTOR* SIMULATOR

3.1 Description of Program

Drying Doctor consists of three parts: (1) a graphical user interface (GUI) for defining the dryer, specifying the product and viewing results, (2) the simulation engine, to solve the governing transport equations and (3) a database, to store all information, allowing for a company-wide description of its paper products, dryer specifications, operating conditions and dryer survey results in a standard format.

During this research, the simulator was further refined. The original IBM 486, Windows 3.1 program was modified for Windows 95, installed on a Pentium Pro 200 and P-166+ computers. The simulator has also been successfully tested under Windows NT and Windows 98. Results with *Drying Doctor* versions 2.200-2.400 are presented here. Likewise the GUI underwent a large "facelift", providing a more user friendly, intuitive interface. The layout of all forms was made uniform by introducing a tab structure.

From the Current Simulation (Figure A-1) one chooses the simulation to be run. The bottom left arrows are for scrolling through all simulations in the database, identified by name, name of machine, product name. All process elements are depicted on the main tab. The next tab, Machine Conditions (Figure A-2), includes machine trim and speed, temperature and moisture content of incoming paper. Product Conditions (Figure A-3) include basis weight, outgoing moisture content and caliper. These tabs, for display, cannot be edited.

The next tab (Figure A-4) effects the choice between the three types of *Drying Doctor* simulation. In exit moisture content prediction mode, moisture and temperature history of the sheet through to the dryer exit are predicted for a specified machine speed and entering conditions. In machine speed prediction mode an iterative solution converges, without user intervention, to the speed at which the machine will operate with all incoming and outgoing conditions. As exit moisture content is typically fixed, the machine speed prediction mode is most commonly used, i.e. for examining all effects on production capacity such as increase in machine speed from installation of spoiler bars in drying cylinders or changing air jet temperature in a Yankee dryer.

The final type of simulation is calibration. As *Drying Doctor* uses a full microscale model with no tuning parameters, with numerous machine characteristics and conditions specified, simulated results will always differ somewhat from those measured. As with all simulators of complex systems, the calibration mode uses a complete set of measured conditions to adjust a model parameter so that predicted results conform exactly. Criteria for selection of the adjustable calibration parameter are that the results be quite sensitive to this parameter and that it be one in the model for which there is significant uncertainty. For cylinder and Yankee dryers, the parameter chosen for the *Drying Doctor* calibration is the relationship between moisture content and the cylinder-sheet contact heat transfer coefficient, specifically, the intercept b in the Rhodius and Gottsching (1979) equation. Figure 3-1 shows the default curve, i.e. their correlation, used unless a calibration is carried out. In calibration mode an iterative solution adjusts the parameter to give the measured set of conditions. Machine speed and exit moisture content predictions can be run with or without prior calibration. This tuning method has the greatest effect at the dry end. A change of 20 in the intercept changes the coefficient by 5 % at moisture content of 0.1 kg/kg dry, but by less than 1 % at 1.4 kg/kg dry.

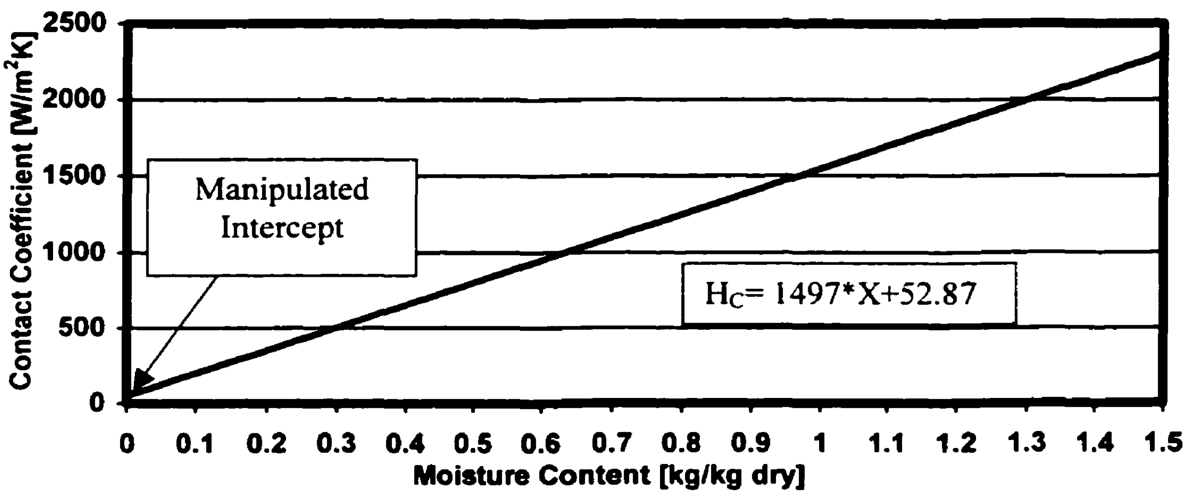

Figure 3-1: Calibration Mode Tuning Equation

The fourth tab describes Computational Details (Figure A-5). Current choices are the correlations for moisture diffusivity and thermal conductivity, these being now the best available from the literature. With research continuing at McGill on the transport properties of paper, the current equations may subsequently be replaced with those results. Other choices available are the output results time interval and the number of numerical solution computation nodes across the sheet. Currently the output results resolution is limited by file size, that is, to 2000 points or 4000 points in the exported Excel results. For purely computational purposes the sheet is treated as 3 plies, this having no operational effect now but in the future will allow describing for each ply its grammage, furnish, fibre saturation point, etc.. The available number of nodes per ply is from 2 to 998, with 10 nodes/ply commonly used, i.e. 30 nodes in all, for which the output results resolution of 0.01 s generally uses less than the maximum number of points in the result file. Simulations have been run with an output interval as small as 0.0001 s. The fifth tab is used for any documentation applicable to the simulation.

Figure 3-2: Product Button

The machine and product form, the remaining two of importance, are accessible in several ways. The paper product form can be accessed either through the product button on the main toolbar or from the Edit Product button on the Product Conditions tab of the Current Simulation form. Clicking on either brings up the Product form (Figure A-6) which has, at the bottom, arrows for scrolling through the grades in the database where dry basis weight, caliper, ash content, fibre saturation point and target final moisture content are recorded. The second tab (Figure A-7) displays the treatment options for pressing, as Drying Doctor simulates pressing as well as drying.

Figure 3-3: Machine Button

The last main window is the Paper Machine form (Figure A-8), accessed through the button on the main toolbar or the Edit Machine button on the Overview and Machine Condition tabs of the Current Simulation form. The dryer section is defined through the toolbar at the bottom, Figure 3-4. The elements from left represent: press, single-tier cylinder, two-tier cylinder, Yankee dryer, coating station/size press, infrared dryer, flotation dryer and black box. The arrows at the bottom facilitate browsing through all machines in the database. Dryer elements selected from the toolbar are added by clicking on the desired space in the layout. Clicking on the pencil eraser, then on an

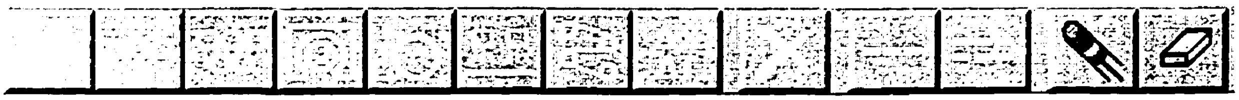

Figure 3-4: Toolbar

element, removes it. The entire dryer section can be erased by clicking on the large eraser. Use of more than one type of process creates a multiple technique dryer. The default layout allows 10 elements, but this can be doubled by clicking on the "two row" button or reversed by the "one row" button. Operating Conditions, the same variables as displayed in the Machine Conditions tab of the Current Simulation form, are entered in the next tab (Figure A-9). Finally, specific variables for each dryer element are input. To enter or edit dryer element variables, one click on the element in the Layout tab brings up the appropriate form. Bars connect each dryer element, representing the inter-element draws, i.e. sheet length between elements. One clicks on these to enter the draw length and felting options. As cylinder dryers and Yankee dryers are the most common types, a description of these forms follows.

In the two-tier cylinder section form, Figure A-10, the default tab is the Geometry tab where the number and geometry of cylinders are entered along with felting options. Figure A-11 shows the Steam System tab where pressure and spoiler bar details are entered. The three options for describing pocket air ventilation conditions in the Air System tab (Figure A-12) are discussed in section 3.3. By choosing the show button from the top of the form, displayed on Figures A-13, 14 & 15, these variables may be manipulated on a cylinder by cylinder basis, including shutting steam off in individual dryers as occurs in industry.

Tissue and toweling are dried on Yankee air impingement dryers. Figure A-16 displays the Geometry tab. Specifications of the cylinder and confinement hood for the array of impinging air jets are entered. The Yankee cylinder steam pressure and impinging jet variables are entered on the Steam System tab (Figure A-17) and Air System tab (Figure A-18). The simulation is started by clicking on the run button.

Drying Doctor returns the results in graphical form (Figure A-19). The 20 graphs available, Figure A-20, may be edited. Results tabulated as a function of drying time or cylinder number may be exported to an Excel spreadsheet.

3.2 Input Variables

The key aspect of any simulation program, i.e. what input data are essential and what optional data may be entered, are shown in the following tables.

Table 3-A: Operating Variables

Variable	Units	Required
Machine Trim	m	Yes
Machine Speed	m/min	Yes
Initial Moisture Content	kg/kg dry	Yes
Initial Sheet Temperature	°C	Yes

Table 3-B: Product Variables

Variable	Units	Required	Default Value
Dry Basis Weight	g/m^2	Yes	none
Dry Caliper	microns	Yes	none
Ash Content	weight %	No	0
Fiber Saturation Point	kg/kg dry	No	none
Final Moisture Content	kg/kg dry	Yes	none
Permeability Proportionality Constant, g	g/m	Pressing Only	Newsprint: 1.129E-12 Bond: 1.505E-11 Market Pulp: 3.872E-10
Compressibility Factor, n	n/a	Pressing Only	Newsprint: 3.28 Bond: 4.03 Market Pulp: 3.55

Table 3-C: Cylinder Geometry and Felting Variables

Variable	Units	Required	Options
Number of Cylinders	n/a	Yes	none
Cylinder Diameter	m	Yes	none
Cylinder Shell Thickness	mm	Yes	none
Sheet Wrap Angle	degrees	Yes	none
Draw Length*	m	Yes	none
Tier of First Cylinder	n/a	Yes	Top/Bottom
Cylinder Contact	n/a	Only Single-Tiered and Unirun Felting	Sheet/Felt
Felting Type	n/a	Yes	Single/Top/ Bottom/Double/None
Felt Wrap Angle	degrees	If Felted	none
Felt Thickness	mm	Yes	none
Sheet length in dryer	m	No	none
Steam Pressure*	kPag	Yes	none
Spoiler Bars*	n/a	Yes	None/Profiling/ Full-Width

*** May be specified individually for each cylinder**

Table 3-D: Cylinder Dryer Pocket Variables

Variable	Units	Required	Default Value	Options
Pocket Type*	n/a	Yes	none	**Known Pocket Conditions/ Unknown Pocket Conditions/ Pocket Ventilation
Pocket Air Temperature*	°C	Depends on pocket type	60	none
Pocket Air Humidity*	kg/kg dry air		0.15	
Ventilation Air Supply Temp.*	°C	Depends on pocket type	120	none
Ventilation Air Supply Flowrate*	m^3/min-m width		14	

*** May be specified individually for each cylinder**
**** Detailed in Section 3.3.3**

Table 3-E: Yankee Dryer Variables

Variable	Units	Required	Default Value	Options
Cylinder Diameter	m	Yes	none	none
Cylinder Shell Thickness	mm	Yes	none	none
Wrap Angle Before Hood	°	Yes	0	none
Wrap Angle Inside Hood	°	Yes	none	none
Wrap Angle After Hood	°	Yes	0	none
Sheet length on cylinder	m	No	none	none
Impingement Side (sheet)	n/a	Yes	none	Top/Wire
Nozzle Diameter	mm	Yes	none	none
Nozzle to Web Distance	mm	Yes	none	none
Nozzle Pattern	n/a	Yes	none	Triangular/Square/ Hexagonal
Nozzle Open Area Ratio	%	Yes	none	none
Steam Pressure	kPag	Yes	none	none
Nozzle Exit Temperature	°C	Yes	none	none
Nozzle Exit Humidity	kg/kg dry air	Yes	none	none
Jet Velocity/Reynolds no.	m/s, or none	Yes	none	none

3.3 *Modifications to* Drying Doctor

The several important additions to *Drying Doctor* during this study have increased the accuracy and scope of this dryer simulator. The option to export results to Microsoft Excel was added. The graphical results were modified to allow printing, editing and faster graphing. The interface structure was modified for consistency, with tab controls to organize data. Changes to the model are now described.

3.3.1 Treatment of the Four Phases of Cylinder Drying

A major improvement for cylinder drying were changes in felting options and more detailed treatment of the four phases of drying. Sheet and felt wrap angle are now specified independently, with sheet wrap angle required to be the larger value. For example, with a cylinder having 270° and 180° sheet and felt wrap angles, *Drying Doctor* now divides the difference in angles between the drying Phase I and III, Figure 2-1. That is, Phase I consists of 45° of air-sheet-cylinder contact, Phase II has 180° of felt-sheet-cylinder contact and Phase III has 45° of air-sheet-cylinder contact. The simulator calculates sheet moisture content, temperature and pore air humidity at each node in the sheet and returns to the user four point values for each variable as well as average moisture content for each third of the sheet. The local values returned are at the two surfaces ("top" and "bottom") and the 1/3 and 2/3 points within the sheet. The local average moisture contents returned for each third of the sheet are designated "top", "middle" and "bottom" third. Here "top" and "bottom" are the sides of the sheet which were top and bottom in the papermachine drainage section.

For a single cylinder the Figure 3-5 profiles of internal sheet conditions during each phase, determined with the microscale model, show local point values of moisture (red circles), temperature (blue lines) and sheet pore air humidity (green squares). These results are for 161 g/m^2 paper at the two tier double felted cylinder #15 (lower tier) where the pocket air is at 0.2 kg/kg dry and 68°C (65°C wet bulb) in the dryer specified in Section 5.3.1. In Phase I, the contact (top) side on this lower tier cylinder is heated rapidly, by about 10°C, with conduction from the steam condensing at 180°C. The remainder of the sheet continues to cool from the effects of the convective heat and mass transfer conditions in the previous draw, until warming from the heated side begins. The

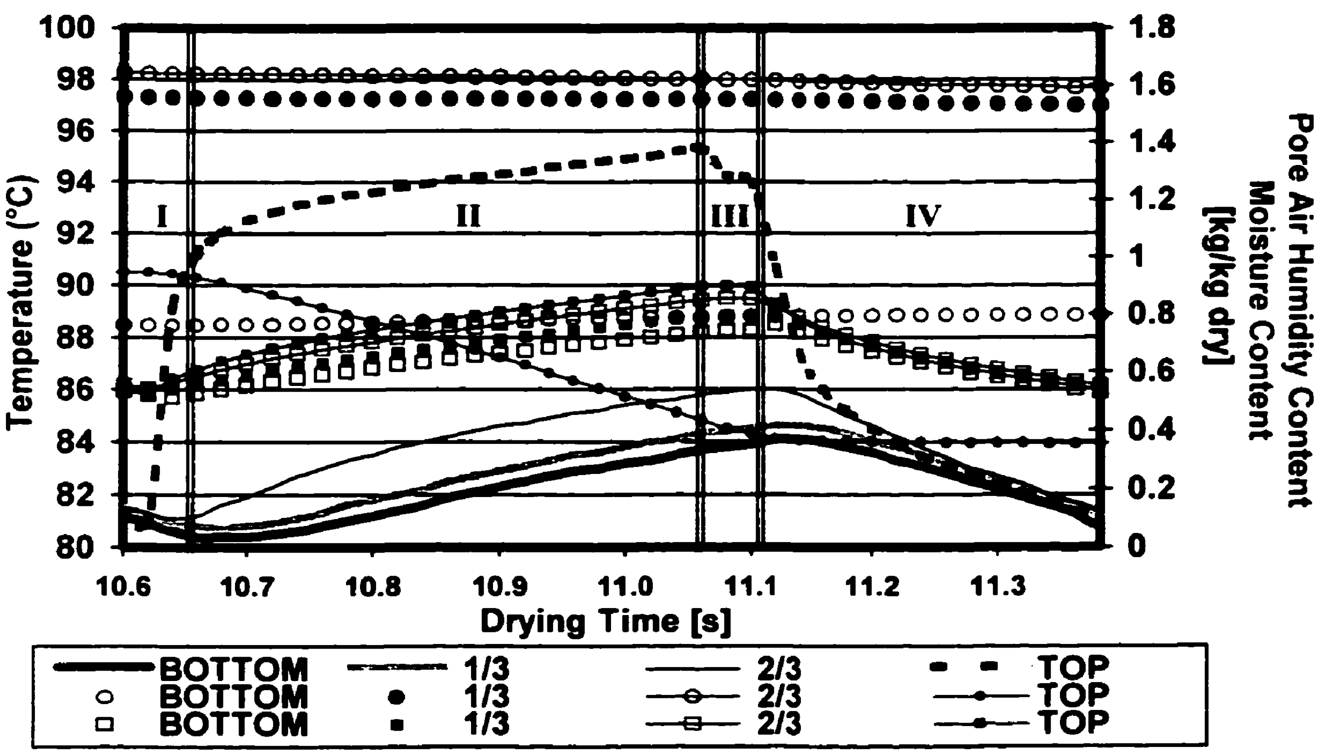

Figure 3-5: ***Drying Doctor*** **Prediction of Sheet Internal Conditions during Four Phases of Cylinder Drying**

transport rates and coefficients are such that the sheet supports large thickness gradients in temperature and moisture but only a small humidity gradient. The local moisture content at the contact side (top) of the sheet on this lower tier cylinder begins to drop from evaporation of moisture as the sheet is heated from this side while the rest of the sheet remains at essentially constant moisture.

In Phase II, the top side temperature continues to rise as the felt now presses the sheet on the cylinder while the sheet at the three other positions warms by heat transport from the heated side. The large drop in moisture content at the top side reflects substantial evaporation in Phase II. Note particularly that the top side of the sheet is getting much drier in spite of liquid moisture diffusion to this side from the wetter interior of the sheet. Thus not only is there counter-current liquid and vapor phase transport on this half of the sheet, but vapor transport is thereby demonstrated to be very much faster than liquid moisture transport. Vapor transport from the top to bottom side is reflected by the continuous humidity decrease from the top to bottom side of the sheet. That the rise in moisture content at the bottom is only marginal in spite of the very large difference in moisture content between the 1/3 position and the bottom again confirms that liquid moisture transport is almost negligible relative to vapor transport.

In Phases I, II and III, the heat transferred from the cylinder surface goes partly into sensible heat, seen in the temperature profiles, and partly into evaporating moisture, seen in the rapid decrease in moisture content at the cylinder contact surface. The top surface temperature increase ends in Phase III, while the top moisture content continues dropping by moisture evaporation and humidity transport. As this cylinder is from a two tier dryer, the moisture contents at the top and bottom of the sheet cross within the four phases of every cylinder. The local pore air humidity, a distributed variable across the sheet thickness, is seen to follow sheet temperature trends.

In the draw between cylinders, Phase IV, both sides contact the 68°C pocket air. The entire sheet cools but the hotter side that has just lost contact with the cylinder naturally cools more quickly, soon eliminating the thickness direction temperature gradient. Likewise the pore air humidity and its gradient drops, paralleling this trend for temperature. The average of the moisture contents at the 1/3 and 2/3 positions decreases from 1.60 to 1.56 from Phase I start to the Phase IV end, this small decrease corresponding to the need for 48 cylinders for complete drying. The moisture difference between top and bottom is larger exiting than entering this cylinder (#15) due to an asymmetry in the moisture profile across the sheet, caused by the large increase in steam pressure at the lower tier cylinder 13 where the top of the sheet was the first side to contact the much hotter cylinder surface. Phase IV demonstrates the ineffectiveness of pocket ventilation in this machine. With 0.2 kg/kg dry pocket air at 68°C (wet bulb 65°C) there is negligible decrease in sheet moisture content in the draw.

Figure 3-5 shows that, with a rigorous microscale model, the *Drying Doctor* precise simulation of paper drying provides unique understanding of what occurs within the sheet during drying, such internal measurements being impossible. As paper properties are developed during drying, knowledge of temperature and moisture evolution within the sheet will enable relating paper properties to drying conditions.

3.3.2 Felting and Pocket Ventilation of Cylinder Dryers

Many two tier dryers have felting arrangements other than the single and double felting originally treated. Figure 3-6 shows that all configurations currently used industrially are now available in *Drying Doctor*: single felted (unirun), top only, bottom

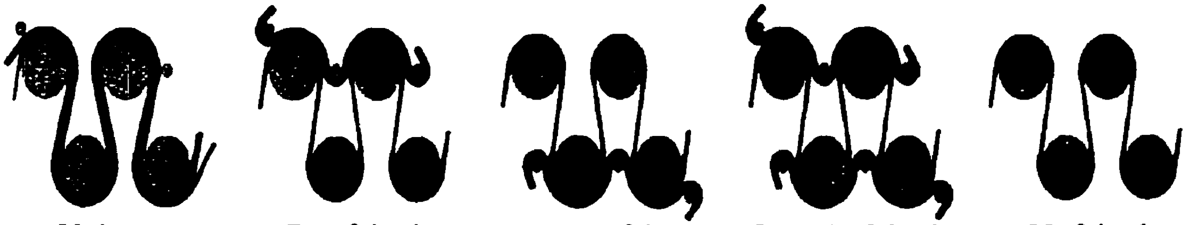

Figure 3-6: Felting Arrangements-Unirun, Top, Bottom, Double & None

only, double felted or no felting. In single felting, on one tier the felt is sandwiched between the sheet and cylinder, reducing heat transfer and drying rate but improving runnability through continuous sheet support. The program treats felting by relating heat transfer to the thermal conductivity and thickness of the felt and by using the heat-mass transfer analogy with Sherwood and Nusselt numbers.

Another improvement was adding simulation of dryer pocket ventilation. Pocket conditions (green areas, Figure 3-7) determine phase IV sheet boundary conditions.

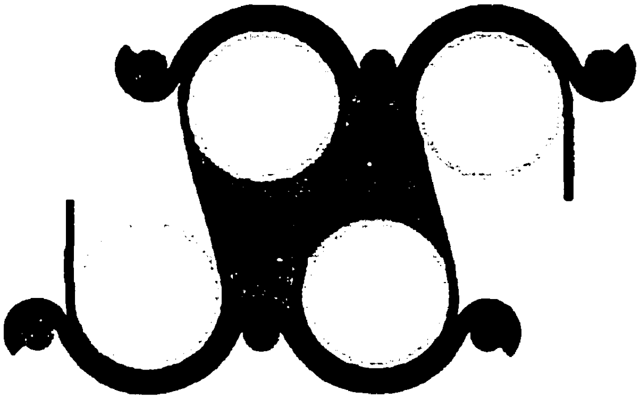

Figure 3-7: Cylinder Pockets

Without pocket ventilation, a substantial gradient in air humidity develops from the machine centerline to its edges, producing a corresponding cross direction gradient in sheet moisture content, i.e. CD moisture non-uniformity. Many machines utilize a ventilation system supplying hot, relatively dry air to the pockets, thereby promoting both higher drying rate and less CD nonuniformity of drying and hence of sheet moisture content. Only closed pockets are ventilated, i.e. top tier for top felting, bottom tier for bottom felting, or both with double felting. The three simulation options now are:

- Known Pocket Conditions

  Used when pocket air temperature and humidity is measured.

- Unknown Pocket Conditions

  When pocket conditions are unknown, default values currently are 60°C and 0.15 kg/kg dry air (wet bulb 59.8°C). This single default condition for all pockets from wet to dry end typically does not represent conditions well at either end. This high humidity would cause condensation on the sheet at the wet end where it is usually cooler than the 60°C air wet bulb temperature, and cause unrealistically low drying rates at the dry end due to the low driving force for evaporation into such high humidity pocket air. An improvement would clearly be to use a machine direction humidity profile. For now, the humidity is set lower (usually 0.1 kg/kg dry air, wet bulb 53°C) in the first and last dryer sections to approximate a humidity profile.

- Pocket Ventilation Supply Air Conditions

  The variables entered are the ventilation supply air temperature and flowrate or, if unknown, default values of 120°C and 14 m^3/min-m width are used. The supply air is considered dry (0 kg/kg dry air).

3.3.3 Cylinder Report

The final substantial improvement was addition of a cylinder report. Previously, all output variables were available only as a function of drying time from entry into the dryer. Steam pressure, average solids and moisture content, evaporation rate, condensate flow rate, cylinder surface temperature, pocket air humidity and temperature are now tabulated and plotted by cylinder number, as in dryer survey reporting.

3.3.4 Yankee Dryer

In a Yankee dryer the cylinder is surrounded by a hood to confine the hot air which issues from arrays of jet nozzles. Although there is heat conduction from steam condensing in the Yankee cylinder, typically of much larger diameter than cylinder dyers, sheet drying normally is predominantly by the high convection heat and mass transfer coefficients typical of turbulent impinging jets. The hood is usually constructed in two sections, Figure 5-8, operated at different conditions. The impingement variables

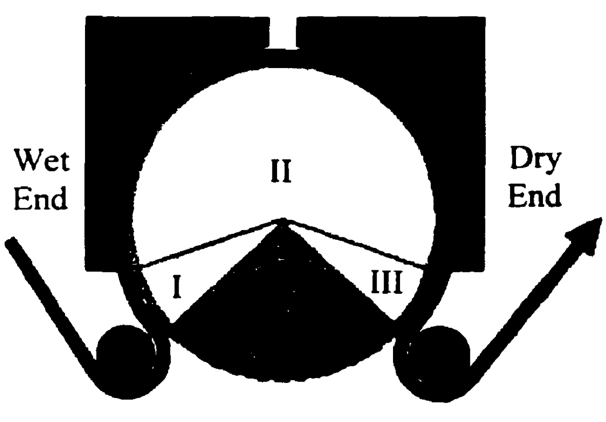

Figure 3-8: Three Phases of Yankee Drying

can now be specified independently for the wet and dry end, corresponding to industrial practice. The simulation was also modified to allow for the region where the sheet contacts the cylinder, but is not inside the hood, Figure 3-8. Thus, the paper wrap is now specified as the amount before the hood (I), inside (II) and after it (III).

3.3.5 Calibration

A major *Drying Doctor* modification was addition of a third simulation mode, calibration, which applies to both cylinder and Yankee dryers as described in Section 3.1. For most machines and grades the iterative procedure required by both calibration and machine speed prediction modes needs about 5 minutes on a P-166+ computer, with no intervention by the user.

4 VALIDATION

The results produced by any process simulation software must be tested and successfully validated against industrially measured data to earn confidence for its use. As most paper is dried over steam-heated cylinders, validation of the *Drying Doctor* simulator for this application is a priority. As all tissue and toweling is dried entirely or in part on Yankee dryers, of which there are thousands in the world, validation of this simulator for Yankee dryers is likewise essential. Moreover, a new development is the potential for the combination of cylinder drying with high intensity drying processes such as air impingement drying in what would thereby become "multiple technique drying" for printing and linerboard grades of paper. This possibility further increases the importance of validating the Yankee dryer model. Thus results from simulations of both Yankee dryers and steam-heated cylinder dryers are validated using mill measured data.

4.1 Air Impingement Convection Drying

4.1.1 Simulator Demonstration for Base Case

In the industrial configuration known as the Yankee dryer the dominant mechanism is by air impingement convection drying. The general characteristics of this process are first presented for a generic case prior to using three sources of paper mill data for validation of the air impingement drying capability of the *Drying Doctor* software. The generic case demonstration shows the type of variation in dryer performance associated with this process. Table 4-A gives the base case specification.

As the industrial focus of the present thesis is linerboard, a thicker grade (50 g/m^2) than the typical Yankee dryer application to tissue/toweling is used for this base case. Realistic choices for the moisture content of heavier papers in and out of a dryer are 1.5 and 0.07 kg/kg dry. Paper at any commercial machine speed for a 50 g/m^2 sheet could not be dried completely on a single Yankee dryer of cylinder diameter in the range used industrially. The use for this base case of a number of Yankee dryers in series would make a purely demonstration case unnecessarily complex. The alternative of a realistic machine speed and a single Yankee dryer would correspond to only a small change in moisture content in and out of the dryer. For a demonstration case this procedure is unsatisfactory because the nature of drying differs greatly between the wet sheet entering and the dry end conditions. For the Yankee dryer demonstration case then, moisture contents into and from the dryer were kept at the 1.5 and 0.07 kg/kg dry values by using atypically low machine speeds. This base case does however illustrate realistically the trends of performance with Yankee dryer design and operating variables.

Table 4-A: Yankee Impingement Dryer Base Case Specification

Variable	S.I. Units	Alternate Units
Cylinder diameter	3.66 m	12 ft
Cylinder shell thickness	25 mm	0.98 in
Nozzle diameter	5 mm	0.20 in
Nozzle to web distance	20 mm	0.78 in
Nozzle plate open area ratio	2 %	
Nozzle pattern	equilateral triangular	
Sheet wrap angle before and after hood	20°	
Hood wrap angle	230°	
Sheet length in dryer	8.6 m	28.3 ft
Condensing steam	500 kPag/159°C	72.5 psig/318°F
Jet air temperature	400°C	752°F
Jet air velocity	100 m/s	19,685 fpm
Jet air humidity	0.2 kg/kg dry	
Basis weight	50 g/m^2	10.2 lb/1000 ft^2
Inlet moisture content	1.50 kg/kg dry	40 % solids
Exit moisture content	0.07 kg/kg dry	93.5 % solids
Inlet sheet temperature	40°C	104°F
Dry sheet caliper	200 microns	
Fibre saturation point	0.8 kg/kg dry	55.6 % solids

Yankee drying process parameters may be divided into equipment design specifications and operating variables. The principal equipment characteristics are diameter of the air jet nozzles, ratio of jet nozzle area to nozzle plate area (commonly referred to as the nozzle plate open area ratio), nozzle pattern in the nozzle plate and nozzle to web spacing. The operating variables illustrated here are velocity, temperature and humidity of the air jets at the nozzle exit, moisture content and temperature of the sheet and steam pressure inside the Yankee dryer cylinder. The effect of the three equipment specifications is shown first, Figures 4-1 to 4-3, then for the six operating variables as Figures 4-4 to 4-9. The large squares indicate the base case condition.

In the complex interaction between the effects of the three equipment specifications, that for nozzle diameter, Figure 4-1, reflects the combined effects on heat and mass transfer at the moist sheet impingement surface from two non-dimensional variables, jet Reynolds number and nozzle spacing H/d. Impingement surface transfer coefficients increase monotonically with jet Reynolds number, but pass through a maximum with H/d. Thus the representation of dimensional variables in Figure 4-1 reflects the interaction between the non-dimensional variables as reported in extensive studies of transport phenomena under impinging jets.

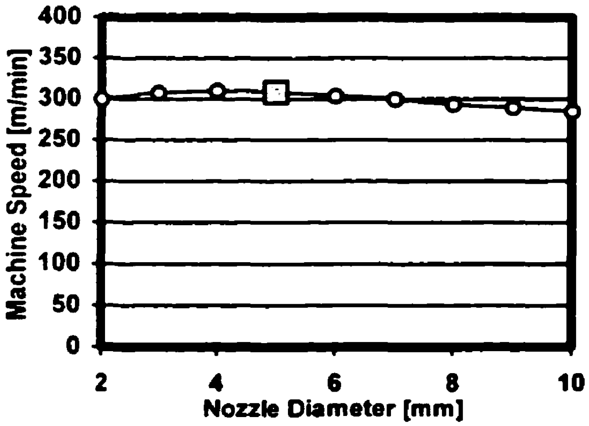

Figure 4-1: Effect of Nozzle Diameter

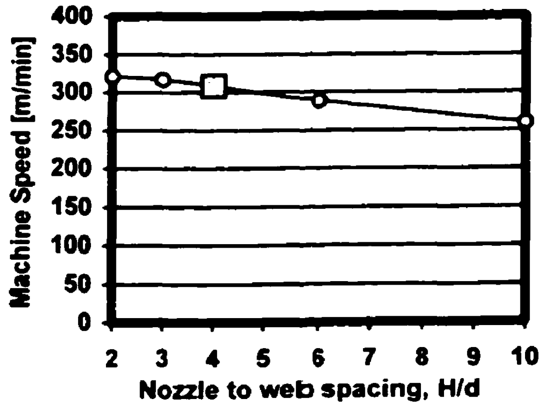

Figure 4-2: Effect of Nozzle to Web Distance

In Figure 4-2, changing nozzle diameter with the open area ratio fixed at the base case value changes every non-dimensional variable, i.e. Reynolds, Nusselt and Sherwood numbers, the nozzle to sheet spacing, H/d, and inter-nozzle spacing, S/d. Transport phenomena under impinging jets is an extensive field beyond the scope of this thesis. Appendix C shows the correlation used for the heat and mass transfer coefficients along with its range of validity, the latter providing the limits for Figures 4-1 to 4-3.

At very low values of nozzle plate open area ratio, Figure 4-3, the impinging jets are so far apart that a substantial fraction of the moist sheet is in a wall jet region of relatively low convection transfer coefficients while only a small fraction of the sheet experiences the high transfer coefficients characteristic of the impingement region. As open area ratio is increased by decreasing inter-nozzle spacing at constant nozzle diameter d, the extent of the wall jet region decreases, then vanishes. Transfer coefficients thereby become insensitive to further increases in open area ratio, seen on Figure 4-3. Thus as percent open area in the Yankee dryer hood increases from low values, the associated increase in convection transfer coefficients change from substantial to negligible, as is seen in the machine speed dependency. From purely drying rate considerations, *Drying Doctor* gives this maximum at about 4-5 % open area. However, as shown by Martin (1977) and confirmed in practice, industrial Yankee dryer hoods are usually designed for open area ratios in the 1-2 % range because the incremental cost of blower power for the impinging air jets at higher open area ratio exceeds the value of the higher drying rate. The complex techno-economic interaction between these parameters, being beyond the scope of the present work, is not discussed further.

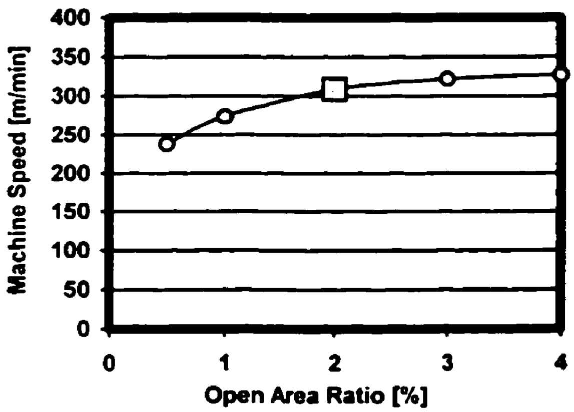

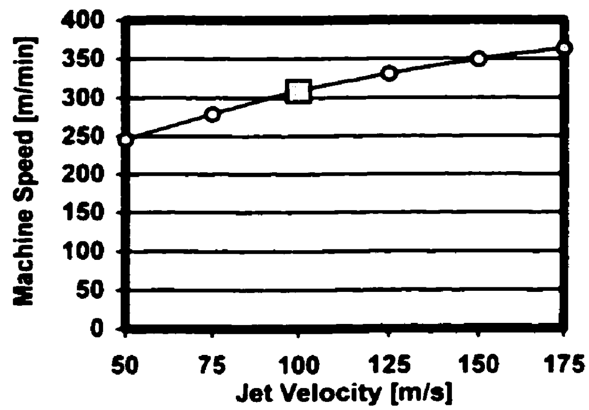

Figure 4-3: Effect of Nozzle Plate Open Area Ratio **Figure 4-4: Effect of Jet Air Velocity**

The trends with varying operating conditions are now presented. The extensive examination by Martin (1977) of the many geometric and flow variables involved in impingement drying of paper showed that maximums in drying rate occur relative to geometric variables. Economic as well as technical factors influence the optimum choices of equipment specifications and operating variables in Yankee drying of paper. For example, cost of fan power limits the maximum jet velocity, Figure 4-4, to about 125 m/s. As jet air temperature increases, Figure 4-5, the machine speed increases due to higher heat and mass transfer rates, but hood construction material cost and product quality considerations determine the operating value. The small decrease in machine speed with increasing humidity, Figure 4-6, shows the drying process is more controlled by impingement heat than mass transfer. The default humidity value of 0.2 kg/kg dry air is an industrially realistic value used for the demonstration purposes of this section.

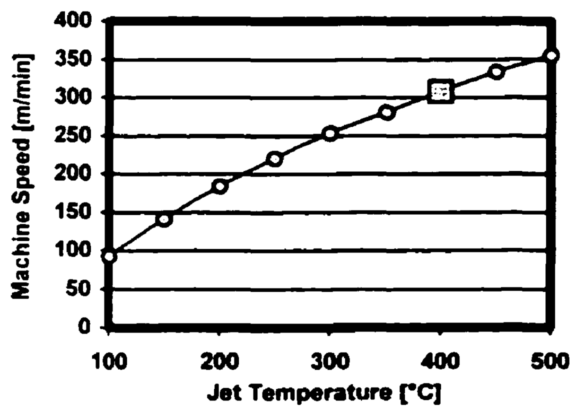

Figure 4-5: Effect of Jet Air Temperature

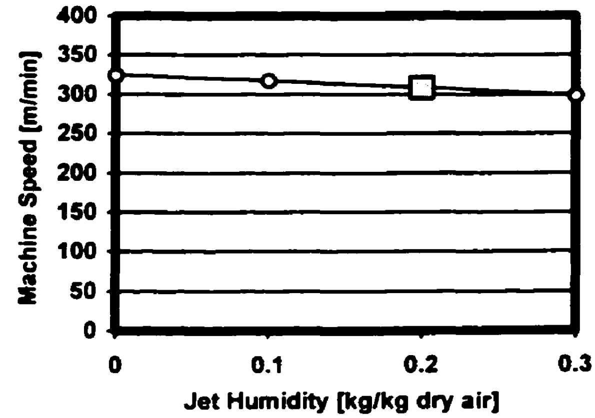

Figure 4-6: Effect of Jet Air Humidity

As Yankee dryers of tissue machines are normally controlled by adjusting internal steam pressure, not impingement hood conditions, Figures 4-7 and 4-8 show the steam pressure effect. The average drying rate for a Yankee dryer can be expressed as:

$$\overline{R} = \frac{60}{1000} \cdot \frac{S_M * B * \Delta X}{L}$$, where

S_M	machine speed [m/min]
B	basis weight [g/m^2]
ΔX	water removed [kg/kg dry]
L	dryer length based on sheet wrap angle [m]
$\overline{R}$	average drying rate [kg/m2h]

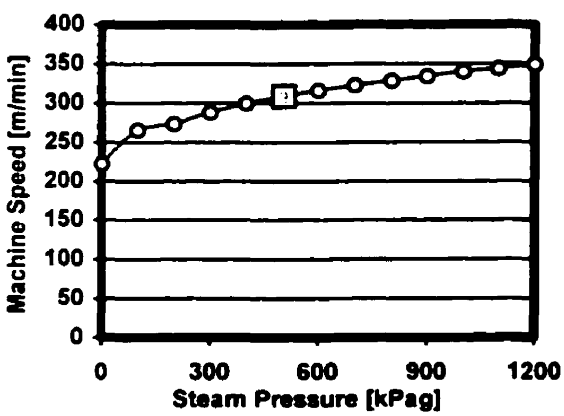

Figure 4-7: Effect of Steam Pressure

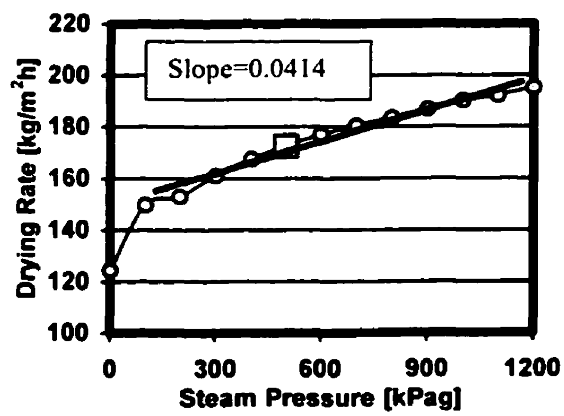

Figure 4-8: Drying Rate Dependence on Steam Pressure

In the typical steam pressure operating range of 300 to 1000 kPag, the slope corresponds to a pressure increase of about 40 kPa for a 1 % increase in average drying rate or machine speed. The sensitivity of drying rate to steam pressure is relatively low because the high convection transfer coefficients under impinging jets result in the drying being dominated on the air impingement side. The machine speed (i.e. average drying rate) is 38 % greater with the 500 kPag steam pressure of the base case than without steam, corresponding to 71 % of the drying of 50 g/m^2 paper coming from the impinging jets. The greater sensitivity of the Yankee dryer to air jet velocity and temperature is seen by reference to Figures 4-4, 4-5 and 4-7. Thus for a change in machine speed from 250 to 300 m/min, the increase required in jet velocity is about 40 m/s, in jet temperature about 100°C but in steam pressure the increase would be large, about 500 kPa. Fine tuning Yankee dryer operation is therefore done conveniently by adjusting cylinder steam pressure. In practice, economic and practical factors as well as paper property considerations influence the choice of dryer control strategy.

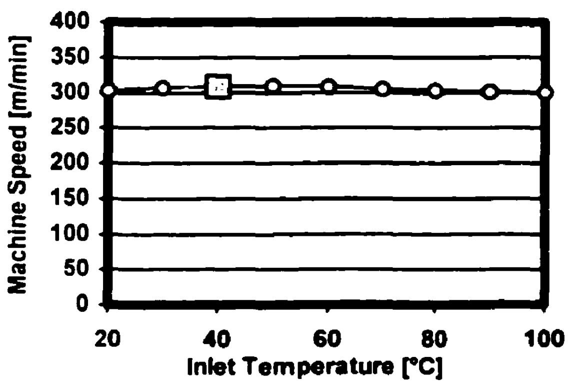

Figure 4-9: Effect of Inlet Temperature

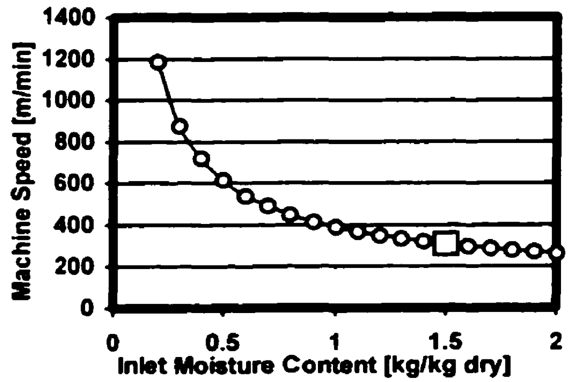

Figure 4-10: Effect of Inlet Moisture Content

Figures 4-9 & 10 show the effect of incoming paper conditions. Inlet sheet temperature has negligible effect because paper sensible heat effects are minimal relative to the latent heat of evaporation. From the average drying rate relation, $\overline{R} \propto \dfrac{S_M \cdot B \cdot \Delta X}{A}$, machine speed S_M would be approximately inversely proportional to the amount of water removed from the sheet, ΔX, hence the hyperbolic shape of the Figure 4-10 relation. In Figure 4-11 the effect of incoming sheet moisture content is

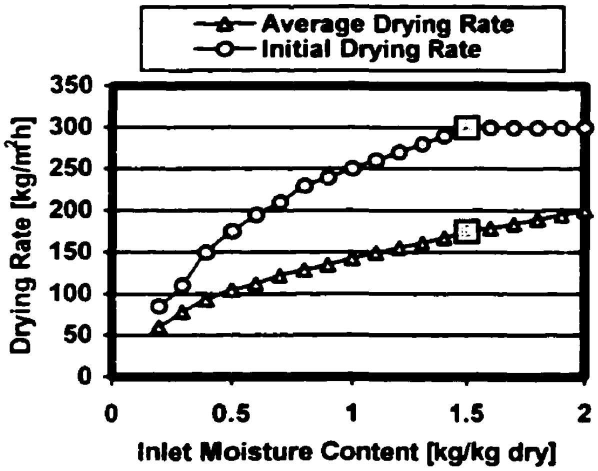

Figure 4-11: Drying Rate Dependence on Inlet Moisture Content

expressed in terms of initial and average (to 7 % exit moisture content) drying rate. The initial drying rate decreases with decreasing inlet sheet moisture content even at values greater than the fibre saturation point, 0.8 kg/kg dry for the base case, a prediction which might be considered suspect. In fact what occurs with such high intensity drying is that a thin layer of the sheet at the impingement surface side is dried below the fibre saturation point extremely quickly. As will be detailed in Section 4.1.4, the thermal conductivity and moisture diffusivity of moist paper decrease very sensitively with decreasing moisture content. Thus under high intensity drying conditions this rapid increase in the resistance to heat and mass transfer in a thin layer of relatively dry paper near the impingement surface causes the surprisingly early onset of falling rate drying, even at sheet average moisture contents well above the fibre saturation point value.

4.1.2 Perkins Tissue Machine

The operating conditions and design specifications for the Yankee dryer of a tissue machine, gathered from a 1989 mill visit to Perkins Paper Ltd., were entered in *Drying Doctor* as in Table 4-B. As the specifications available were incomplete, those assumed from typical industrial operation appear here in bold type. As will be the case in all dryer validation tests in this thesis, two absolute simulations were run with *Drying Doctor*, an uncalibrated exit moisture content prediction and an uncalibrated machine speed prediction. As a simulator machine speed prediction within 5% can be considered satisfactory, the results in Table 4-C constitute successful validation.

Table 4-B: Design Specifications and Operating Conditions: Perkins Paper Yankee Dryer

Variable	**S.I. Units**	**Alternate Units**
Machine width	3.33 m	10.9 ft
Cylinder diameter	3.66 m	12 ft
Cylinder shell thickness	24 mm	0.94 in
Nozzle diameter	7.9 mm	0.31 in
Nozzle to web distance	**20 mm**	**0.78 in**
Nozzle spacing/nozzle diameter	**2.5**	
Nozzle plate open area ratio	**2 %**	
Nozzle pattern	**equilateral triangular**	
Hood and paper wrap angle	260°	
Draw after Yankee	1.0 m	3.3 ft
Total sheet length	9.3 m	30.5 ft
Machine speed	1038 m/min	3400 fpm
Drying time on cylinder	0.54 s	
Condensing steam	**600 kPag/165°C**	**87 psig/329°F**
Jet temperature	454°C	850°F
Jet velocity	112 m/s	22,000 fpm
Jet humidity	0.2 kg/kg dry air	
Basis weight	19 g/m^2	3.9 $lb/1000\ ft^2$
Sheet inlet moisture	1.50 kg/kg dry	40 % solids
Sheet exit moisture	0.064 kg/kg dry	94 % solids
Sheet inlet temperature	**40°C**	**104°F**
Dry sheet caliper	**50 microns**	
Fibre saturation point	0.7 kg/kg dry	59 % solids

Table 4-C: Uncalibrated Validation for Air Impingement Dryer: Perkins Tissue Machine

Exit moisture content	
Validation simulation	6.5 % d.b.
Measured	6.4 % d.b.
Machine speed	
Validation simulation	1027 m/min
Measured	1038 m/min
Difference	-1.1 %

Figures 4-12 to 4-16 show the simulation results for local moisture content, local sheet temperature and drying rate as a function of drying time and position within sheet. As consistently used throughout the present work, "top" and "bottom" denote the top and bottom of the sheet in the drainage section. Here the top side is the air impingement side. Even with a sheet of very low basis weight, 19 g/m^2, only 50 μm thick, Figures 4-12 and 4-13 show impressively large moisture gradients developing during drying. This characteristic shows the necessity of modeling that is microscale, not based on sheet average conditions. The Figure 4-13 profiles of the predictions at four points (at the two surfaces and the interior one-third points) are very informative. Until 0.1 s, almost all drying occurs within the top third of the sheet. At 0.2 s the steep moisture gradients are now in the middle third while in the third adjacent to the cylinder there is slower drying by evaporation from heat conduction at the cylinder surface. By 0.3 s almost all remaining moisture is in the third of the sheet adjacent to the cylinder.

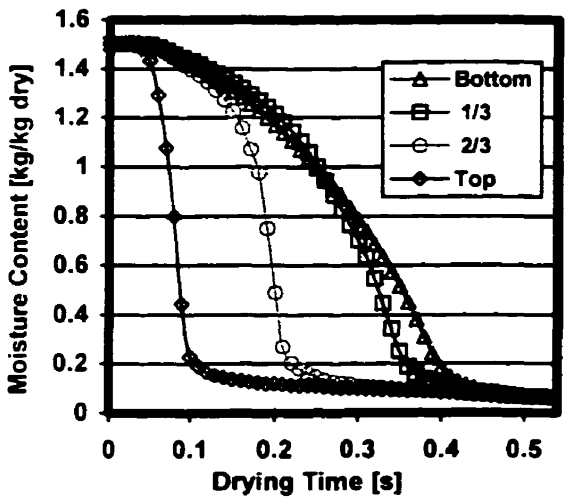

Figure 4-12: Local Moisture Content Drying History: Perkins Tissue Machine

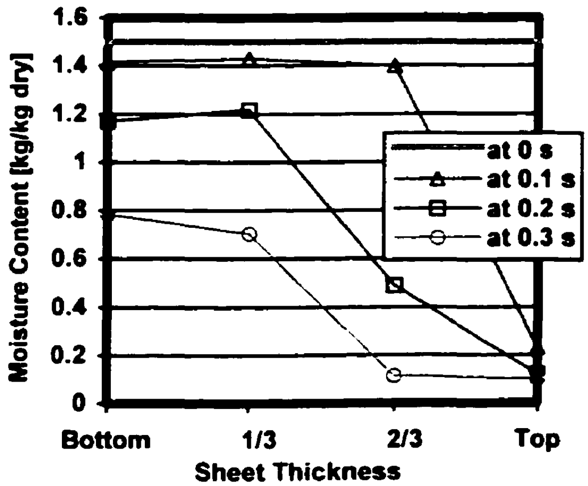

Figure 4-13: Moisture Content Thickness Profiles: Perkins Tissue Machine

The local temperature history recorded on Figures 4-14 and 4-15 at the "top", 1/3, 2/3 and "bottom" points of the sheet shows that under the high heat flux from the impinging air jets the sheet is heated very rapidly during the first 0.05 s of drying from 40° to 90-100°C. The thermal conductivity of paper with some water in the pores above its fibre saturation point moisture content (here 0.7 kg/kg dry fibre) is sufficiently high that this rapid heating in the first 0.05 s is accomplished with only the small temperature gradient in the thickness direction seen in Figure 4-14. By 0.2 s when the impingement surface and the adjacent 1/3 of the sheet approach dryness, the thermal conductivity in this third of the sheet drops sharply and the corresponding large increase in thickness direction temperature gradient is apparent on Figure 4-15. The discontinuity between 0.24 and 0.25 s in sheet temperature and drying rate, Figures 4-14 and 4-17, is a result of boundary conditions being calculated only once for each half of the Yankee dryer. As computer speeds have increased dramatically since development of *Drying Doctor* began,

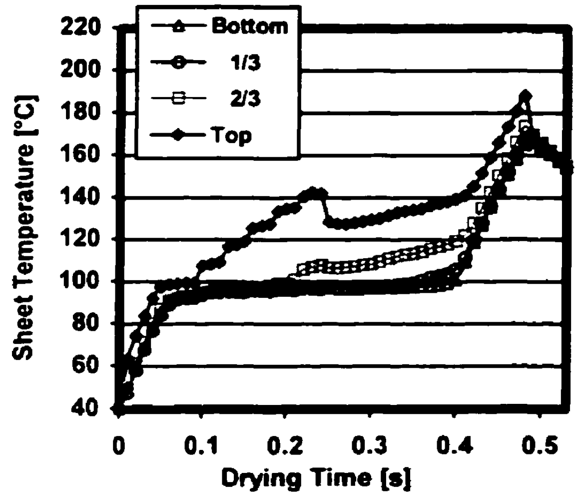

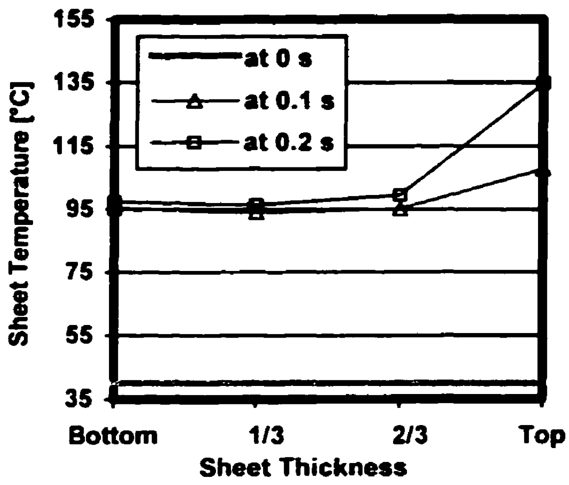

Figure 4-14: Sheet Temperature Drying History: Perkins Tissue Machine

Figure 4-15: Sheet Temperature Thickness Profiles: Perkins Tissue Machine

boundary conditions may now be changed more often, which will be implemented. In the 0.05 s of the 1 m draw after the Yankee (0.48 to 0.53 s) sheet temperature drops by 20-40°C and bound moisture content from 7.0 to 6.5 % d.b..

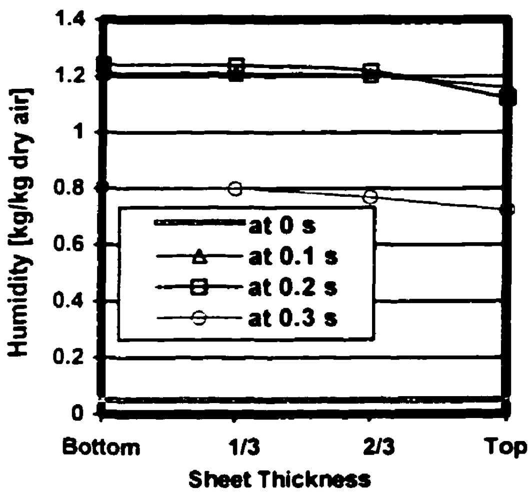

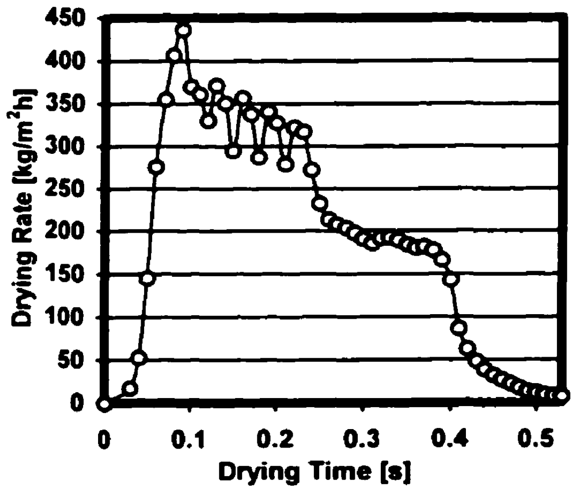

Figure 4-16: Pore Humidity Thickness Profiles: Perkins Tissue Machine

Figure 4-17: Drying Rate History: Perkins Tissue Machine

Figure 4-16 shows the pore humidity thickness profiles to be much smaller than for either liquid moisture or temperature. Profiles of liquid moisture and temperature have a counterbalancing effect. Thus at the impingement surface the liquid moisture content is lowest but the temperature is highest and vice versa at the cylinder side.

The evolution of drying rate, Figure 4-17, shows the increasing rate period occupies the first 0.09 s as the sheet is heated from its initial 40°C to about 90-100°C, Figure 4-14. This 0.09 s constitutes 17 % of the drying time of 0.54 s to the measured exit moisture content of 6.4 %. Under the strong heat flux from the high temperature air impinging jets there is no constant rate drying as the transition is directly to the falling rate period. The oscillations in calculated drying rate from 0.1 to 0.22 s are simply artifacts of the adaptive time step used in the simulations. In high temperature impingement air drying of tissue most of the drying, over 80 %, is seen to take place in the falling rate period during which the drying rate is increasingly dominated by the resistance to heat and mass transfer within the sheet. This characteristic is apparent also in the moisture content drying history of Figures 4-12 and 4-13. At t=0.1 s the Figure 4-13 moisture profile shows that only a very thin layer of low moisture content near the impingement surface is sufficient to cause this transition at about 0.1 s on Figure 4-17 from increasing to falling rate drying while about 90 % of the sheet still has water in the pores. The much lower thermal conductivity and moisture diffusivity in just this surface layer without pore water has caused the transition to falling rate drying. At t=0.2 s, well into the falling rate period according to Figure 4-17, Figures 4-12 and 4-13 show that half the sheet still has free water in the pores but the moisture content at the impingement surface is only 0.12 kg/kg dry. A sharp drop in the drying rate is also seen at about 0.4 s. At this time the moisture content at all points in the sheet is below about 0.15 kg/kg dry and moisture diffusivity is so low that this transport mechanism makes a negligible contribution, drying being now by heat conduction into the sheet, evaporation of the non-diffusing liquid water, and water vapor transport out. Thus from this time until dryness the water bound to the fibres is removed, with this desorption accounting for the final sharp drop in drying rate. At 0.54 s, when the sheet average moisture content is 0.064 kg/kg dry, the drying rate controlled by this desorption is only 8 kg/m^{2}h. A dryer survey from the mill gives the hood and cylinder average drying rates as 131 kg/m^{2}h and 78 kg/m^{2}h respectively, for a total rate of 209 kg/m^{2}h, corresponding to 63 % of the drying from impingement air, 37% from the Yankee cylinder. The drying rate predicted by *Drying Doctor*, 204 kg/m^{2}h from the inlet to the exit moisture content, matches very well the measured rate.

Some time prior to the Perkins Paper dryer survey used here, steam was turned off when a crack appeared in the Yankee cylinder. To achieve the same final moisture content, machine speed was reduced from 1038 m/min to between 868-914 m/min, a reduction in drying rate of 12 to 16 %. This decrease does not agree with the cylinder drying rate contribution of 37 % recorded in the report. This 37 % is not based on

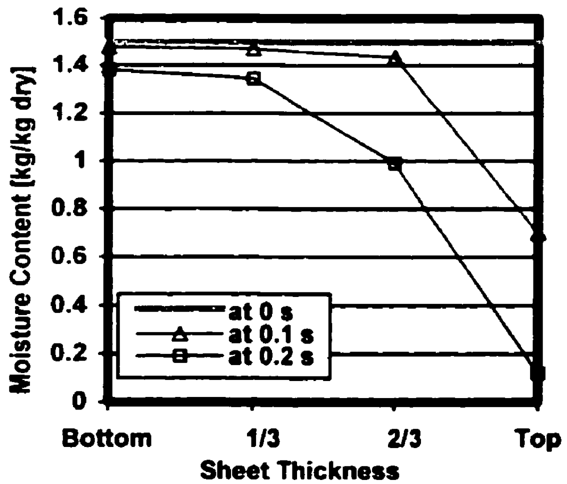

Figure 4-18: Moisture Content Thickness Profiles: Perkins Tissue Machine- Steam off

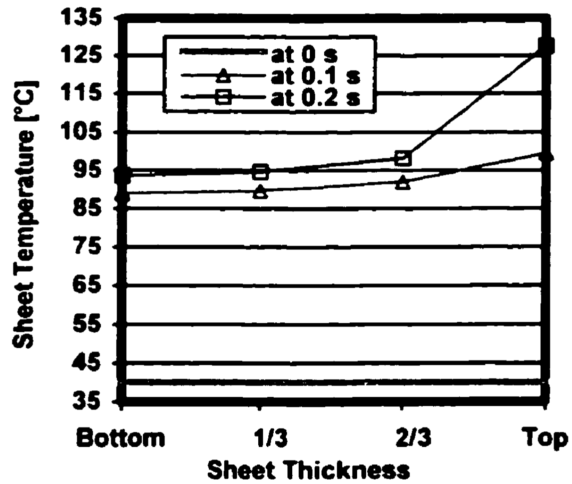

Figure 4-19: Sheet Temperature Thickness Profiles: Perkins Tissue Machine- Steam off

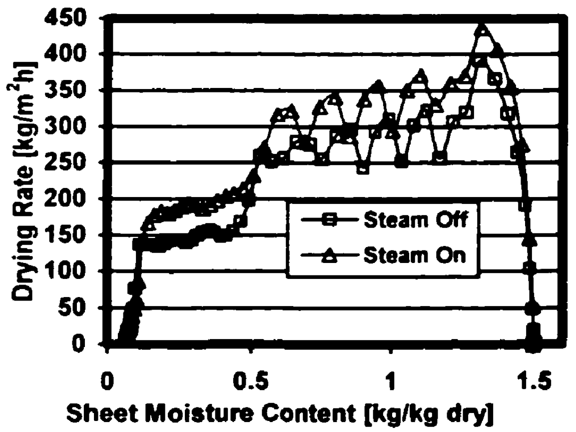

Figure 4-20: Drying Rate Curve: Perkins Tissue Machine

measurements, but on the manufacturers specifications. This specification may not be correct and may not apply to the slower machine speed. Without steam in the cylinder, the uncalibrated moisture content simulation at the average reduced speed, 892 m/min, Figures 4-18, 4-19 and 4-20, predicts final moisture content of 6.3 %, matching the measured 6.4 %. The predicted average drying rate is 177 kg/m^{2}h, lower by 13.5 % than the 204 kg/m^{2}h predicted for steam in the Yankee cylinder, which is consistent with the 12-16 % reduction experienced in machine speed.

This good agreement shows that *Drying Doctor* produces acceptable predictions both for Yankee dryers with steam, as used normally, and for drying purely by air impingement drying. Here, the second case occurred exceptionally for this damaged

Yankee dryer, but air impingement is the only mode of drying in air flotation dryers used for non-contact drying of coated paper and occasionally for other grades such as sack paper. The thickness direction moisture content profiles of Figures 4-13 and 4-18 show the slower drying on the side of the sheet in contact with the cylinder when there is no steam in the cylinder. Comparison of the Figure 4-15 and 4-19 profiles of local temperature shows that even for the sheet adjacent to the cylinder, most of the heating comes from the impinging jets, not from the steam condensing in the cylinder.

The trends in drying rate curves with and without cylinder steam pressure, Figure 4-20, are similar. The source of the discontinuity in Figure 4-20 at a moisture content of 0.5 kg/kg dry, as already noted concerning Figures 4-14 and 4-17, is a numerical problem stemming from the way in which boundary conditions are updated in the sectioned Yankee hood, for which a better procedure is to be implemented.

4.1.3 Scott Tissue Machine

At a 1992 survey of a Yankee dryer of a tissue-toweling machine of Scott Paper Co. attended by McGill University personnel, measurements were taken on its newly installed hood. The design specifications and operating conditions for the two grades produced, 14 g/m^2 tissue and 21.1 g/m^2 toweling are given in Tables 4-D and 4-E. Again those values appearing in bold type were assumed. This dryer differs from that of Perkins, Table 4-B, in having 20° of paper-cylinder wrap outside the hood on both sides.

Table 4-D: Design Specifications: Scott Paper Yankee Dryer

Variable	S.I. Units	Alternate Units
Machine width	3.68 m	12.1 ft
Cylinder diameter	3.66 m	12 ft
Cylinder shell thickness	**24 mm**	**0.94 in**
Nozzle diameter	9.5 mm	3/8 in
Nozzle to web distance	19 mm	3/4 in
Nozzle spacing/nozzle diameter	2.0	
Nozzle plate open area ratio	2.5 %	
Nozzle pattern	**equilateral triangular**	
Wrap angle before and after hood	20°	
Wrap angle inside hood	230°	
Draw after Yankee	1.0 m	3.3 ft
Sheet length in dryer	9.6 m	31.6 ft

Table 4-E: Operating Conditions: Scott Paper Yankee Dryer

Variable	21.1 g/m^2		14 g/m^2	
	S.I. Units	**Alternate Units**	**S.I. Units**	**Alternate Units**
Machine speed	924 m/min	3033 fpm	1218 m/min	4000 fpm
Drying time	0.62 s		0.47 s	
Condensing steam	613 kPag/166°C	88 psig/330°F	634 kPag/167°C	92 psig/332°F
Jet temperature	346°C	654°F	400°C	750°F
Jet velocity	**125 m/s**	**24,600 fpm**	91.5 m/s	18,000 fpm
Jet humidity	0.1 kg/kg dry air		0.1 kg/kg dry air	
Sheet inlet moisture	1.22 kg/kg dry	45 % solids	1.50 kg/kg dry	40 % solids
Sheet exit moisture	0.058 kg/kg dry	94.5 % solids	0.053 kg/kg dry	95 % solids
Sheet inlet temperature	90°C	194°F	90°C	194°F
Dry sheet caliper	60 microns		45 microns	
Fibre saturation point	0.7 kg/kg dry	58 % solids	0.7 kg/kg dry	58 % solids

Table 4-F: Uncalibrated Validation for Air Impingement Dryer: Scott Tissue Machine

Basis Weight	21.1 g/m^2	14 g/m^2
Exit moisture content		
Validation simulation	6.0 % d.b.	7.6 % d.b.
Measured	5.8 % d.b.	"5.3 % d.b."
Machine speed		
Validation simulation	919 m/min	1081 m/min
Measured	924 m/min	"1218 m/min"
Difference	- 0.5 %	"-11.2 %"

The uncalibrated validation results, Table 4-F, show that *Drying Doctor* under-predicts drying rate, the machine speed predictions being just 0.5 % slow for 21 g/m^2 toweling but significantly slow, by 11 %, for 14 g/m^2 tissue. The data for the 14 g/m^2 tissue are only design values for the hood, not measured data, so the difference may be attributed to this as the results for the measured 21 g/m^2 toweling match very well.

Exceptionally during this dryer survey the sheet moisture content was determined not only entering and leaving, but also at the middle of the dryer hood. The moisture content of these sheet samples, taken with a special "paper scoop-plastic bag" device, was determined gravimetrically to be 0.52 kg/kg dry. The Figure 4-21 drying history includes moisture content at the sheet "top" and "bottom" surfaces. The predicted drying history is seen to match extremely well that measured at the middle of the dryer hood.

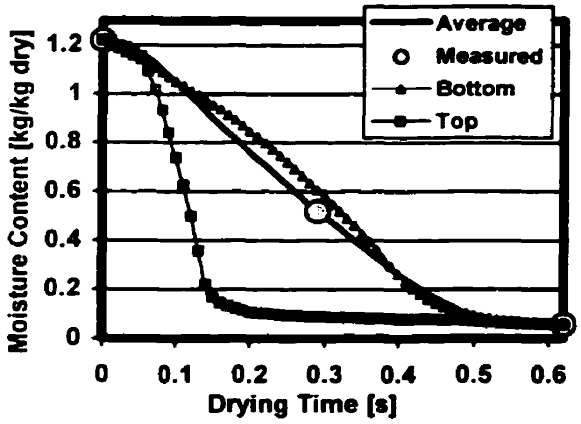

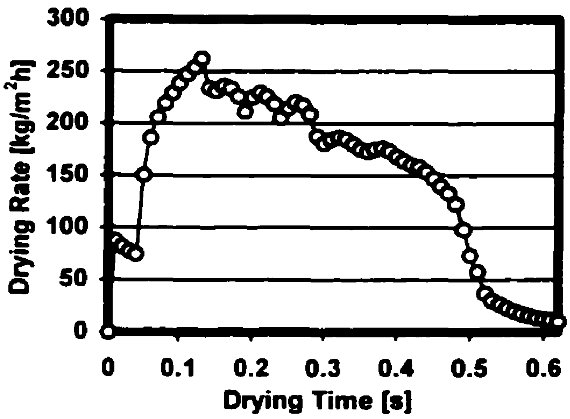

Figure 4-21: Moisture Content Drying History: Scott Tissue Machine, 21.1 g/m^2

Figure 4-22: Drying Rate History: Scott Tissue Machine, 21.1 g/m^2

Concerning drying rate, Figure 4-22, the drop predicted over the first 0.04 s results from cooling the sheet from 90°C, its initial high temperature, to 87°C as the sheet is heated only by heat conduction while in contact with the cylinder prior to entering the impingement hood. This feature is not present in for the Perkins tissue machine, Figure 4-17, because there was no sheet wrap to the cylinder prior to the impingement hood. The predicted drying rate then rises to its maximum, this rise being less steep than for the Perkins simulation, Figure 4-17, because the air jet temperature is about 100°C lower, 454°C at Perkins and 346°C at Scott. When the drying rate reaches this maximum at 0.14 s, the moisture content at the impingement surface, Figure 4-21, has just dropped below the fibre saturation point. Thus, as in the Perkins machine, there is transition directly from the increasing to falling rate drying period, with no constant rate drying. From the dryer survey the measured average drying rates for the wet and dry half of the hood were also supplied, Table 4-G, which are very well matched by the *Drying Doctor* predictions.

Table 4-G: Drying Rates: Scott Tissue Machine, 21.1 g/m^2

Average Drying Rate	Wet End	Dry End
Measured	190 kg/m^{2}h	144 kg/m^{2}h
Simulated	189 kg/m^{2}h	143 kg/m^{2}h

When a calibration simulation was run on the 14 g/m^2 tissue, the method of adjusting the calibration parameter, cylinder-sheet contact heat transfer coefficient, was not able to increase the drying rate sufficiently to lower the exit moisture content from the predicted 7.6 % to the manufacturers design value of 5.3 %. Even with the contact heat transfer coefficient increased to give a minimal resistance, the limiting simulated exit moisture content was 6.0 %. This finding demonstrates how dominant and effective impingement drying is relative to cylinder drying. The sheet is about 1/2 dry at 0.3 s, at which time the sheet temperature is about 120°C at the impingement surface, but only 100°C at the cylinder surface. With air jets at 346°C and steam condensing at 166°C, at this point the sheet receives heat by a ΔT about 225°C at a high heat convection transfer coefficient from the impinging jets, by a ΔT about 65°C at a low contact conduction heat transfer coefficient from the condensing steam, hence the low sensitivity of drying rate to the contact heat transfer coefficient.

In the future *Drying Doctor* will be able to calibrate Yankee dryers more effectively through implementation of a feature allowing different parameters to be calibrated as appropriate for different drying processes. This capability is also required for machines having on-line coating or a size press. Such machines usually have known moisture contents at the entrance to the dryer section, entering and exiting the coater or size press as well as at the end of the after-dryer. For calibration, one must fit both the moisture content into the coater or size press and that exiting the after-dryer. To do so currently requires definition of two paper machines. The first of these machines, the cylinders up to the coater, is calibrated to the moisture content entering the coater while the second machine, the coating station and the after-dryers, is calibrated to the dryer exit moisture content.

4.1.4 Laboratory Impingement Dryer

Bond and Douglas (1997) obtained laboratory data for air and superheated steam impingement drying of linerboard of three equal plies. The results of two sets of air impingement experiments for basis weight 205 and 430 g/m^2 are used here for validation. Their sheet was supported on an unheated base plate, corresponding to a Yankee dryer with no steam pressure in the cylinder. They determined the complete drying history by monitoring temperatures continuously at the sheet surfaces and the two internal ply boundaries, and by gravimetric determination of the moisture content of each ply at the end of incomplete drying experiments. The dryer specifications and operating conditions are given in Tables 4-H and 4-I.

Table 4-H: Design Specifications: Laboratory Dryer

Variable	S.I. Units	English Units
Nozzle diameter	6.35 mm	0.25 in
Nozzle to web distance	23 mm	0.9 in
Nozzle spacing/nozzle diameter	3.6	
Nozzle plate open area ratio	4.1 %	
Nozzle pattern	equilateral triangular	

Table 4-I: Operating Conditions: Laboratory Dryer

Variable	430 g/m^2		205 g/m^2	
	S.I. Units	Alternate	S.I. Units	Alternate
Jet temperature	400°C	750°F	400°C	750°F
Jet Reynolds number	2000		2000	
Sheet inlet moisture	1.5 kg/kg dry	40 % solids	1.0 kg/kg dry	50 % solids
Sheet inlet temperature	35°C	95°F	35°C	95°F
Dry sheet caliper	1260 microns		750 microns	
Fibre saturation point	0.8 kg/kg dry	55.5 % solids	0.8 kg/kg dry	55.5 %

Figure 4-24 shows the evolution of point values of local sheet temperature at the two external surfaces of the sheet and at the one-third positions within the sheet. The evolution of the local average moisture content for each one third of the sheet on Figure 4-23 shows that *Drying Doctor* overpredicts impingement drying rate with this very heavy sheet. These results are for 430 g/m^2 paper, over 10 times that of the tissue and toweling for which Yankee dryers are normally used. As the simulated values of

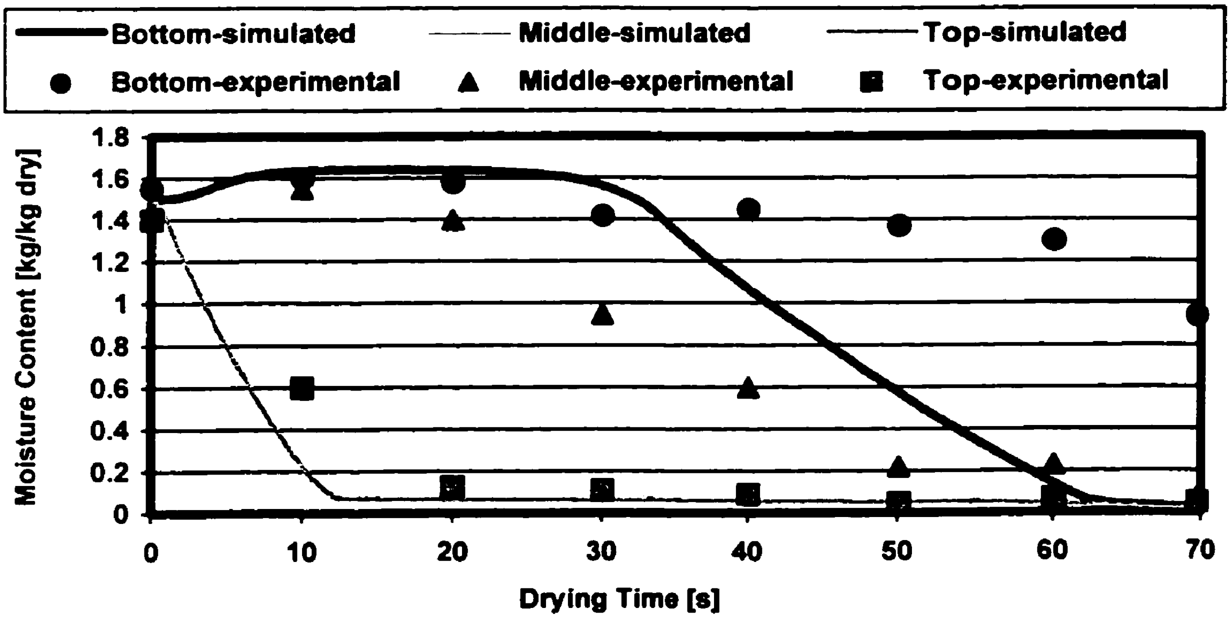

Figure 4-23: Moisture Content Drying History: Laboratory Impingement Dryer, 430 g/m^2 paper

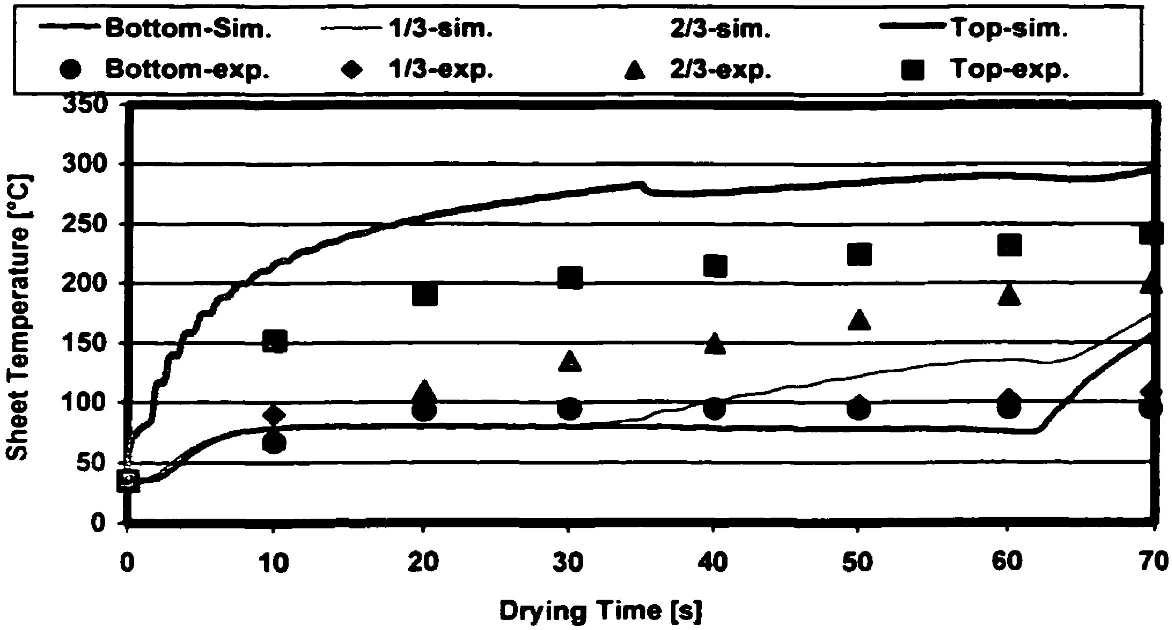

Figure 4-24: Sheet Temperature Drying History: Laboratory Impingement Dryer, 430 g/m^2 paper

moisture content decrease more rapidly than those measured, these differences indicate that the rates of heat and mass transfer predicted are higher than measured, i.e. drying rate is over- predicted. Figure 4-24 likewise shows that the simulated rate of heat transfer into the sheet is higher than that measured, consistent with drying rate being over-predicted.

Figure 4-24 shows that early in the drying, at 10-20 s for this thick paper, the region of the sheet adjacent to the impingement surface is quite hot and dry while the bottom of the sheet remains cool and wet. This large difference provides the driving force for some of the water vapor generated near the surface to diffuse to the cool, wet interior where it would condense. This mechanism provides the basis for the predicted and observed increase in moisture content at the bottom at 10 s and 20 s and at the middle third of the sheet at 10 s for the 430 g/m^2 paper, Figure 4-23, and quite similarly for the 205 g/m^2 sheet, Figure 4-25.

With a lighter grade, 205 g/m^2, dried from a lower initial moisture content, 1.0 kg/kg dry, Figure 4-26 shows results comparable to Figure 4-25. The difference between simulated and measured results for the 430 and 205 g/m^2 paper indicates less over-drying with the lighter sheet. For comparison, at 10 s, the R simulated is 49.6 kg/m^{2}h, 32 % higher than that measured, 37.6 kg/m^{2}h. At t=20 s, the difference is smaller yet, R measured being 31.2 kg/m^{2}h, 17 % lower than that simulated, 36.4 kg/m^{2}h. From Figure

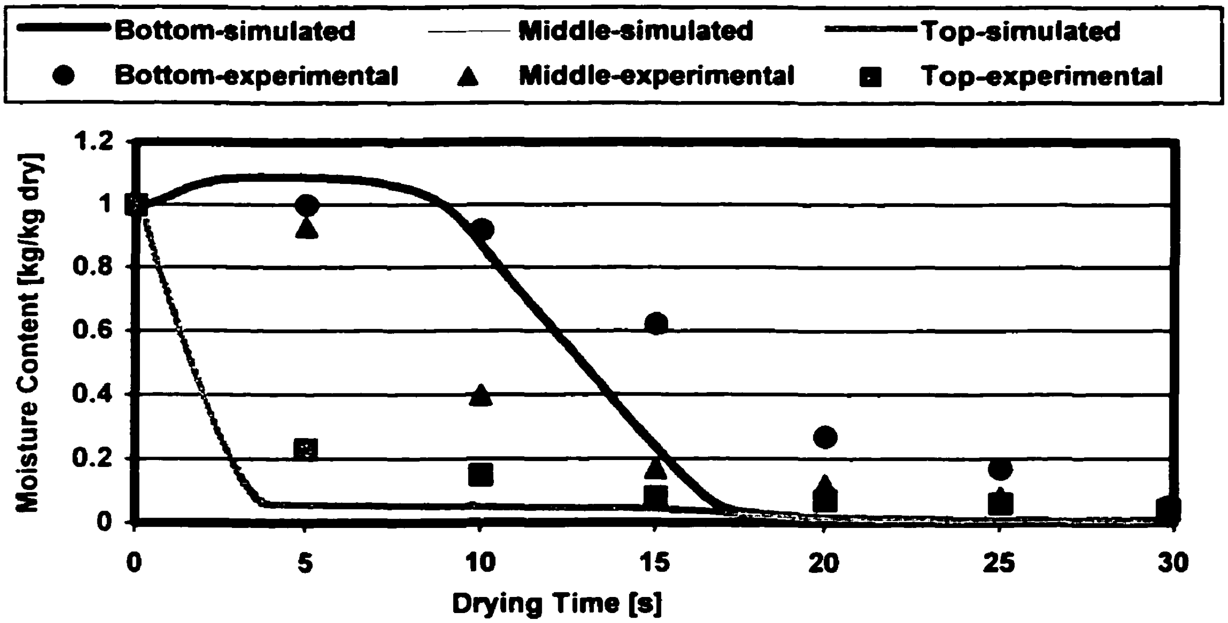

Figure 4-25: Moisture Content Drying History: Laboratory Impingement Dryer, 205 g/m^2 paper

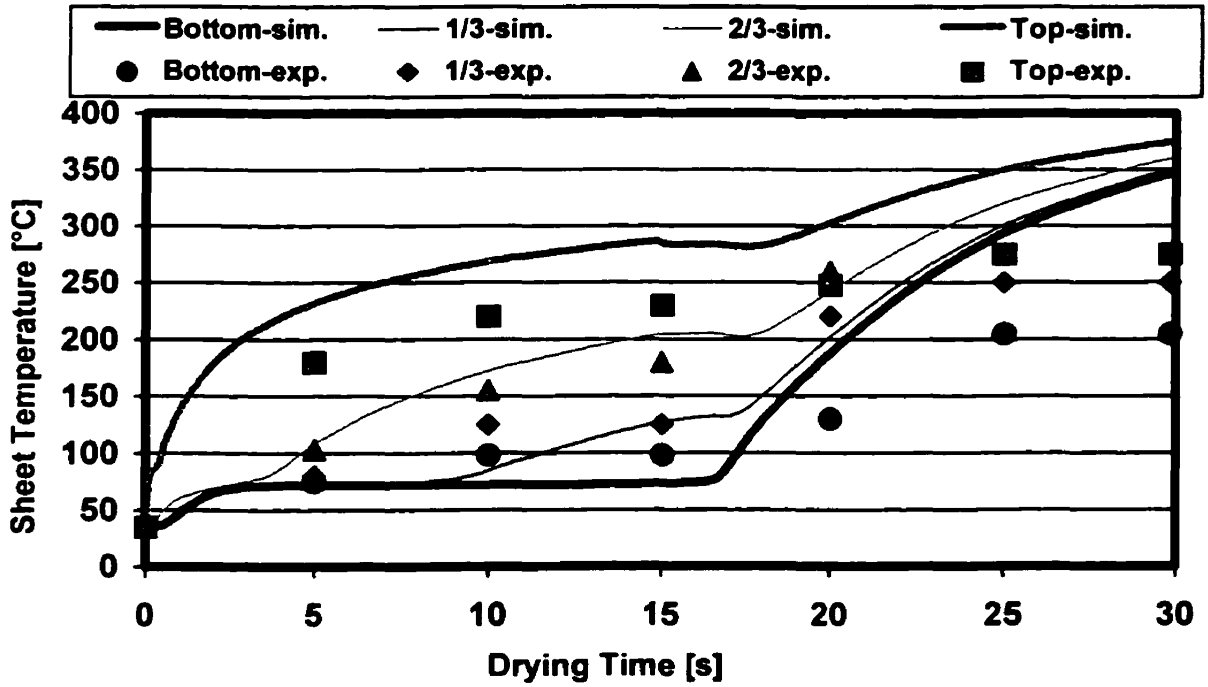

Figure 4-26: Sheet Temperature Drying History: Laboratory Impingement Dryer, 205 g/m^2 paper

4-23, these differences are much larger with the 430 g/m^2 paper. As with the 430 g/m^2 grade, the "top" layer is overheated in the simulation, but until the lower layers are predicted to be dry, at about 17 s, at those depths the temperatures predicted are quite close to those measured. That the prediction is more accurate for the 205 g/m^2 paper reflects the fact that for impingement drying, the overall resistance to heat and mass transfer from essentially the start of drying is dominantly within the sheet, hence the predicted drying rate and drying history is very sensitive to the transport properties of moist paper.

As a microscale based model, *Drying Doctor* is very sensitive to the choice of transport properties used for the various processes occurring within the moist, porous sheet. For one key parameter, diffusivity of moisture in the thickness dimension, the following four correlations have been published:

- Lee and Hinds (1980):

$$D_L = 1.4 * 10^{-10} * (X - 0.15)^{2.2} \qquad X \geq 0.15$$
$$D_L = 1 * 10^{-15} \qquad X < 0.15$$

- Hartley and Richards (1974):

$$D_L = \frac{3 * 10^{-13}}{\mu}$$

- Navarri (1992):

$$D_L = 9.386 * 10^{-10} * e^{\frac{-0.332}{X}} * e^{\frac{-31700}{R * T}}$$

- Lin (1991):

$$D_L = 2.616 * 10^{-11} * e^{0.5 * X} * e^{\frac{16100}{R} * \left(\frac{1}{298.15} - \frac{1}{T}\right)}$$

A critical evaluation of the basis of these 4 correlations, including the experimental work from which they were derived, indicates that the Lee and Hinds work provides the most credible correlation for the diffusivity of liquid moisture in paper. Therefore this correlation is used throughout this thesis, where a high degree of success in the many validations of diverse paper dryers is recorded. This finding does not constitute validation of the Lee and Hinds correlation but does indicate that, until such time as a more definitive study is reported, their representation of moisture diffusivity in paper may be used.

4.2 Steam Heated Cylinder Conduction Drying

As most paper is dried on steam heated cylinders, validation of *Drying Doctor* for cylinder dryer sections is essential. *Drying Doctor* has been used in four design projects at McGill to simulate numerous steam heated cylinder dryer sections, to design modifications for machine speed-ups, to suggest modifications to the process to increase papermachine profitability and to design rebuilds for more substantial changes yet. The rebuild designs have included major press section changes, changes in furnish, addition of a size press and conversion of a machine from uncoated to on-line coated paper with the addition of high intensity dryers. One such project provided the detailed dryer surveys for three newsprint machines, used here in section 4.2.3 to validate *Drying Doctor* for cylinder drying.

4.2.1 Simulator Demonstration for Base Case

As with impingement drying, a generic base case of cylinder drying is presented first to demonstrate the general process characteristics before treating validation. The base case variables are listed in Table 4-J.

Table 4-J: Cylinder Dryer Section Variables

Variable	S.I. Units	Alternate Units
Number of cylinders	50	
Cylinder diameter	1.52 m	5 ft
Condensing steam	400 kPag/152°C	58 psig/305°F
Cylinder shell thickness	25 mm	0.98 in
Draw length	1 m	3.28 ft
Dryer section sheet length	202.5 m	664.5 ft
Felt thickness	2 mm	0.08 in
Felting	Double (see Figure 3-6,p.27)	
Sheet wrap angle	230°	
Felt wrap angle	180°	
Ventilation air supply temp.	120°C	248°F
Ventilation air supply rate	14 m^3/min-m width	150 ft^3/min-ft width
Basis weight	127 g/m^2	26 lb/1000 ft^2
Sheet inlet moisture	1.4 kg/kg dry	41.67 % solids
Sheet exit moisture	0.08 kg/kg dry	92.6 % solids
Sheet inlet temperature	35°C	95°F
Dry sheet caliper	220 microns	
Fibre saturation point	0.75 kg/kg dry	57.1 % solids

The first variable examined is sheet wrap angle, varied between 180 and 270°. Drying rate was calculated according to the TAPPI standard method:

$$R_T = \frac{60}{1000} \cdot \frac{S_M * B * \Delta X}{N * \pi * D} \qquad \Delta X = X_O - X_F \text{, where:}$$

S_M:	machine speed	[m/min]
B:	basis weight (dry basis)	[g/m^2]
N:	number of cylinders	
D:	cylinder diameter	[m]
X_O:	moisture content entering (dry basis)	[kg/kg dry]
X_F:	moisture content leaving (dry basis)	[kg/kg dry]
ΔX:	water removed	[kg/kg dry]
R_T:	TAPPI drying rate (total cylinder area)	[kg water/m^{2}h]

The TAPPI standard drying rate is the ratio to total cylinder area of the total amount of drying in the 4 phases of drying on the cylinders and in the draws. By contrast, in modeling and simulating a cylinder dryer section each change in boundary conditions defines a new sub-section, and the area basis of drying rate is the actual one-sided area of the sheet. As the actual length of sheet in dryer sections is 10-25 % less than the total circumferential length of the cylinders, TAPPI average drying rates are therefore about 10-25 % below the true values based on actual sheet area in the dryer. In the following graphs the large squares indicate the default values.

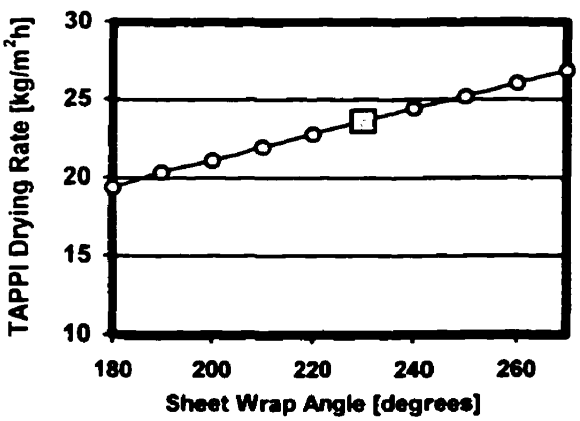

Figure 4-27: Effect of Sheet Wrap Angle on Drying Rate

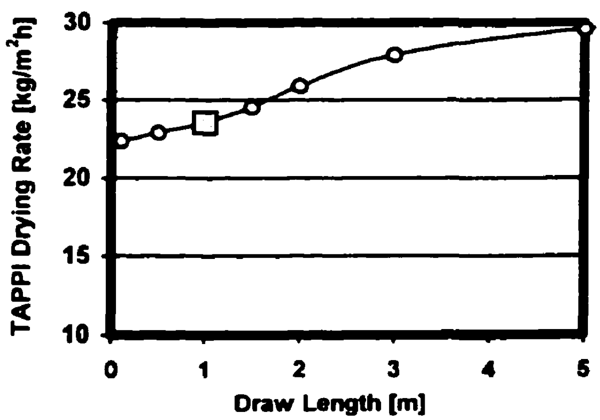

Figure 4-28: Effect of Draw Length on Drying Rate

As Figure 4-27 shows that each 10°C increase in sheet wrap angle increases drying rate by about 4-5 %, the advantage of using the largest practical sheet wrap angle is evident. The draw, phase IV in Nissan's (1955) use of phases, Figure 2-1, is the length of sheet between loss of contact from one cylinder to making contact with the next, and is where both sheet surfaces contact the dryer pocket air. By its definition, the standard TAPPI drying rate must increase as draw length increases, Figure 4-28, due to evaporative drying in the draws. As boundary conditions experienced by the sheet, the pocket air temperature and humidity conditions play a large role in determining drying in the draws. For the 9 cylinder dryer sections used in this thesis, the draws range from 0.7 to 1.6 m, with shorter draws for the weaker newsprint sheets and longer draws for stronger kraft linerboard. Longer draw lengths are limited by the associated increased sheet breaks and ventilation costs.

Steam condensate and evaporation rates by cylinder, useful in dryer analysis, are *Drying Doctor* outputs that are displayed in Figure 4-29 for this generic case. The condensate rate is very large in the cylinders at the wet end, where heat transfer is favored by the low sheet temperature. The low evaporation rate in the early cylinders increases as the sheet warms. Steam generally cascades from high pressure at the dry end to low at the wet end. In this demonstration case however, specifying steam pressure constant enables seeing a period of approximately constant rate drying develop over cylinders 8-12. The predicted ratio of condensate to water evaporated is 0.99.

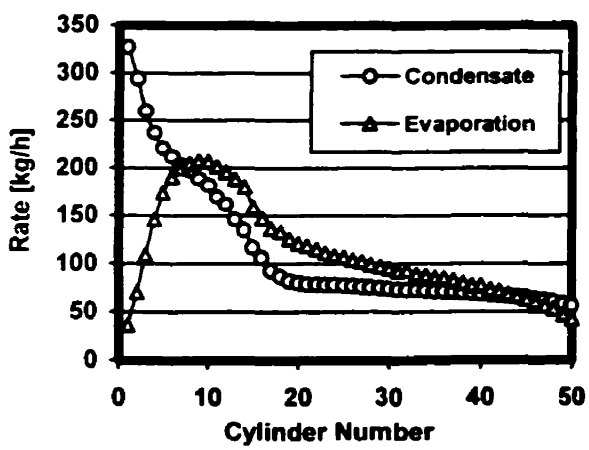

Figure 4-29: Steam Condensate and Evaporation Rates

As all the above simulations were with the default ventilation supply air conditions of *Drying Doctor*, the pocket ventilation effect is now demonstrated. Figure 4-30 shows the simulator form with three options. The first option accommodates pocket conditions when known for each cylinder. The second option invokes the default conditions of 60°C pocket air of humidity 0.15 kg/kg dry air, for which the wet bulb temperature is 59.8°C. For the third option, conditions of ventilation supply air to the pockets are specified, either as known values of supply air flowrate and temperature, or the default ventilation supply conditions of 14 m^3/min-m width of 120°C dry air, for which wet bulb temperature is 36.8°C. These choices of default conditions were based on numerous dryer surveys.

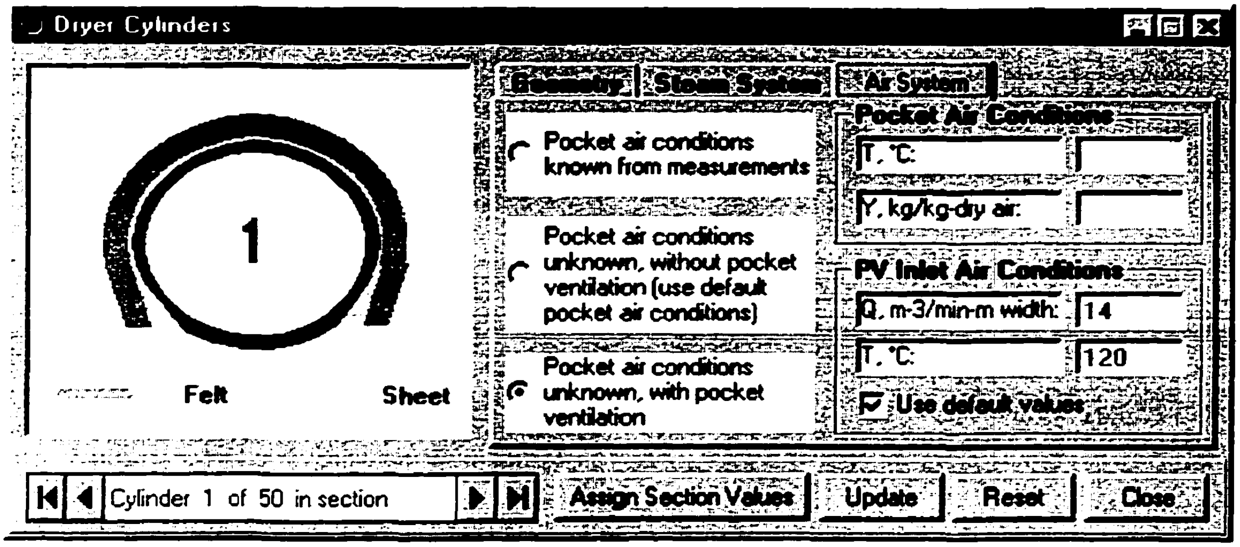

Figure 4-30: ***Drying Doctor*** **Pocket Air Form**

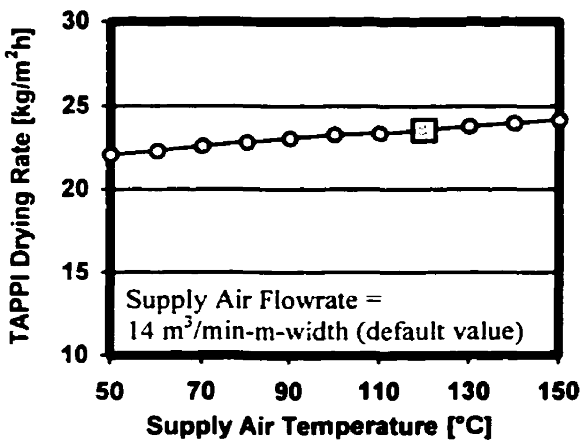

Figure 4-31: Effect of Ventilation Air Supply Temperature on Drying Rate

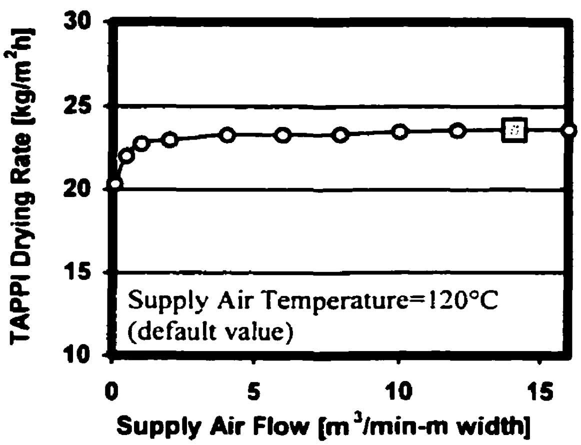

Figure 4-32: Effect of Ventilation Air Supply Flowrate on Drying Rate

For the effect of ventilation supply air conditions, Figures 4-31 & 32, the default conditions are shown as large squares. Air supply conditions affect pocket conditions, which in turn determine the boundary conditions in the draw phase. The initially large benefit with ventilation air supply flowrate, Figure 4-32, becomes asymptotic to about a 17 % increase in drying rate as the default supply air flowrate, 14 m^3/min-m width, is relatively large. At this flow the mean residence time (assuming plug flow) for the air in the pocket is only about 3 s. Figure 4-33 shows that the temperature in the pocket predicted by *Drying Doctor* begins dropping sharply below a supply air flowrate about half the default value. In practice, optimum pocket ventilation conditions involve an economic balance between the value of the higher drying rate and cost of the flowrate of low humidity, high temperature air.

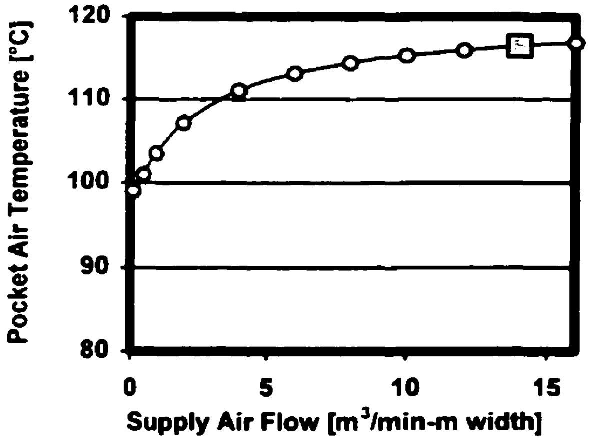

Figure 4-33: Calculated Pocket Air Temperature at Cylinder #10

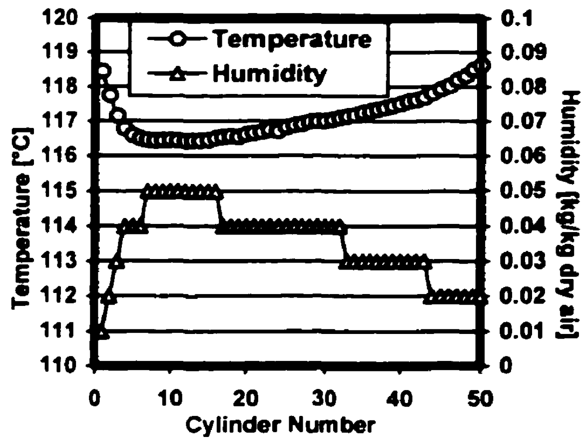

Figure 4-34: Calculated Pocket Air Temperature and Humidity for Default Supply Conditions

When ventilation air supply temperature and flowrate are entered in *Drying Doctor* the pocket air temperature and humidity are calculated, as shown in Figure 4-34 for the default conditions of 120°C supply air at 14 m^3/min-m width. As shown by Figure 4-29, evaporation rate is low in the cylinders near the wet end due to sheet warm-up, and low near the dry end due to sensible heat input to the sheet and to low drying rate near the end of the falling rate period. With a uniform ventilation supply flow to all pockets, this profile in evaporation rate is reflected exactly in the maximum in pocket air humidity and minimum in pocket temperature, Figure 4-34. The 0.01 pocket air humidity resolution in Figure 4-34 is due to rounding of the output only, the precise value being used for calculations in the simulator.

The option with specified pocket air temperature and humidity is used only when measurements are available. As there are default conditions for ventilated sections, the pocket air default values reflect an unventilated dryer section. For this reason the default pocket air temperature, 60°C, is much lower than that for ventilation supply air temperature, 120°C, for which the wet bulb temperatures are 59.8 and 36.8°C. As the use of a single default pocket air humidity for the entire section is seen from Figure 4-34 to be unrealistic, currently the profile is changed manually at the wet and dry ends. Use of too high a default humidity, 0.15 kg/kg dry air, leads to condensation on the cool sheet at the wet end as well as stopping drying at the dry end before the target exit moisture content. For unventilated machines Figures 4-35 and 4-36 illustrate the sensitivity of average drying rate to pocket air temperature and humidity when pocket temperature and humidity are specified directly.

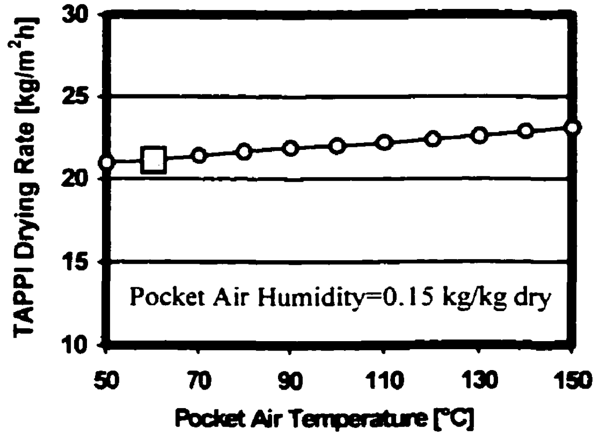

Figure 4-35: Effect on Drying Rate of Pocket Air Temperature in Unventilated Machine

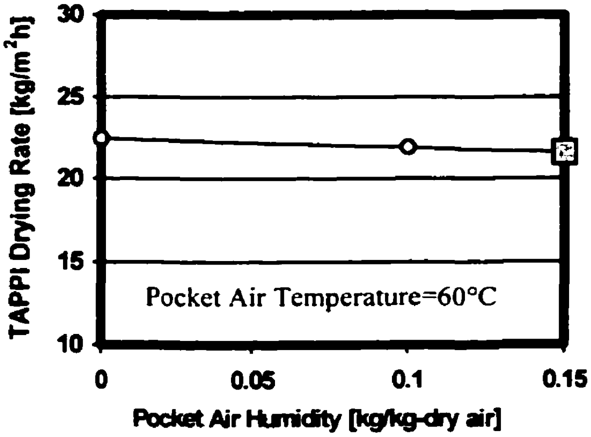

Figure 4-36: Effect on Drying Rate of Pocket Air Humidity in Unventilated Machine

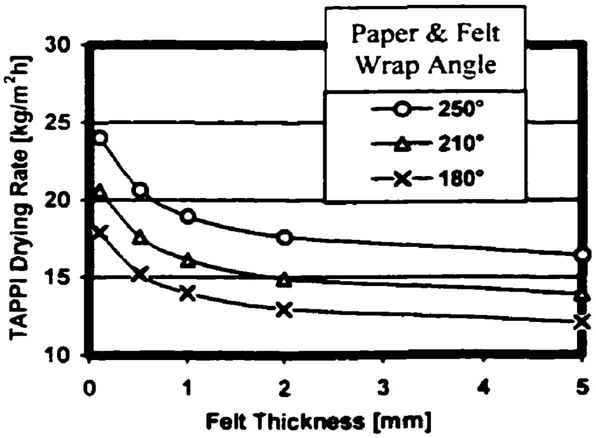

Figure 4-37: Effect on Drying Rate of Felt Parameters: Unirun Felting

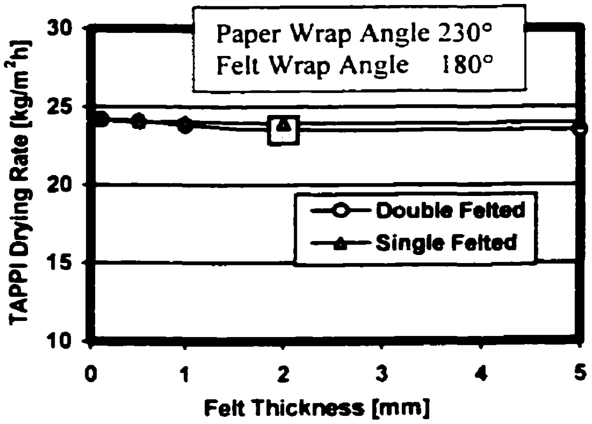

Figure 4-38: Effect on Drying Rate of Felt Thickness: Double Felting and Single Felting

The effects of felting, i.e. wrap angle and felt thickness, are now demonstrated. With the unirun sheet-cylinder configuration the sheet is separated from the lower tier cylinders by the felt. For felt thickness more than 2mm thick, Figure 4-37 shows that there is little further reduction in drying rate, i.e. a 2mm thick felt insulates the sheet almost completely from the lower cylinder. The Figure 4-38 simulations with double felting and top (or bottom) felting, rather similar configurations show that there is negligible drying rate disadvantage for the case of double felting where twice as many cylinders are felted. As expected, felt thickness has nearly no effect on drying rate for either double or single felting. Felt wrap angle was also found to have a much smaller effect on drying rate with double and single felting (under 2 mm thick) when compared to the variation found with unirun felting. For comparison, Figure 4-39 shows the significant effect of sheet wrap angle for unfelted machines. For the final parameter demonstrated, Figure 4-40 shows the sensitivity of drying rate to the resistance to heat transfer across the cylinder shell thickness. In the 9 cylinder dryer sections used in this thesis, felt thickness varied between 1.8 and 2.0 mm, while the cylinder shells were in the range of 25-30 mm.

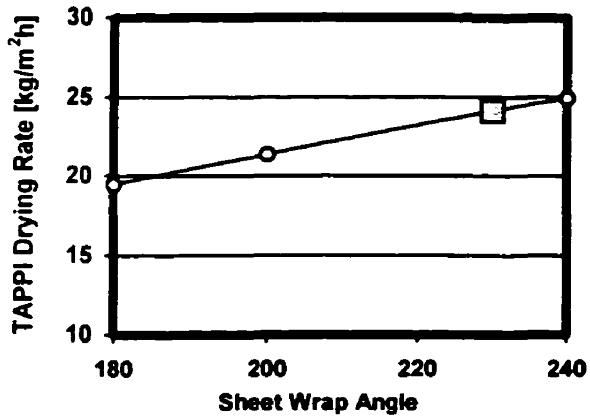

Figure 4-39: Effect of Sheet Wrap Angle on Drying Rate: No Felting

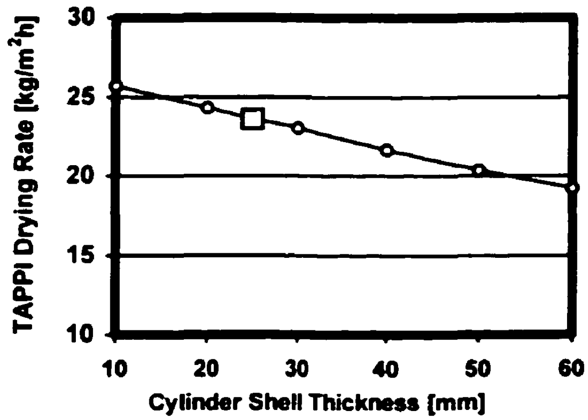

Figure 4-40: Effect of Shell Thickness on Drying Rate

4.2.2 Simulator Demonstration for Effect of Pocket Ventilation and Spoiler Bars

The Technical Association of the Pulp and Paper Industry publishes graphs of TAPPI standard average drying rate to enable comparison of dryer sections to industrially representative data. These curves account for steam condensing temperature, number and diameter of cylinders, machine speed, entering and leaving sheet moisture content, basis weight and paper grade. For paper grade, no further specifications (i.e. furnish) are given. With many of the variables included in Table 4-J left unaccounted and simplifications such as average steam pressure used, there is naturally substantial variability on the TAPPI graphs. Here, three grades are simulated, with and without pocket ventilation, and with variable cylinder steam pressure. The grades are differentiated by basis weight and fibre saturation point moisture content, 0.75, 0.75, and 0.8 kg/kg dry respectively, for newsprint, linerboard and corrugating medium. The TAPPI calculation simply averages the steam pressure of all cylinders. Following industrial practice, for the simulations the steam pressure was ramped up from a lower pressure at the wet end where the sheet is first heated to the wet bulb temperature, Figure 4-14. The TAPPI curves used are those from Reese (1988) and Robinson et al. (1989). All specifications are for the TAPPI 50 cylinder machine in Table 4-K unless otherwise noted. With pocket ventilation, our standard default ventilation air supply conditions (Table 4-J) are used. For simulations without ventilation, the default pocket air temperature of 60°C is used for all cylinders, with condensation on the sheet at the wet end and incomplete drying at the dry end prevented by the following air humidity profile:

Cylinders 1-10: 0.1 kg/kg dry air

Cylinders 11-40: 0.15 kg/kg dry air

Cylinders 41-50: 0.1 kg/kg dry air.

Table 4-K: Operating Conditions and Results: Newsprint

Condensing Steam		Average Condensing Steam Temperature [°C]	Machine Speed [m/min]	
Cyl. 1-10 [kPag/°C]	Cyl. 11-50 [kPag/°C]		Ventilated	No Ventilation
100/120°	100/120°	120	998	813
100/120°	162.5/129°	128	1101	876
100/120°	225/136°	134	1194	931
100/120°	287.5/143°	139	1243	985
100/120°	350/148°	144	1320	1039

For 48 g/m^2 newsprint entering and leaving at moisture contents of 1.4 and 0.08 kg/kg dry, the machine speed predictions are shown on Table 4-K and Figure 4-41. These *Drying Doctor* simulations show the strong drying rate sensitivity to the boundary conditions for heat and mass transfer at the free surface of the sheet. The full lines are the TAPPI standards for its designation of maximum, average and poor drying rates. The unventilated and ventilated sets of simulator predictions approximate the TAPPI average and maximum lines. The good agreement, including the slopes of the dashed lines through the simulator predictions, supports validation of the *Drying Doctor* simulator for newsprint.

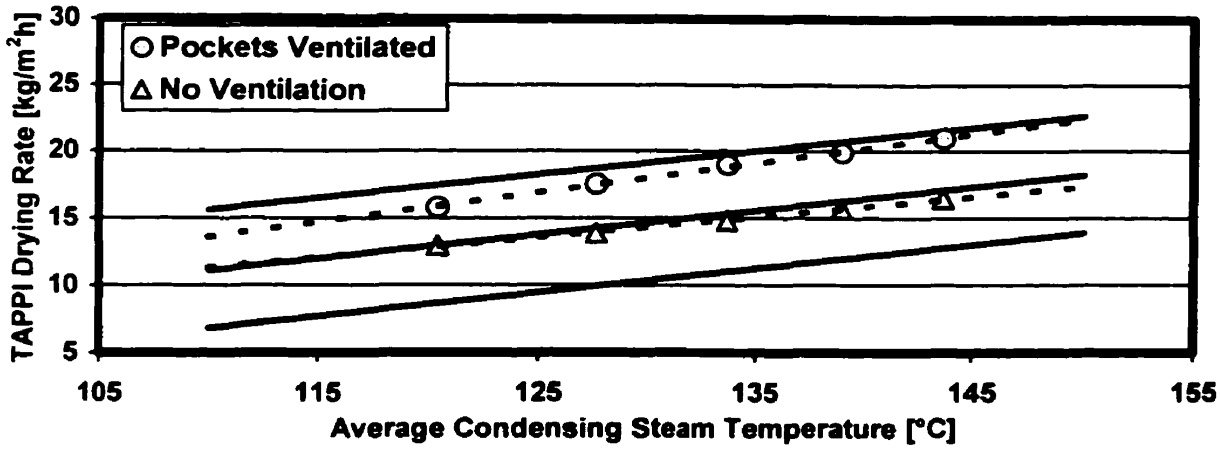

Figure 4-41: Dryer Simulator Predictions and TAPPI Drying Rate Curves, TIS 0404-15: Newsprint

Table 4-L and Figure 4-42 provide data for simulations for 127 g/m^2 linerboard with inlet and exit moisture content of 1.4 and 0.06 kg/kg dry. The steam conditions for the first 10 cylinders are as follows:

Cylinders 1-2: 100 kPag/120°C

Cylinders 3-4: 200 kPag/134°C

Cylinders 5-6: 300 kPag/144°C

Cylinders 7-8: 400 kPag/152°C

Cylinders 9-10: 500 kPag/159°C

Table 4-L: Operating Conditions and Results: Linerboard

Condensing Steam Cyl. 11-50 [kPag/°C]	Average Condensing Steam Temperature [°C]	Machine Speed [m/min]	
		Ventilated	No Ventilation
675/169°	165	610	558
800/175°	170	633	582
925/181°	175	659	604
1050/186°	180	675	624
1175/191°	184	691	642

Predicted drying rates, Figure 4-42, are slightly above the TAPPI average drying rate for non-ventilated machines by about 5-10 %, while ventilated dryers are again approximately the TAPPI maximum line. The slopes of the simulated rates approximate the TAPPI curves. As linerboard is much thicker than newsprint, the greater resistance to internal heat and mass transfer provides a more critical test yet of any drying simulation.

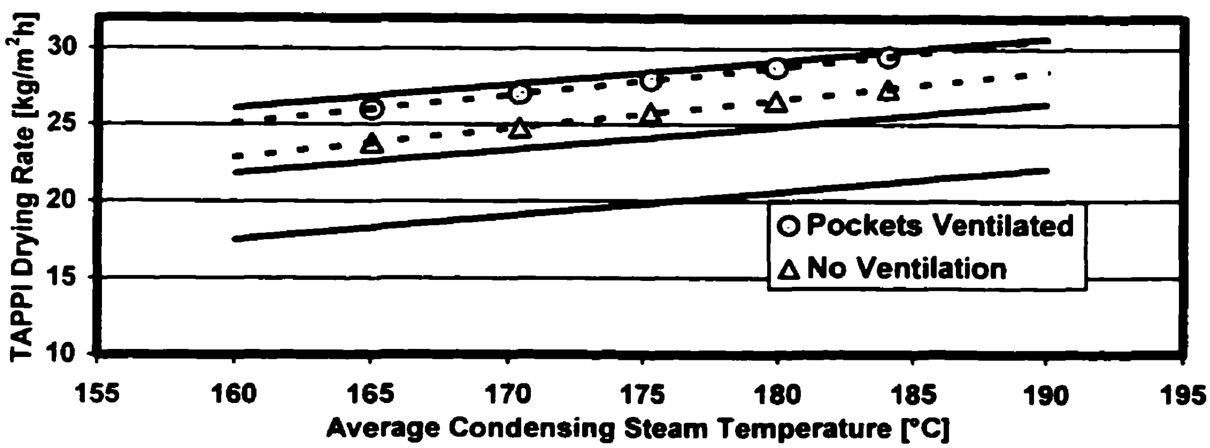

Figure 4-42: Dryer Simulator Predictions and TAPPI Drying Rate Curves, TIS 0404-09: Linerboard

The data for drying 337 g/m^2 corrugated medium from 1.4 to 0.07 kg/kg dry are shown in Table 4-M and Figure 4-43. The steam conditions in the first 10 cylinders is ramped as follows:

Cylinders 1-3: 100 kPag/120°C

Cylinders 4-6: 200 kPag/134°C

Cylinders 7-10: 300 kPag/144°C

Table 4-M: Operating Conditions and Results: Corrugated Medium

Condensing Steam Cyl. 11-50 [kPag/°C]	Average Condensing Steam Temperature [°C]	Machine Speed [m/min]	
		Ventilated	No Ventilation
322.5/146°	144	164	151
447.5/155°	152	181	169
572.5/163°	159	194	184
697.5/170°	165	207	197
822.5/176°	170	218	208
947.5/182°	175	228	218
1072.5/187°	180	238	227
1197.5/191°	184	247	235

The predicted average drying rate without pocket ventilation, Figure 4-43, is somewhat higher than the TAPPI average curve and the slope of both sets of predictions are slightly greater than the TAPPI curves. These simulations for the heaviest basis weight are with the greatest resistance to internal heat and mass transfer. Comparison of Figures 4-41, 4-42 and 4-43 shows that as the sheet gets thicker, the difference in drying rate from pocket ventilation is progressively reduced, which is logical as the role of internal transport increases. Thus the enhancement in drying rate through use of the simulator default pocket ventilation conditions is about 20 %, 10 % and 5 % for increasing basis weight of 48, 127 and 337 g/m^2.

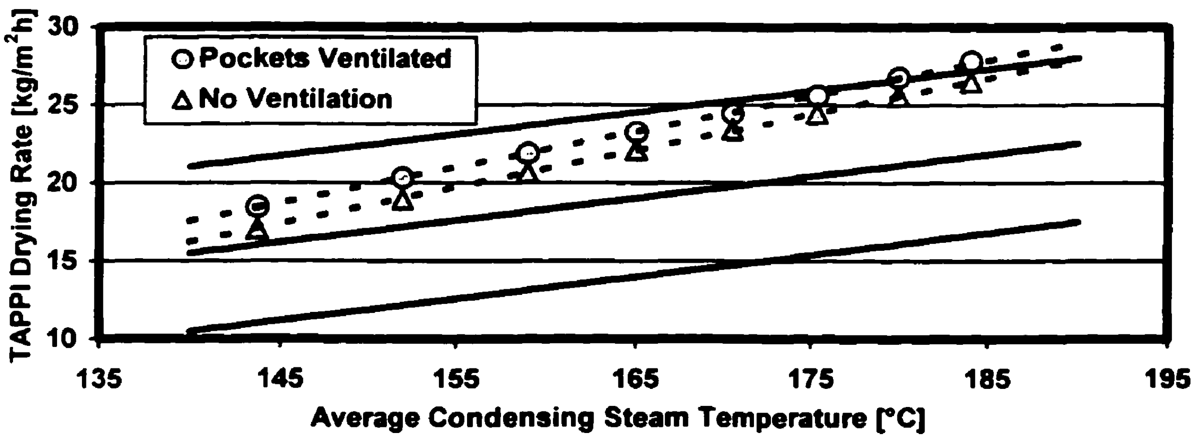

Figure 4-43: Dryer Simulator Predictions and TAPPI Drying Rate Curves, TIS 0404-08: Corrugating Medium

TAPPI has standard curves showing the effect of spoiler bars in dryer cylinders. Spoiler bars within the cylinder shell are turbulence promoters that disturb the condensate layer. They vary from full cylinder length to only 1-2 m long when used for moisture profiling. The dimensions of the bars vary with the desired condensate layer thickness and siphon clearance. Typically 18 to 30 bars are equally spaced in a cylinder. For a two-tier, double felted 50 cylinder newsprint dryer section running at 1070 m/min the TAPPI curves give the drying rate increase with spoiler bars.

As the specifications of the machine stated by TAPPI to have "effective pocket ventilation" are not given, the default ventilation air supply conditions of the *Drying Doctor* simulator were used. With machine speed fixed at 1070 m/min and for the steam pressures of Table 4-N, simulations without spoiler bars were run to determine the inlet moisture content required to give the specified outlet moisture content of 8 %. To find the increase in dryer capacity with spoiler bars, machine speed predictions were run with these inlet and exit moisture contents. The rate increase with spoiler bars is predicted well, Figure 4-44. The simulated rates both with and without spoiler bars are about 10 to 15 % higher than the TAPPI curves. As the simulator default conditions for ventilation air supply (14 m^3/min-m width of 120°C air) qualify more as highly effective pocket ventilation than the TAPPI reference to "effective" ventilation, the predicted results should indeed be slightly higher than the TAPPI curves. As it is centrifugal force which maintains the insulating layer of condensate around the cylinder interior, spoiler bar effectiveness depends on machine speed. The diverging curves with and without spoiler bars show a greater advantage at higher steam temperature where the condensation rate and consequently, machine speed are greater. The simulations correctly show this effect.

Table 4-N: Operating Conditions and Results: Spoiler Bars

Condensing Steam [kPag/°C]		Average Condensing Steam Temperature [°C]	Inlet Moisture Content [kg/kg dry]	Machine Speed With Spoiler Bars [m/min]
Cyl. 1-10	Cyl. 11-50			
50/112°	50/112°	111	1.155	1383
100/120°	100/120°	120	1.305	1413
150/128°	162.5/129°	127	1.437	1426
200/134°	225/136°	133	1.563	1425
250/139°	287.5/143°	139	1.664	1425

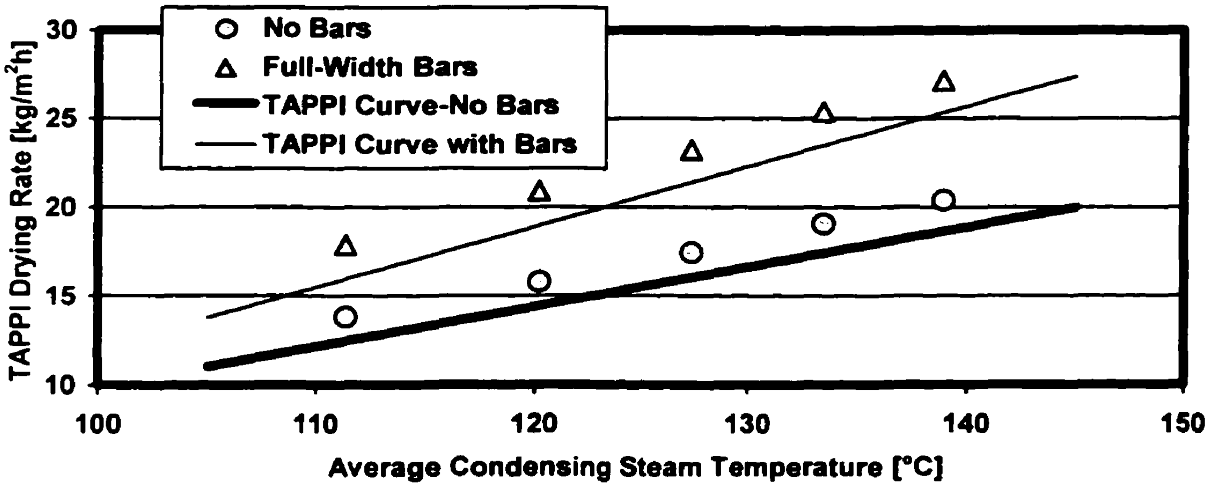

Figure 4-44: Dryer Simulator Predictions and TAPPI Drying Rate Curves, TIS 0404-15: Spoiler Bars with Newsprint

4.2.3 Simulator Validation for Newsprint

Fralic et al. (1997) of McGill University applied an incompletely developed version of *Drying Doctor* to three newsprint machines of Kruger Inc. at Bromptonville, Quebec.

The results of the numerous dryer surveys from that study are used here to validate the improved simulator now available.

(a) Kruger Bromptonville Paper Machine #1

Three validation tests with three dryer surveys were made for this 46 cylinder machine, specified in Table 4-O. The first 16 cylinders were felted on the top tier only, the remainder being double felted. Table 4-P lists the April 12, 1988 operating conditions from the Albany Inc. dryer survey with steam off in cylinders 8, 17, 19, 22, 23, 25, 26, 28, 34, 36, 38, 43 & 44. The measured dryer pocket air temperature and humidity for each cylinder were entered into the simulator. The validation simulation results, Table 4-Q, show drying is over-predicted somewhat, by 6.4 % relative to machine speed.

As the survey also contained measured cylinder surface and sheet temperatures, the simulation was calibrated to the measured final moisture of 8.4 % to compare these values. That some measured sheet temperatures are higher than the cylinder surface is evidence of measurement error. Cylinder surface temperatures from the uncalibrated simulation, Figure 4-45, are lower than those measured but the trends are similar, with lower temperature at cylinders without steam. The 13 cylinders without steam correspond to the gaps in the record of condensing steam temperature. Figure 4-46 shows the simulated sheet temperatures match those measured very well in the first half, but are somewhat low in the later cylinders. The simulation sheet average temperature shown is

Table 4-O: Design Specifications: Kruger Paper Machine #1

Variable	S.I. Units	Alternate Units
Cylinder diameter	1.22 m	4 ft
Cylinder shell thickness	23.6 mm	0.93 in
Machine width	3.65 m	12 ft
Draw length (varies)	0.87 - 1.4 m	2.85 - 4.59 ft
Dryer section sheet length	159 m	523 ft
Felt thickness	1.8 mm	0.07 in
Top felted felt wrap angle	180°	
Double felted felt wrap angle	180°	
Paper wrap angle	230°	
Spoiler bars	none	

Table 4-P: Operating Conditions: Kruger Paper Machine #1-April 1988

Variable	S.I. Units	Alternate Units
Machine speed	534 m/min	1751 fpm
Drying time	17.9 s	
Basis weight	48.8 g/m^2	10 lb/1000 ft^2
Inlet moisture content	1.27 kg/kg dry	44 % solids
Exit moisture content	0.084 kg/kg dry	92.25 % solids
Sheet inlet temperature	56°C	133°F
Fibre saturation point	0.7 kg/kg dry	58.8 % solids
Section 1	16 cylinders (1-16), top felting	
Condensing steam	84.8 kPag/118°C	12.3 psig/244°F
Section 2	14 cylinders (17-30), double felting	
Condensing steam	84.4 kPag/118°C	12.2 psig/244°F
Sections 3	16 cylinders (31-46), double felted	
Condensing steam	115.1 kPag/123°C	16.7 psig/253°F
Pocket conditions	varies-taken from dryer survey	

Table 4-Q: Uncalibrated Validation for Newsprint: Kruger Paper Machine #1-April 1988

Exit moisture content	
Validation simulation	6.8 % d.b.
Measured	8.4 % d.b.
Machine speed	
Validation simulation	568 m/min
Measured	534 m/min
Difference	6.4 %

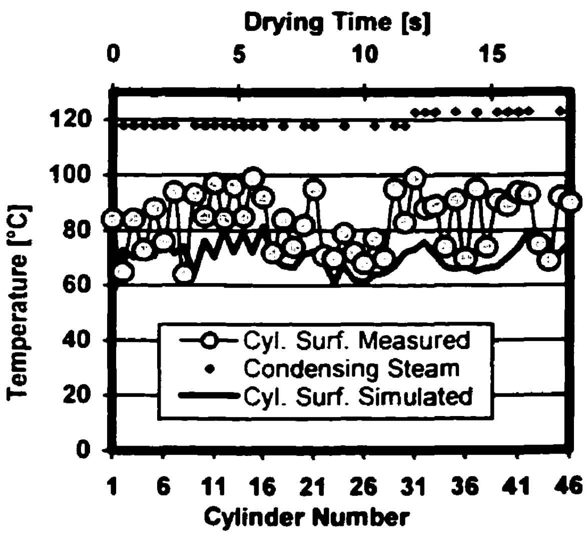

Figure 4-45: Cylinder Surface Temperature: Kruger Paper Machine #1-1988

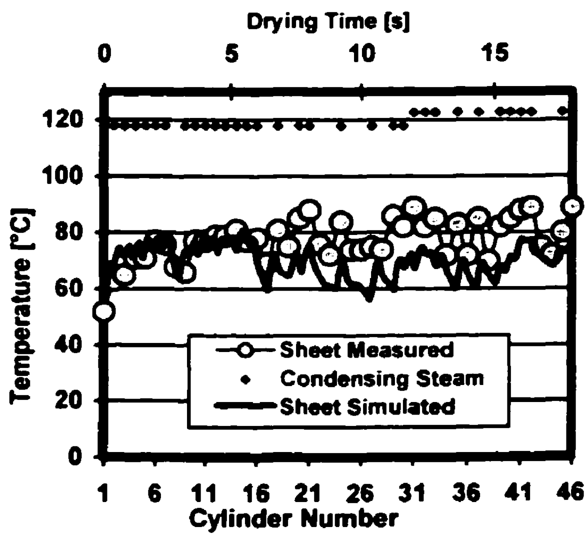

Figure 4-46: Sheet Temperature: Kruger Paper Machine #1-1988

taken as a weighted average of that at the two surfaces (w=1) and at the interior 1/3 points (w=0.5). The difference between the simulated sheet and cylinder temperatures is smaller than that measured, which suggests that the simulated contact resistance to heat transfer is too low, i.e. the contact heat transfer coefficient may be too high.

For the operating conditions of the two later dryer surveys, Table 4-R, the absolute validation results are given in Table 4-S. For both cases, validation tests in the exit moisture prediction mode give moisture contents within 1 %, while the machine speed predictions were just 2.3 % slow and 1.1 % fast. Such close agreement for the absolute predictions with the uncalibrated *Drying Doctor* simulator constitute highly satisfactory validation tests. Any use of the simulator would be after calibration for which, at the survey operating conditions, the small deviations noted above go to zero.

Table 4-R: Operating Conditions: Kruger Paper Machine #1-1994

Variable	**March 1994**		**November 1994**	
	S.I. Units	**Eng. Units**	**S.I. Units**	**Eng. Units**
Machine speed	556 m/min	1825 fpm	541 m/min	1776 fpm
Drying time	17.2 s		17.7 s	
Basis weight	48.8 g/m^2	10 lb/1000 ft^2	48.1 g/m^2	10 lb/1000ft
Inlet moisture content	1.53 kg/kg dry	60.5 % solids	1.63 kg/kg dry	62 % solids
Exit moisture content	0.078kg/kg dry	7.2 % solids	0.076 kg/kg dry	7 % solids
Inlet temperature	56°C	132.8 °F	56°C	132.8 °F
Fibre saturation point	0.7 kg/kg dry	58.8 % solids	0.7 kg/kg dry	58.8 %
Condensing steam	S.I. [kPag/°C] and Alternate [psig/°F]			
Section 1 (1-16)	13.8/104°	2/219°	69/115°	10/239°
Section 2 (17-30)	62.1/114°	9/237°	124/124°	18/255°
Sections 3 (31-46)	121/124°	18/255°	166/130°	24/265°
Cylinders turned off	20, 22, 40 & 44		21, 22, 40 & 44	
Pocket conditions	varies-taken from dryer surveys			

Table 4-S: Uncalibrated Validation for Newsprint: Kruger Paper Machine #1-March and Nov. 1994

	March 1994	November 1994
Exit moisture content		
Validation simulation	8.7 % d.b.	6.7 % d.b.
Measured	7.8 % d.b.	7.0 % d.b.
Machine speed		
Validation simulation	543 m/min	547 m/min
Measured	556 m/min	541 m/min
Difference	-2.3 %	+1.1 %

(b) Kruger Bromptonville Paper Machine #2

This 42 cylinder newsprint machine (design specifications given in Table 4-T) with unirun felting on the first 16 cylinders, double felting thereafter, had seven dryer surveys, six by Kruger and one by JWI Inc.. For the six internal surveys, the operating conditions are shown in Table 4-U. For this well ventilated dryer section, those pocket condition records available from surveys were used in the simulations. For the six validations shown in Table 4-V the difference between simulated and measured machine speed is small, averaging only 1.7 %.

Table 4-T: Design Specifications: Kruger Paper Machine #2

Variable	S.I. Units	Alternate Units
Cylinder diameter	1.52 m	5 ft
Cylinder shell thickness	28.6 mm	1.12 in
Machine width	4 m	13.1 ft
Draw length	0.75 m	2.5 ft
Dryer section sheet length	162 m	531 ft
Felt thickness	1.8 mm	0.07 in
Unirun felted wrap angles	210°	
Double felted felt wrap angle	180°	
Paper wrap angle	240°	
Fibre saturation point	0.7 kg/kg dry	58.8 % solids
Spoiler bars	none	

Table 4-U: Operating Conditions: Kruger Paper Machine #2

Dryer Survey	Condensing Steam [kPag/°C]			Machine Speed	Drying Time	Basis Weight	Inlet Moisture Content	Exit Moisture Content
	Cyl. 1-5	Cyl. 6-32	Cyl. 33-42	m/min	s	g/m^2	kg/kg dry	kg/kg dry
June 1992	90/ 119°	350/ 148°	350/ 148°	849	11.43	47.6	1.61	0.073
May 1995	82/ 118°	270/ 141°	275/ 141°	837	11.59	48.08	1.56	0.081
June 1995	84/ 118°	255/ 139°	255/ 139°	839	11.57	49.11	1.56	0.083
August 1 1995	78/ 117°	228/ 137°	282/ 142°	827	11.74	48.25	1.62	0.08
August 9 1995	81/ 117°	235/ 137°	260/ 140°	819	11.85	47.86	1.7	0.079
January 1996	90/ 119°	250/ 139°	250/ 139°	817	11.87	48.9	1.54	0.085

Table 4-V: Uncalibrated Validation for Newsprint: Kruger Paper Machine #2

	June 1992	May 1995	June 1995	August 1 1995	August 9 1995	January 1996
Exit moisture content						
Validation simulation	7.8 %	7.8 %	9.6 %	10.4 %	11.4 %	8.9 %
Measured	7.3 %	8.1 %	8.3 %	8 %	7.9 %	8.5 %
Machine speed [m/min]						
Validation simulation	860	844	825	805	791	811
Measured	849	837	839	827	819	817
Difference	+1.3 %	+0.8 %	-1.6 %	-2.6 %	-3.3 %	-0.8 %

Table 4-W: Validation for Newsprint: Kruger Paper Machine #2-August 22, 1995

	August 22 1995
Exit moisture content	
Validation simulation	8.7 % d.b.
Measured	9.2 % d.b.
Machine speed	
Validation simulation	865 m/min
Measured	861 m/min
Difference	+0.4 %

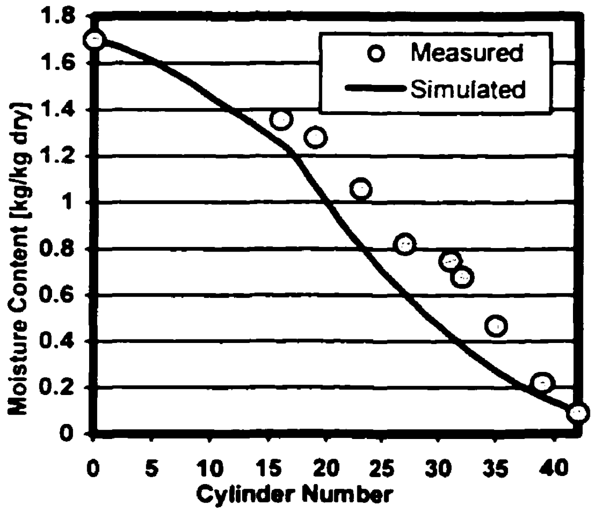

Figure 4-47: Sheet Moisture Content: Kruger Paper Machine #2-August 22,1995

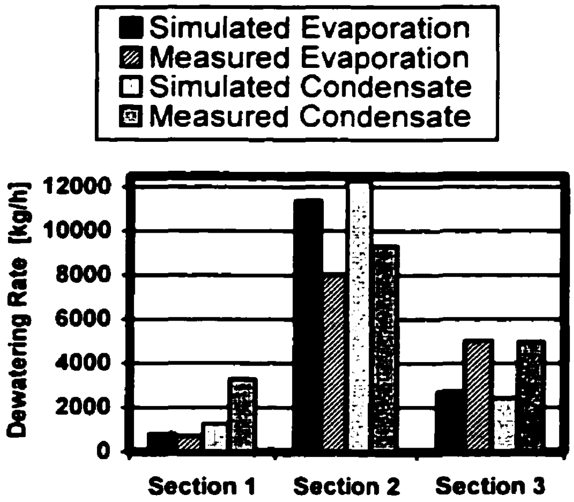

Figure 4-48: Condensate and Evaporation Rate: Kruger Paper Machine #2-August 22,1995

The August 22, 1995 survey by JWI Inc. includes measurements of sheet moisture content at several points in the three dryer sections operated at steam pressures of 90, 255 and 275 kPag. The uncalibrated simulation results, Table 4-W, constitute excellent validation. From the moisture contents on Figure 4-47 the presence of the moisture control device after cylinder 31 is reflected in the sharp change of slope of measured moisture content. The predictions are seen to err on the side of over-drying until a sheet moisture content of 0.75 kg/kg dry, compensated by under-drying thereafter. The survey also provided condensate flow rates for each pressure section and the evaporation rate is calculated from the moisture contents measured. The Figure 4-48 comparison between simulated and measured evaporation and condensate rates shows the same trend, first over-drying, then under-drying. A discrepancy is found in the first section where the predicted condensate flow is much lower than that measured although the moisture contents match well. As results that follow for unirun sections will show, condensate flow is normally over-predicted by the simulator for this felting configuration, giving reason to suspect some measurement error.

(c) Kruger Bromptonville Paper Machine #3

For the final newsprint machine five standard dryer surveys were available as well as a special one in which, exceptionally, the condensate rate from most cylinders was measured. This 46 cylinder machine has unirun felting on the first 29 cylinders, double felting on the remainder. Tables 4-X and 4-Y give the design specifications and operating conditions. Section 1 is not detailed here as the pressure varies from cylinder to cylinder, averaging about 70 kPag, but individual cylinder pressures were used in simulations. Pocket conditions, again measured for most cylinders, were used in simulations.

The Table 4-Z simulation results show on average slight under-drying (a mean of -0.6 %) with the absolute value of machine speed prediction being 3.8 % of actual.

Table 4-X: Design Specifications: Kruger Paper Machine #3

Variable	S.I. Units	Alternate Units
Cylinder diameter	1.52 m	5 ft
Cylinder shell thickness	25.4 mm	1 in
Machine width	3.9 m	12.8 ft
Draw length	0.7 m	2.3 ft
Dryer section sheet length	186 m	610 ft
Felt thickness	1.8 mm	0.07 in
Unirun felted wrap angles	255°	
Double felted felt wrap angle	180°	
Paper wrap angle	250°	
Fibre saturation point	0.7 kg/kg dry	58.8 % solids
Spoiler bars-profiling	16, 18, 20, 22, 24, 26, 28, 29, 31, 33, 35, 37	
Spoiler bars-full-width	39, 41, 43	

Table 4-Y: Operating Conditions: Kruger Paper Machine #3

Dryer Survey	Condensing Steam [kPag/°C]			Machine Speed	Drying Time	Basis Weight	Inlet Moisture Content	Exit Moisture Content
	Sect.2	Sect.3	Sect.4	m/min	s	g/m^2	kg/kg dry	kg/kg dry
June 1992	270/ 141°	360/ 149°	320/ 145°	1080	10.33	48.2	1.33	0.085
Feb. 1995	230/ 137°	350/ 148°	390/ 151°	1160	9.62	48.2	1.173	0.105
April 1995	170/ 130°	260/ 140°	292/ 143°	1130	9.87	49	1.15	0.112
August 1995	200/ 134°	300/ 144°	251/ 139°	1130	9.87	49.2	1.2	0.099
Nov. 1995	190/ 133°	320/ 145°	251/ 139°	1133	9.85	48.4	1.227	0.10

Table 4-Z: Uncalibrated Validation for Newsprint: Kruger Paper Machine #3

	June 1992	February 1995	April 1995	August 1995	November 1995
Exit moisture content					
Validation simulation	10.8 %	8.4 %	10.7 %	11.6 %	11 %
Measured	8.5 %	10.5 %	11.2 %	9.9 %	10 %
Machine speed [m/min]					
Validation simulation	1026	1237	1145	1095	1099
Measured	1080	1160	1130	1130	1133
Difference	-5.0 %	+6.6 %	+1.3 %	-3.1 %	-3.0 %

The data for steam pressure, condensate and water removal rates, Figures 4-49 to 4-51, come from a detailed March 1995 study which also included pocket humidity and sheet and cylinder temperatures for most cylinders. At that time there was no steam to cylinders 1, 3, 5, 7, 9, 11, 13, 15, 19, 30, 32 and 34.

For the unirun cylinders, the predictions of condensate rate are high for cylinders contacting the sheet but accurate for those contacting the felt. The reason for the high predictions may be that the felt is heated when in contact with the lower cylinder, this heated felt in turn heating the sheet. This heating of the sheet by the felt in the unirun configuration is not currently accounted for in *Drying Doctor*, which leads to overprediction of the amount of steam condensing. This trend is seen throughout the unirun section. In the double felted section the predictions are low and show a step pattern between the top and bottom cylinders due to spoiler bars installed only on the bottom cylinders. As the report is not clear on how condensate rate measurements were made, some values may not have been measured directly for each cylinder. As spoiler bars are used to increase the condensation heat transfer, more condensate from such cylinders would be expected.

The simulated evaporation rate, Figure 4-51, gives a predicted ratio of condensate to evaporation rate of 1.11, slightly lower than the measured 1.2. The largest effect on evaporation rate comes from cylinders without steam, seen to lower the rate in the cylinder following. Thus the cylinders following turned off cylinders 30, 32 and 34, would otherwise be expected to have much higher evaporation rates, ca. 400 kg/h. The decrease in evaporation rate in the last 10 cylinders is steeper than the drop in condensate flow, Figure 4-50, due to the sensible heat for raising sheet temperature, Figure 4-53.

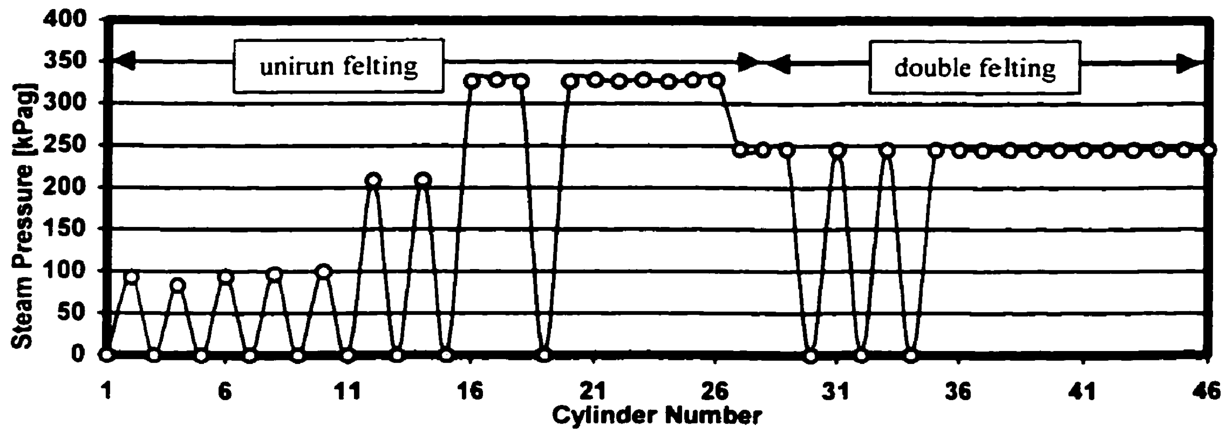

Figure 4-49: Steam Pressure: Kruger Paper Machine #3-March 1995

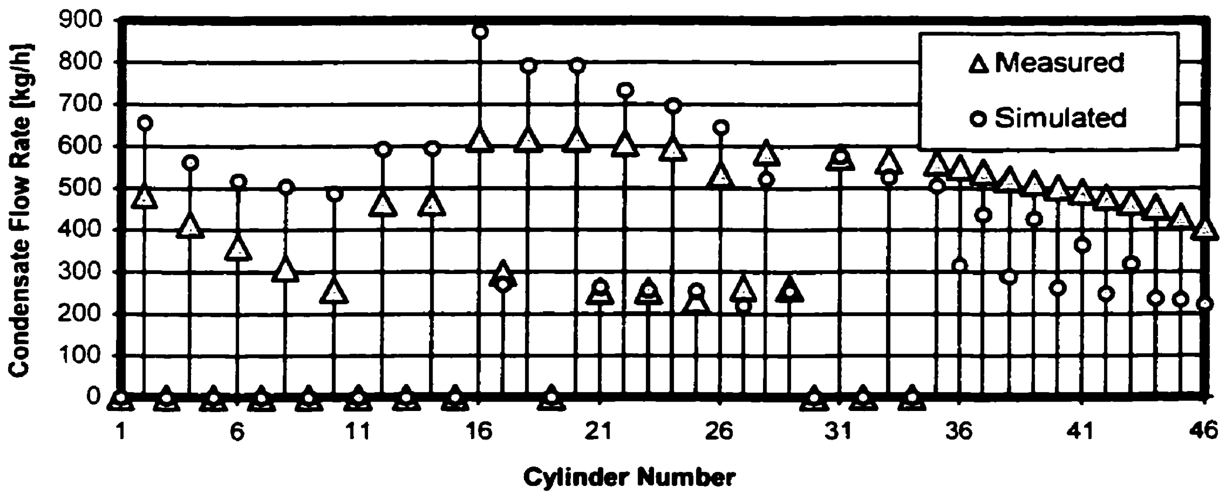

Figure 4-50: Condensate Flow Rate: Kruger Paper Machine #3-March 1995

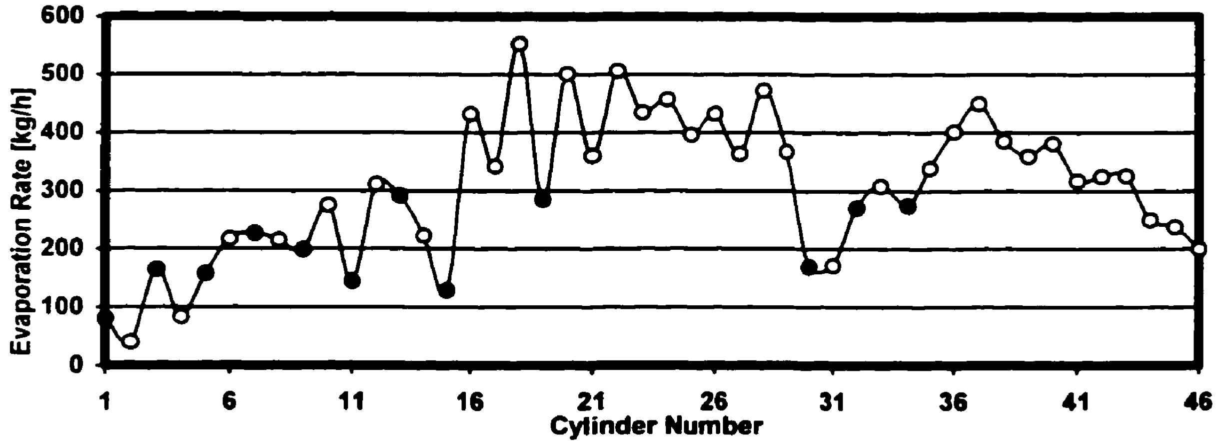

Figure 4-51: Evaporation Rate: Kruger Paper Machine #3-March 1995

Comparison of simulated and measured cylinder surface and sheet temperatures, Figures 4-52 and 53, again shows that predicted values are somewhat low. This difference is greatest at the beginning of the dryer in the unirun felting configuration with no steam in some alternating cylinders. The 12 cylinders without steam correspond to the gaps in the record of condensing steam temperature. As shown earlier, the current version of this simulator predicts temperatures lower than actual on cylinders following those without steam, as seen with the large number of unheated cylinders (9) near the wet end.

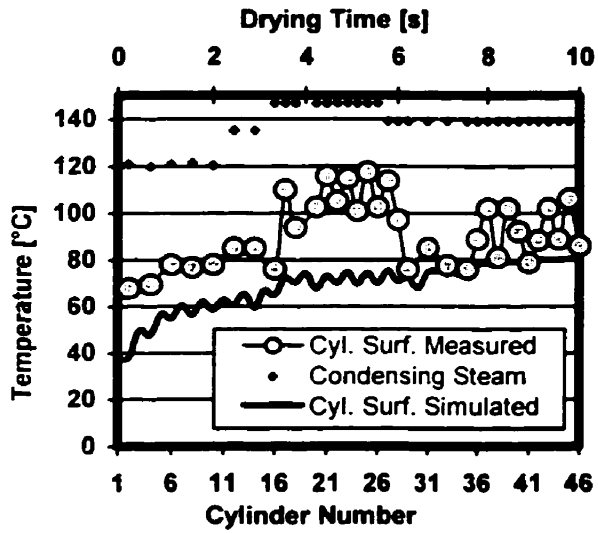

Figure 4-52: Cylinder Surface Temperature: Kruger Paper Machine #3-March 1995

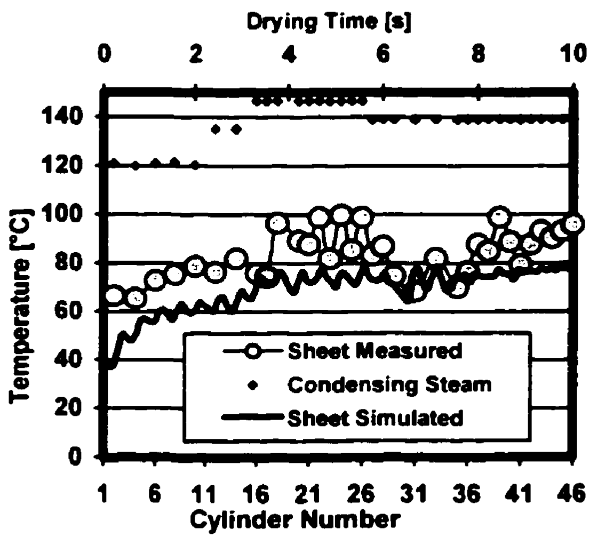

Figure 4-53: Sheet Temperature: Kruger Paper Machine #3-March 1995

4.3 Multiple Technique Drying

To date multiple technique drying is practiced only for drying coated paper, where variations of the sequence IR drying - air impingement flotation drying - cylinder drying are frequently found, and for tissue and toweling where the sequence through air drying-impingement air (Yankee) drying is well established with some paper companies. With these limited exceptions for specialty grades, single technique drying over steam heated cylinders is universal paper industry practice for major grades. However the concept of multiple technique drying is now gaining industrial interest. The high capital costs of paper mill dryers limits the rate of change of this technology, but the concept of multiple technique drying for printing and heavier grades has recently come independently from university researchers, Bond et al. (1996) and all major dryer manufacturers, first from Valmet with Kuhasalo (1995). However, just a few exceptional machines have incorporated Yankee dryers or IR dryers into cylinder dryer sections. Schematics and dryer surveys for two such non-traditional machines incorporating Yankee dryers into cylinder dryers, constituting pioneering multiple technique dryers for uncoated printing and heavier papers, enable validation of the *Drying Doctor* simulator for this trend of the future.

4.3.1 Simulation Validation for Linerboard

(a) Paper Machine of Canadian International Paper

For papermachine #4 at the then Canadian International Paper Co. mill (now Avenor Inc.) in La Tuque, Quebec, a 1961 dryer survey by Ross Air Systems Inc., supplier of the air impingement hoods, provides the basis for a validation test. The machine layout of this multiple technique dryer, Figure 4-54, consisted of 43 double-tier dryer cylinders, 10 with air impingement dryers, sometimes described in industry as "high- velocity hoods". The sectioned air impingement dryers (SIAD units) on the top tier were partitioned in the machine cross-direction (CD) dimension for use in minimizing CD moisture profile variability. Three unsectioned air impingement dryer (IAD) units were installed on five lower tier cylinders. Specifications and operating conditions are given in Table 4-AA. The sheet top side contacts the surface of all lower tier cylinders, the sheet bottom side contacting all upper tier cylinders.

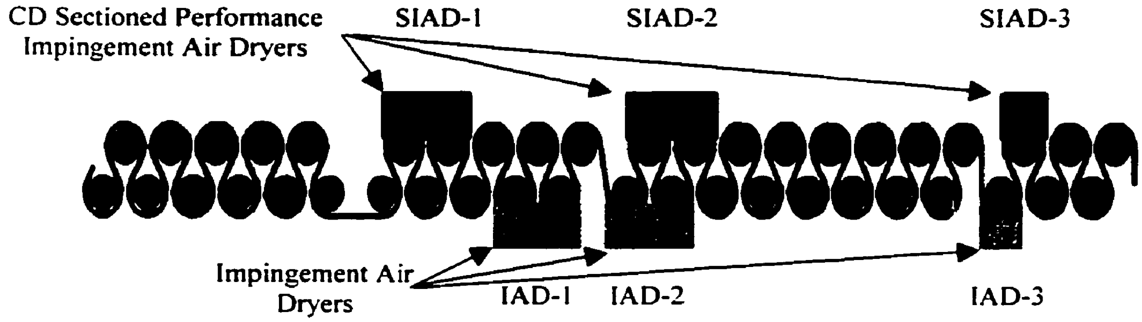

Figure 4-54: Multiple Technique Dryer: Canadian International Paper Machine

Table 4-AA: Design Specifications and Operating Conditions: Canadian International Paper Machine

Variable		**S.I. Units**	**Alternate Units**
Cylinder diameter		1.52 m	5 ft
Cylinder shell thickness		**40 mm**	**1.6 in**
Machine width		4.1 m	13.4 ft
Draw length		1 m	3.3 ft
Dryer section sheet length		156 m	512 ft
Felt thickness		**3 mm**	**0.12 in**
Felted and paper wrap angle		**180°**	
Condensing steam	Section 1 (Cyl. 1-11)	276 kPag/142°C	40 psig/287°F
	Section 2 (Cyl. 12-21)	290 kPag/143°C	42 psig/289°F
	Section 3 (Cyl. 22-37)	228 kPag/137°C	33 psig/278°F
	Section 4 (Cyl. 38-43)	386 kPag/151°C	56 psig/304°F
Machine speed		274 m/min	90 fpm
Drying time		34.2 s	
Basis weight		127 g/m^2	26 lb/100 ft^2
Inlet moisture content		1.941 kg/kg dry	34 % solids
Final moisture content		0.053 kg/kg dry	95 % solids
Fibre saturation point		0.8 kg/kg dry	55.5 % solids
Nozzle exit jet velocity		69 m/s	13,600 fpm
Nozzle exit temperature	SIAD-1	288°C	550°F
	SIAD-2	278°C	533°F
	SIAD-3	238°C	461°F
	IAD-1	263°C	505°F
	IAD-2	257°C	495°C
	IAD-3	238°C	461°F
Nozzle diameter		9 mm	0.35 in
Nozzle to web distance		20 mm	0.8 in
Nozzle spacing/nozzle diameter		2.2	
Nozzle plate open area ratio		1.5%	
Nozzle pattern		equilateral triangle	

The felting arrangement, mentioned briefly but not described in the report, was assumed as a 180° wrap angle for both paper and felt, with all cylinders double felted.

The cylinder shell thickness, not specified, was assumed to be relatively thick, 40 mm, to compensate for subsequent technology advances. With this choice, which gave good agreement between recorded and predicted results, an uncalibrated validation simulation could not be done.

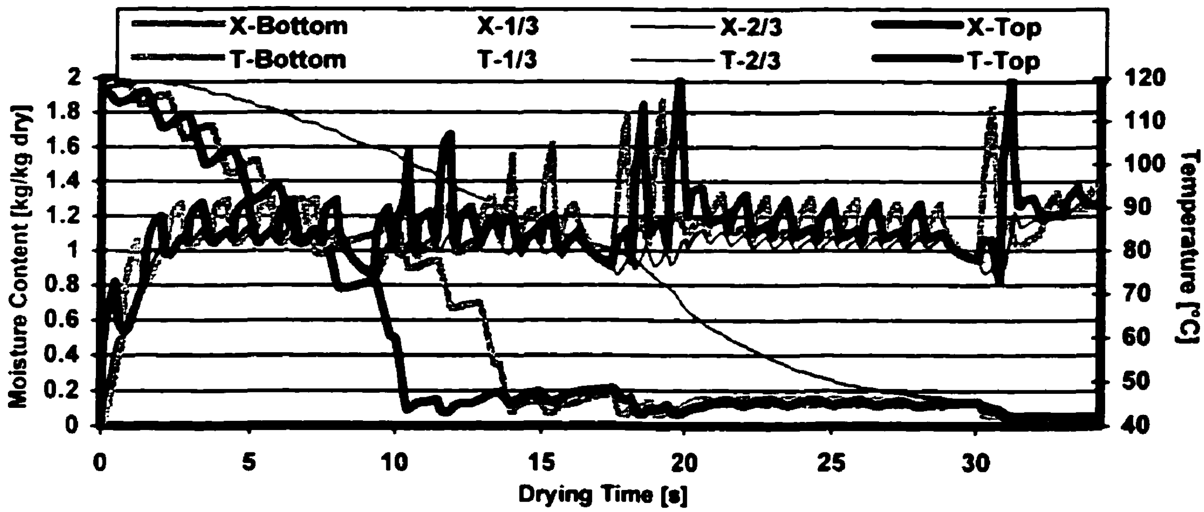

Figure 4-55: Local Moisture and Temperature Profiles: Canadian International Paper Machine

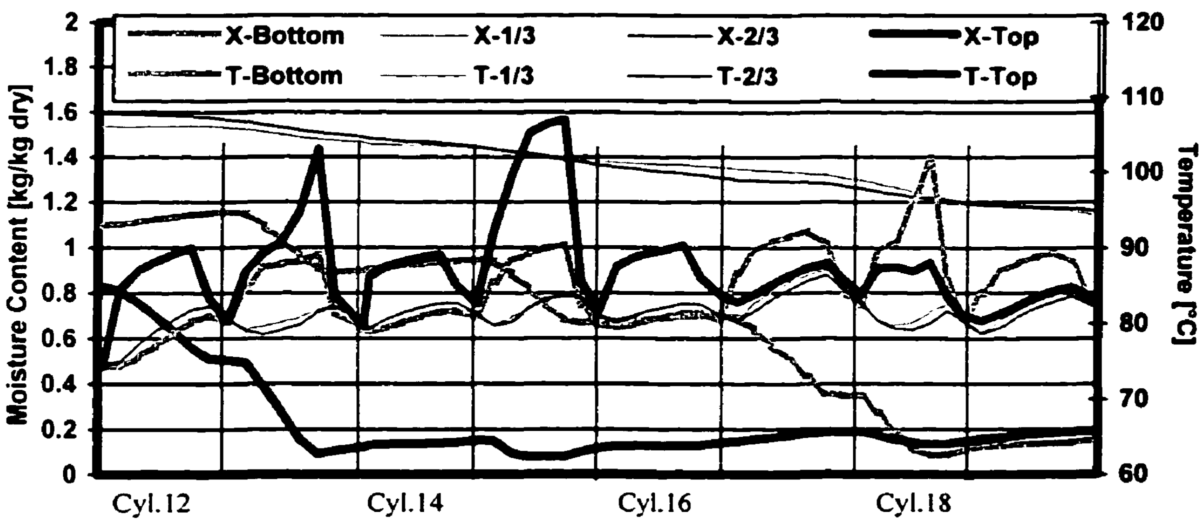

Figure 4-56: Local Moisture and Temperature Profiles: Canadian International Paper Machine-Cylinders 12-19

The necessity of a microscale model for a dryer simulator is demonstrated here by the very large moisture gradients across the sheet, at times over 1.3 kg/kg dry just between the sheet surface and one-third points, as shown by the z-direction moisture profile history, Figures 4-55 and 4-56, the latter an enlargement for cylinders 12-19. To minimize drying asymmetry, the side of the sheet contacting the air jets alternates with successive impingement dryer units. The difference in moisture content from the sheet top to bottom after cylinder 12, Figure 4-56, shows that as lower tier cylinders 11 and 12 both contact the sheet top, Figure 4-54, this surface is considerably drier prior to any air impingement drying. At cylinder 13, the top side of the sheet is the first to be contacted by the impingement air, and the moisture content is thereby reduced sharply relative to the bottom side in contact with the cylinder. The impinging jets are seen to dry the top and bottom of the sheet at cylinders 13 and 18 to 0.1 kg/kg dry, but do not reduce moisture content much further at those surfaces at the subsequent cylinders, 15 and 20. Thus once this much moisture content gradient has been created, the driving force for liquid and vapor transport from the sheet interior to its surfaces is sufficient to maintain this level of moisture content at the surfaces.

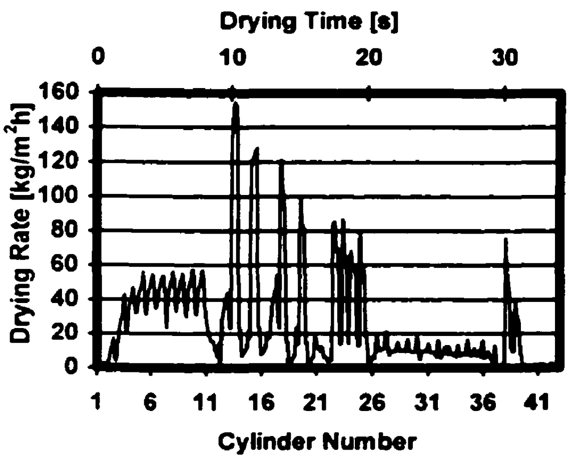

Figure 4-57: Drying Rate: Canadian International Paper Machine-Normal Operation

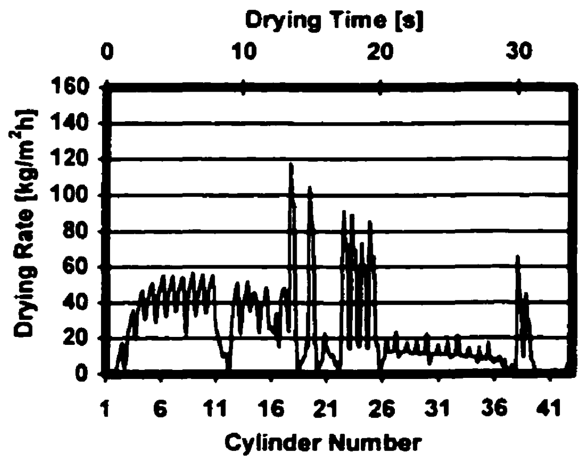

Figure 4-58: Drying Rate: Canadian International Paper Machine With SIAD-1 Impinging Jets Off

With all impingement dryers operating, the dryer survey reported that cylinders 13 and 15, the first with air impingement hoods, provided 10 % of the total heat transfer by the 43 cylinder multiple technique dryer. To quantify the effect of air impingement drying by the first SIAD unit, during the dryer survey the impinging jets on cylinders 13 and 15 were shut off but not the steam. To compensate, the second and third sections (cylinders 12-37) required a steam pressure increase by 103 kPa to reach the same final moisture content at the same machine speed. For this modified operation, a *Drying Doctor* test simulation gave excellent validation, i.e. gave final moisture content 5.1 %, close to the 5.3 % measured, and machine speed 276 m/min, only 0.6 % higher than the measured 274 m/min. In the predicted drying rates for these two cases, the two large spikes, Figure 4-57, from SIAD-1 at cylinders 13 and 15 are absent from Figure 4-58 for the case without this impingement dryer. The drying rates in the second and third dryer sections, from 10-25 seconds, were slightly higher due to the increased steam pressure used to achieve the same exit moisture content. Not only did this non-standard papermachine provide a rare opportunity to test the simulation with data from multiple technique drying of a heavy grade of paper, but the variation in operating conditions provided further opportunities for investigating simulator reliability. These tests establish that *Drying Doctor* simulation of multiple technique drying of linerboard predicts correctly the interaction between the cylinder and air impingement drying.

(b) Paper Machine of Tembec Inc.

The Temboard unit of Tembec Inc., Temiscaming, Quebec produces a high performance grade of linerboard used for printed products. Exceptionally, the dryer section of this papermachine includes a Yankee dryer between cylinders 41 and 42, thereby making it a multiple technique dryer. Two dryer surveys conducted over a sixteen-month period give moisture content and temperature measurements throughout the machine. Figure 4-59, Tables 4-BB and 4-CC give the machine layout, design specifications and operating conditions. The bold values in Table 4-BB were assumed, being not available in the surveys. There are five cylinder dryer sections with the Yankee cylinder between the fourth and fifth. The first two sections (shown in green) are of unirun configuration, the remainder (in red) being double felted. The sheet top side contacts the surface of all lower tier cylinders and the Yankee cylinder, while the sheet bottom is the contact side for all upper tier cylinders and is the air impingement side of the Yankee dryer.

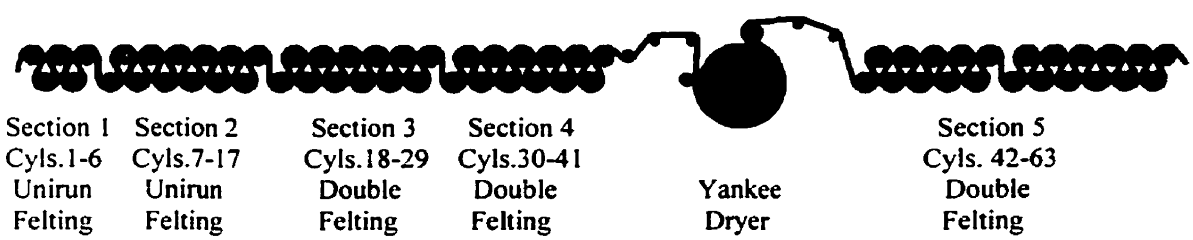

Figure 4-59: Multiple Technique Dryer: Temboard Paper Machine

Table 4-BB: Design Specifications: Temboard Paper Machine

Variable	S.I. Units	Alternate Units
Regular cylinders diameter	1.524 m	5 ft
Yankee cylinder diameter	6.1 m	20 ft
Cylinder shell thickness (both)	**25 mm**	**1 in**
Machine width	4.572 m	15 ft
Draw length (average)	1.2 m	3.9 ft
Dryer section sheet length	306 m	1003 ft
Felt thickness	**2.0 mm**	**0.08 in**
Unirun felt & paper wrap angle	250°	
Double felted paper/felt wrap angle	230°/182°	
Paper wrap angle before and after hood	15°	
Paper wrap angle in Yankee hood	250°	
Nozzle exit temperature	110 °C	230 °F
Nozzle exit jet velocity	**100 m/s**	**19,700 fpm**
Nozzle diameter	**7 mm**	**0.28 in**
Nozzle to web spacing	**20 mm**	**0.79 in**
Nozzle spacing/nozzle diameter	**2.9**	
Nozzle pattern	**equilateral triangle**	
Nozzle plate open area ratio	**1.5%**	

Table 4-CC: Operating Conditions: Temboard Paper Machine

Variable	June 1996*		October 1997	
	S.I. Units	Alternate	S.I. Units	Alternate
Machine speed	344 m/min	1130 fpm	436 m/min	1430 fpm
Drying time	53.3 s		42.1 s	
Basis weight	202 g/m^2	41 $lb/1000ft^2$	152 g/m^2	31 $lb/1000ft^2$
Inlet moisture content	1.27 kg/kg dry	44 % solids	1.41 kg/kg dry	41.5 % solids
Exit moisture content	0.07 kg/kg dry	93.4 % solids	0.073 kg/kg dry	93.2 % solids
Inlet sheet temperature	40°C	104°F	40°C	104°F
Fibre saturation point	0.75 kg/kg dry	57.1 % solids	0.75 kg/kg dry	57.1 % solids
Condensing steam	S.I. Units [kPag/°C] Alternate [psig/°F]			
Section 1	6 cylinders (1-6), unirun felting			
Cylinder #1	-5/99°	-0.7/209°	25/106°	3.6/223°
Cylinder #2	0/100°	0/212°	50/112°	7.3/233°
Cylinders #3-6	5/101°	0.7/214°	70/115°	10.2/240°
Section 2	11 cylinders (7-17), unirun felting			
Upper cylinders	100/120°	14.5/249°	100/120°	14.5/249°
Bottom cylinders	40/110°	5.8/229°	300/144°	43.5/291°
Sections 3 & 4	24 cylinders (18-41), double felted			
Upper cylinders	140/126°	20.3/259°	124/124°	18/255°
Bottom cylinders	140/126°	20.3/259°	180/131°	26.1/268°
Yankee Cylinder	233/137°	33.8/279°	300/144°	43.5/291°
Section 5	22 cylinders(42-63), double felted			
Upper cylinders	182/132°	26.4/269°	131/125°	19/257°
Bottom cylinders	182/132°	26.4/269°	181/131°	26.3/269°

***Cylinders #10, 18, 33 & 63 were without steam for these measurements**

The uncalibrated validation simulations, Table 4-DD, give machine speed predictions on average within 3.4 %. Both data sets were then calibrated for actual machine speed and exit moisture content prior to production of the profiles of local moisture content and temperature, Figures 4-60 to 4-63. The moisture gradients across the sheet are very large, to about 0.9 kg/kg dry between the surfaces and one-third points of the sheet. The top side, that which is not in direct contact with the surfaces of upper tier cylinders in the unirun felting configuration of Sections 1 and 2, is seen to dry very much slower than the bottom side which experiences direct contact with upper tier cylinders. On alternate cylinders, where the top side would otherwise contact the lower cylinder, with the unirun configuration the felt is sandwiched between the sheet and cylinder, insulating the sheet from heat conduction.

Table 4-DD: Uncalibrated Validation for Multiple Technique Dryer: Temboard

	June 1996	October 1997
Exit moisture content		
Validation simulation	9.6 % d.b.	6.7 % d.b.
Measured	7.0 % d.b.	7.3 % d.b.
Machine speed		
Validation simulation	324 m/min	439 m/min
Measured	344 m/min	442 m/min
Difference	-6.1 %	+0.7 %

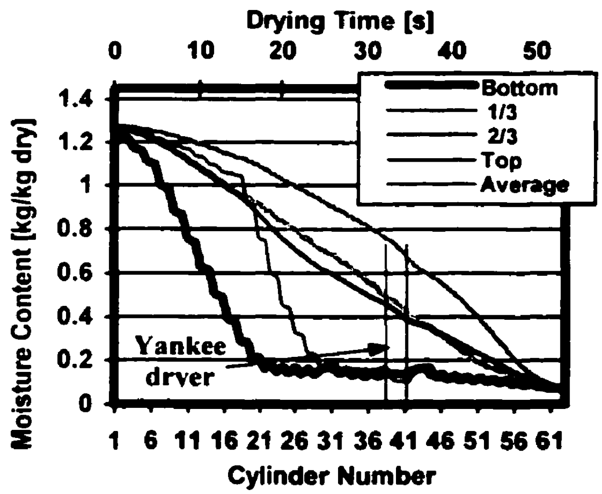

Figure 4-60: Sheet Moisture Content Profile: Temboard Paper Machine-June 1996

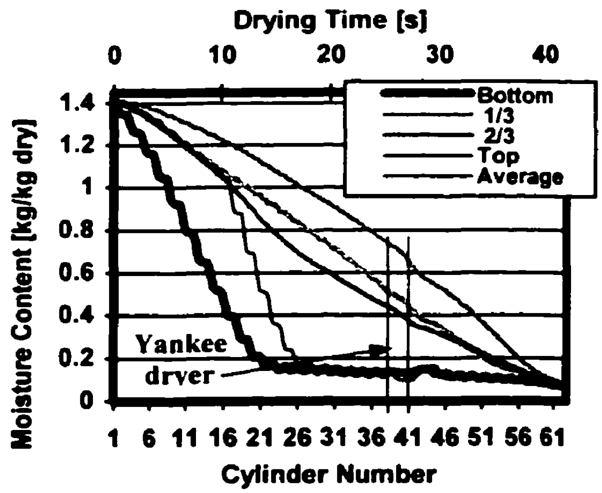

Figure 4-61: Sheet Moisture Content Profile: Temboard Paper Machine-October 1997

The maximum difference in moisture content between the top and bottom surfaces of the sheet naturally occurs at the end of the unirun section, after cylinder 17.

By the end of the 12 double felted cylinders (18-29) of Section 3 this large moisture difference, about 0.9 kg/kg dry, is seen in Figures 4-60 and 4-61 to have almost disappeared with heat transfer to both sides of the sheet. Although several effects combine to allow this convergence, probably the most important of these is that the cylinder to sheet contact heat transfer coefficient is larger by about a factor of 5 at sheet moisture content of 1.1 kg/kg dry compared to that at 0.2 kg/kg dry. After cylinder 17 this effect enables drying on the more moist side to catch up to that on the dryer side.

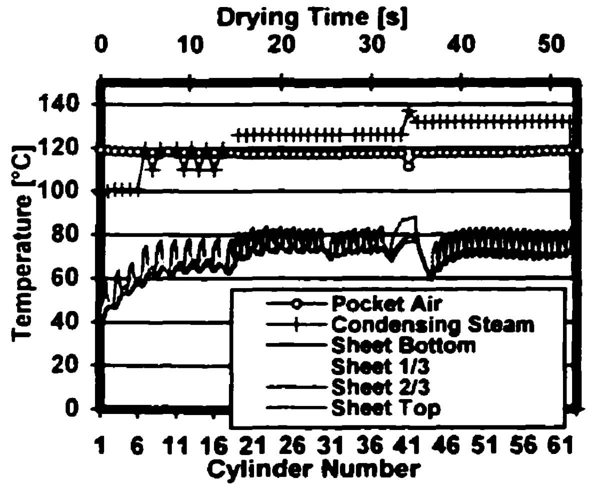

Figure 4-62: Sheet Temperature Profile: Temboard Paper Machine-June 1996

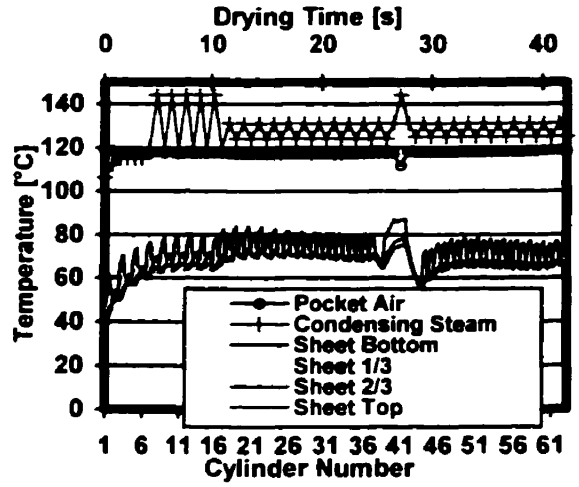

Figure 4-63: Sheet Temperature Profile: Temboard Paper Machine-October 1997

The effect of the Yankee dryer is seen clearly in the sheet moisture and temperature profiles, Figures 4-60 to 4-63. With the Yankee dryer location, Figure 4-59, the sheet bottom side, that which had direct upper tier cylinder contact in the unirun felted sections, is contacted by the impinging air jets. The top surface warms to a higher temperature than the bottom as it contacts the Yankee cylinder that has steam condensing at a temperature higher than the impinging air, Tables 4-BB and 4-CC. Without a dryer simulator based on microscale modeling, the rise and fall of these large moisture and temperature gradients across the sheet would not be detected. As paper properties are developed during drying they depend on the evolution of paper temperature and moisture content, including thickness direction profiles, hence are affected by the microscale drying history.

The microscale modeling of the *Drying Doctor* simulator is thus essential for both process engineering and paper properties aspects. One example of the latter is sheet curl, caused by unbalanced shrinkage forces created by unsymmetrical moisture profiles during drying. As shrinkage starts when local moisture content drops below the fibre saturation point of the pulp, a curl propensity index was defined based on the extent of thickness direction asymmetry in local moisture content below that value, 0.85 kg/kg dry in this case. The greater this asymmetry, the larger the curl propensity index. The predicted curl propensity indices are 86 and 64 for the 1996 and 1997 conditions, respectively. The greater curl propensity for the 1996 conditions is logical as the unirun section creates large moisture gradients, apparent in Figures 4-60 and 4-61, with the slower machine speed increasing this effect.

Figures 4-64 and 4-65 show the reasonable agreement between simulated sheet average moisture content and that measured at several intermediate points in these surveys. As the simulation over-predicts drying rate in the unirun section, an effect also found in two previous cases, sections 4.2.3 (b) and (c), this implies that the simulation uses too low a resistance to drying in tiers where the sheet is insulated from the cylinder by the felt. The deviation by the end of the unirun section is also larger for the 1997 than 1996 data (about 0.1 vs. 0.08 kg/kg dry), consistent with one more unirun cylinder in 1997.

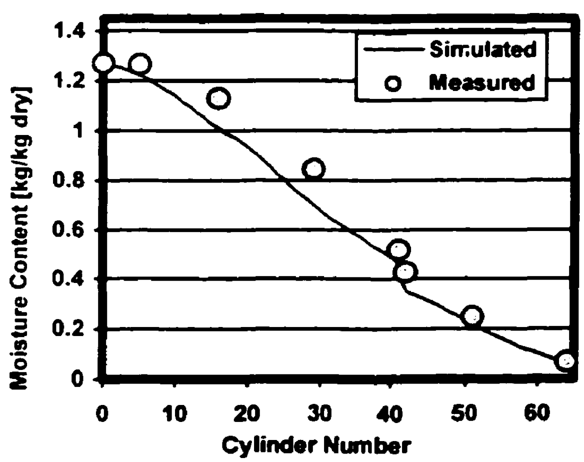

Figure 4-64: Sheet Moisture Content: Temboard Paper Machine-June 1996

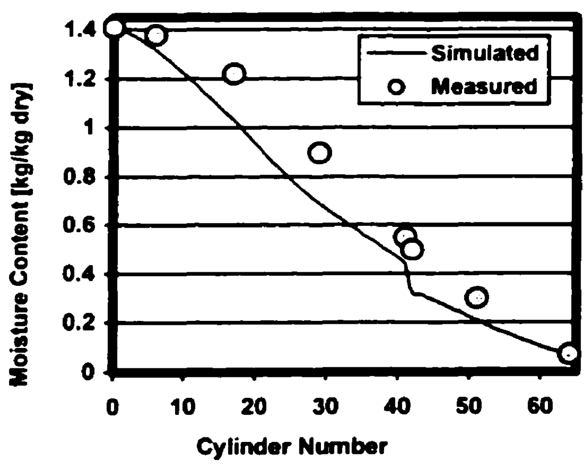

Figure 4-65: Sheet Moisture Content: Temboard Paper Machine-October 1997

Figures 4-66 and 4-67 show measured sheet temperatures significantly higher than those simulated. However some 1996 measured temperatures are evidently in error. The dryer surveys, where some reported sheet temperatures exceed the shell temperature, in fact caution that because of the difficulty in measuring paper temperature, only the trends are reliable. The uncertainty of these measured temperatures appears to be about 10°C. However Figures 4-66 and 4-67, combined with evidence from other cases, indicate that the *Drying Doctor* simulator predicts sheet temperatures that are too low.

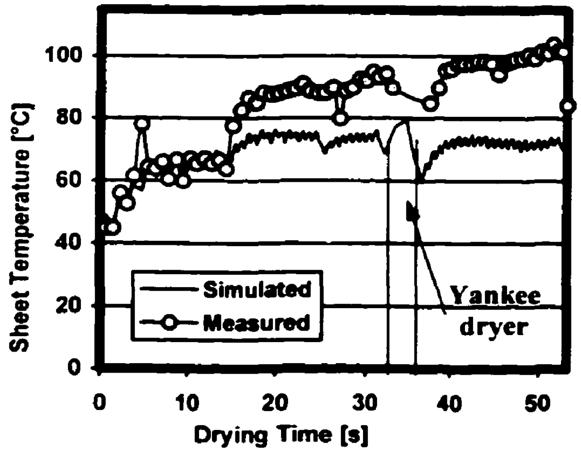

Figure 4-66: Sheet Temperature: Temboard Paper Machine-June 1996

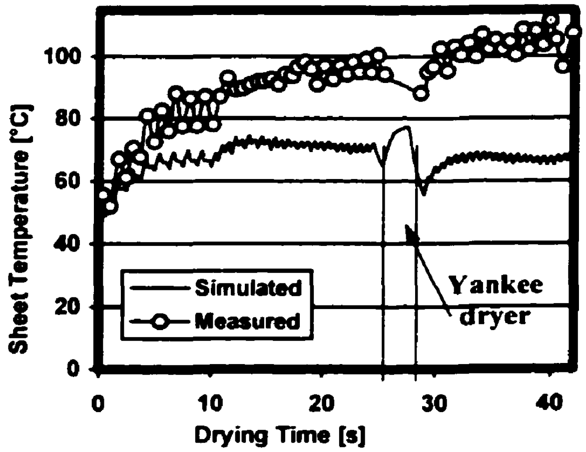

Figure 4-67: Sheet Temperature: Temboard Paper Machine-October 1997

Drying Doctor records for each cylinder: moisture and solids content, cylinder surface temperature, steam pressure, pocket air temperature and humidity, evaporation rate and condensate flow rate. This cylinder report is now presented for the unusually detailed Temboard dryer survey of 1996. Figure 4-68 shows the predicted condensate and evaporation rates. That in 1996 cylinders 10, 18, 33 and 63 were not in use is seen from the Figure 4-68 condensate rates. The predicted overall ratio of condensate to water evaporated, 1.0, is lower than that measured, 1.1, due in part to the current version of the simulator not predicting condensate rates for Yankee cylinders. In the first 17 cylinders, the unirun section, the upper cylinders which directly contact the sheet have condensate rates in the range 800 kg/h while the lower cylinders, where the felt insulates the sheet from the cylinder, have only about 150-200 kg/h condensate. The evaporation rate through the section averages about 300 kg/h, near that measured. In the third section, cylinders 18-29, the lower cylinders now have the higher rate. As Figure 4-60 shows, when the sheet leaves the unirun section its top side is much wetter than the bottom. Thus the top is still substantially above the fibre saturation point and thus locally still in the constant rate drying condition, while the bottom is much below that moisture content and locally is far into the falling rate period. With the lower cylinders contacting the side of the sheet where water is easier to remove and where the contact heat transfer coefficient may be higher by about a factor of 5 as previously noted, the lower cylinders naturally condense more steam. Due to a program limitation, the evaporation and condensate rates for Yankee cylinders are not yet calculated. However on Figure 4-68 the high intensity drying of the Yankee is visible at cylinder 42 which currently shows its relatively small evaporation rate combined with that of the Yankee.

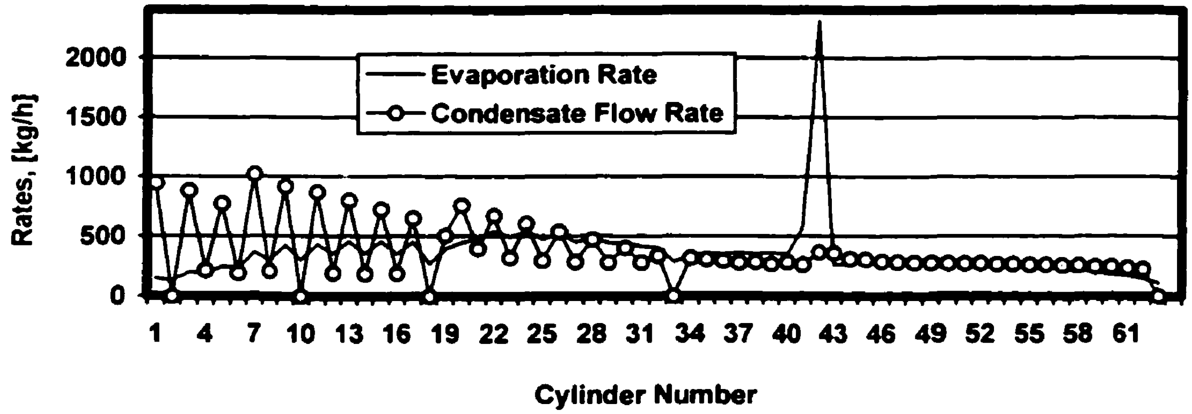

Figure 4-68: Evaporation and Condensate Flow Rates by Cylinder: Temboard Paper Machine-1996

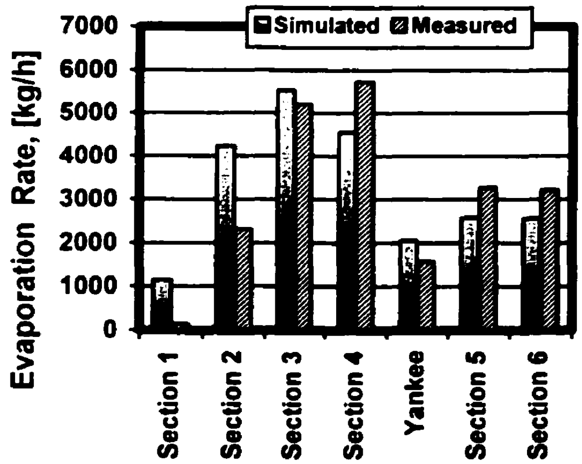

Figure 4-69: Evaporation Rate Comparisons: Temboard Paper Machine-June 1996

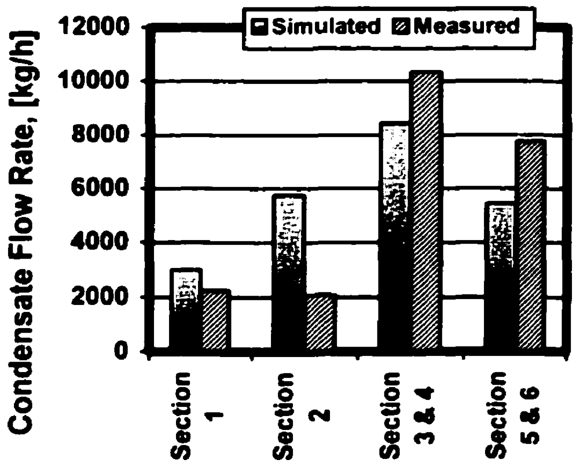

Figure 4-70: Condensate Rate Comparisons: Temboard Paper Machine-June 1996

In the dryer survey, condensate and evaporation rates are supplied only by section. In Figure 4-69 the predicted evaporation rate is seen to be high in unirun sections 1 and 2 while the predictions for the subsequent sections are quite close to the measurements. The condensate flow rate comparison of Figure 4-70 shows a corresponding drying over-prediction for unirun sections, under-prediction in double felted sections. These results provide further evidence that the treatment of unirun sections in the *Drying Doctor* simulator requires improvement.

The dryer survey also supplied cylinder surface temperatures, compared in Figure 4-71 with those predicted. The fluctuations indicate measurement error up to about 20 °C. Simulated cylinder surface temperatures appear low by about 10°C in the early part of drying, by about 20°C later in the dryer. Consistent with papermachines considered earlier, this evidence again shows the predicted sheet temperature is low, especially at sheet moisture content below the fibre saturation point. This deficiency will be corrected in the future from research currently underway here on heat and mass transfer phenomena within the sheet.

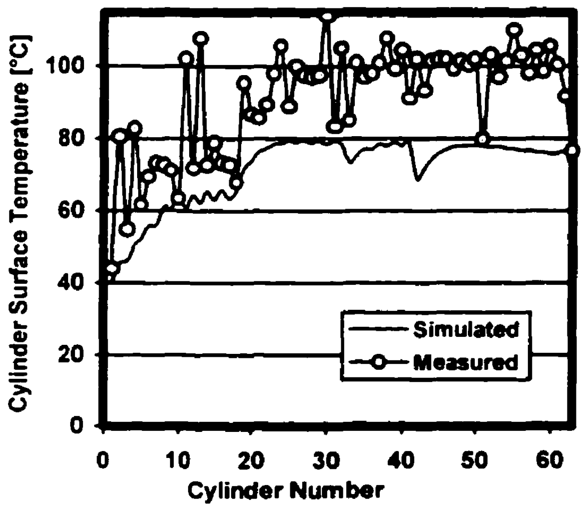

Figure 4-71: Cylinder Surface Temperature: Temboard Paper Machine-June 1996

A general observation from treating these various modifications is that this simulator would provide an effective tool in searching for the economic optimum in the distribution of water removal between conduction drying over steam heated cylinders and convective drying in dryer pockets.

4.4 Simulator Validation Summary

To provide a comprehensive representation of the extensive validation tests of the *Drying Doctor* simulator, Figure 4-72 displays the actual and predicted machine speeds for every case tested, i.e. for grades from tissue through newsprint and linerboard, in cylinder drying, air impingement and multiple technique dryers. As the standard use of a dryer simulator would be in machine speed prediction mode, it is uncalibrated machine speed validation simulations which are presented here. The outer lines show the limits of 5 % from the actual speed. Only a few predictions of 31 validation tests clearly fall outside this 5 % window. The standard deviation of the absolute value of the difference between actual and simulated machine speed is 24 m/min.

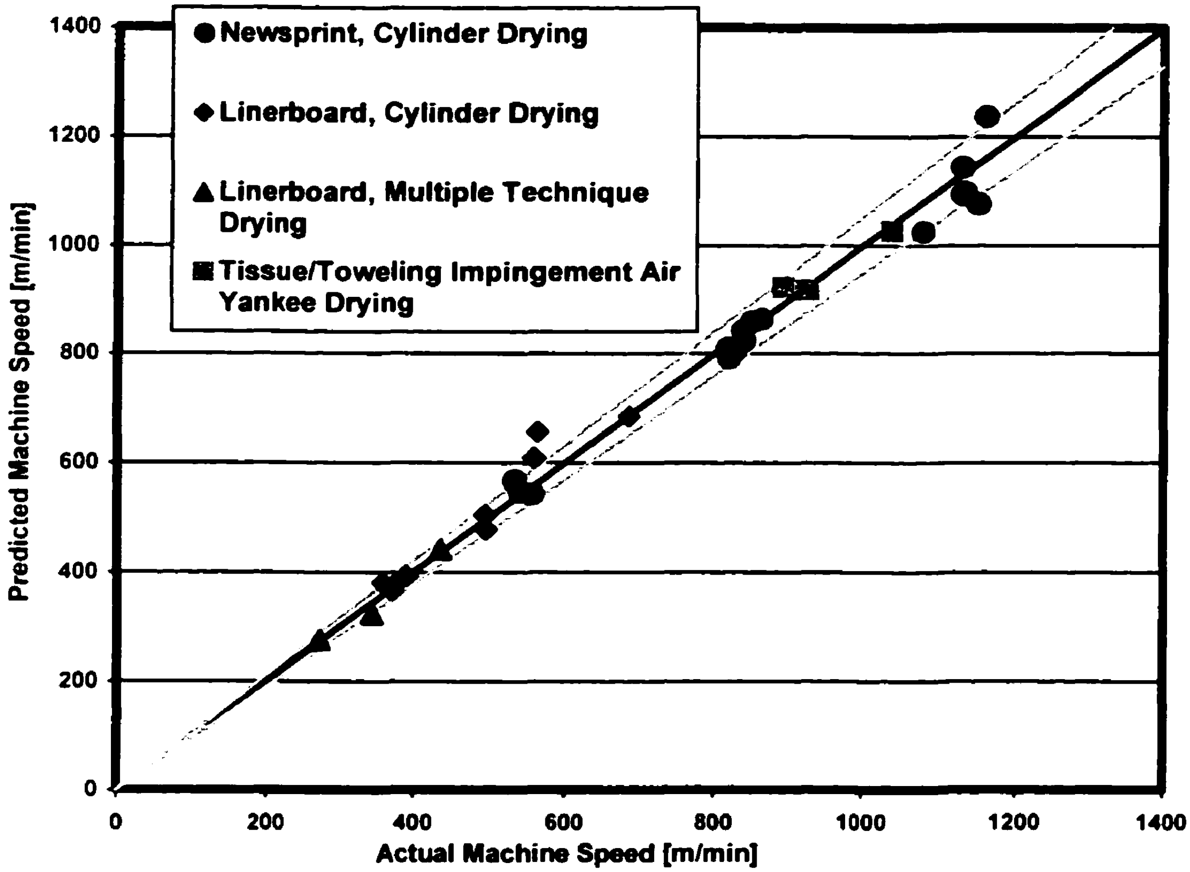

Figure 4-72: ***Drying Doctor*** **Machine Speed Validations: All Paper Machines Tested**

All measurements have some error, including those from the dryer surveys used in the simulations. Some errors in dryer survey recorded measurements are evident, such as sheet temperatures exceeding cylinder temperatures or impossible dryer pocket humidities. As the sheet travels at high speed and dryer sections are typically contained in hoods where the air is hot and humid, these measurements are in fact very difficult to make. For these reasons errors are normal and expected in dryer survey measurements.

These errors in the measurements of the many dryer conditions that are input to the dryer simulator provide one source of error in the simulator predictions. The simulation program itself provides the other source of error. For example, *Drying Doctor* consistently under-predicts sheet and cylinder surface temperatures somewhat and does not completely describe the felting effects in unirun sections.

There is an important distinction between these two kinds of errors. Errors in the dryer simulator are systemic errors, as the simulator calculation procedure is always identically the same. However the errors in dryer survey results are random, as each survey is carried out with staff and measurement instruments specific to that survey. These random errors in measurement appear as random errors in the predicted machine speed because of faulty input data. Thus predicted machine speed includes systematic error from the simulation program, and random error from the measured input conditions to the simulator.

The average error of predicted machine speed from 31 validation tests is +0.6 %. Thus the systematic errors in the *Drying Doctor* simulator program result in it predicting a machine speed which is on average 0.6 % more than actual machine speed. On the other hand the standard deviation of the absolute value of % error in machine speed prediction is 3.4 %, which reflects the effect of random error coming from incorrect dryer survey measurements of input data used by the simulator.

The results of Figure 4-72 demonstrate the accuracy and flexibility of the *Drying Doctor* simulator for the prediction of the performance of dryers of paper from the grades of tissue to containerboard, dried on processes ranging from low intensity cylinder dryers of many configurations, to high intensity air impingement dryers.

5 DOMTAR CONTAINERBOARD MACHINES

The industrial focus of this thesis is simulation of the four papermachines located in Trenton, Mississauga and Red Rock, Ontario of the Domtar Packaging Division, now merged with the containerboard division of Cascades Inc. to form Norampac Inc.. These 127 g/m^2 to 337 g/m^2 sheets, Figure 5-1, considerably thicker those simulated previously, provide a demanding test for *Drying Doctor*. Results are presented of simulations for operating conditions currently used, as modified, and for major dryer section rebuilds.

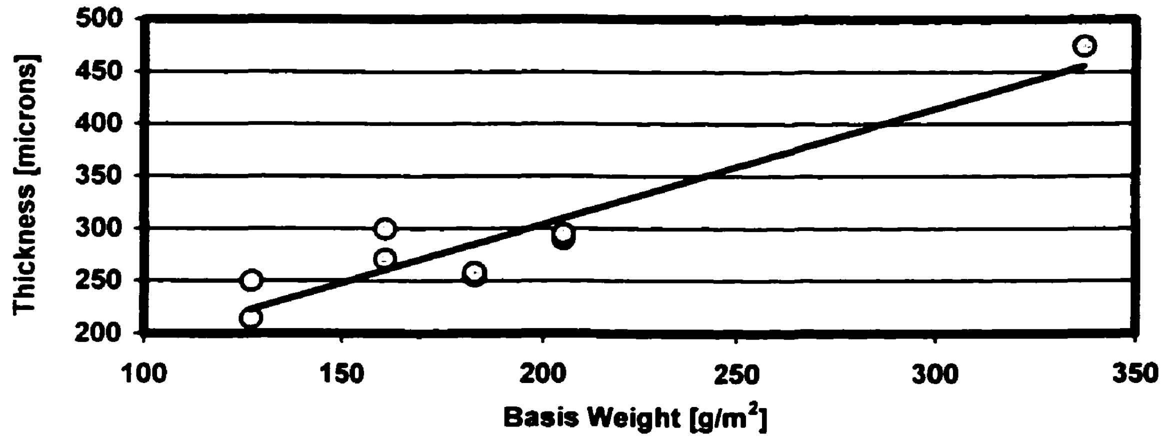

Figure 5-1: Domtar Containerboard Grades

5.1 Trenton Corrugated Medium Machine

5.1.1 Current Operation

The 160,000 t/y Trenton 3-ply corrugated medium machine, Figure 5-2 and Table 5-A, operates with a unique closed-loop water system that nearly eliminates discharge into the Trent River. The furnish is a mixture of recycled old corrugated containers (OCC) and semi-chemical hardwood pulp from a carbonate cook, less harmful to the environment than the sulfite process. Work here is with the 127 and 161 g/m^2 grades.

All 51 cylinders have full-width spoiler bars. They are all double felted with four pressure sections of 6, 14, 14 and 17 cylinders, all pressure sections but the first with fully ventilated pockets. For the two grades, Table 5-B gives the operating conditions as specified by mill personnel. In the first section, the humidity of the 60°C pocket air is 0.15 kg/kg dry air, while in the other three sections the ventilation supply air temperature and flowrate were supplied by dryer surveys as 120°C and 10 m^3/min-m width.

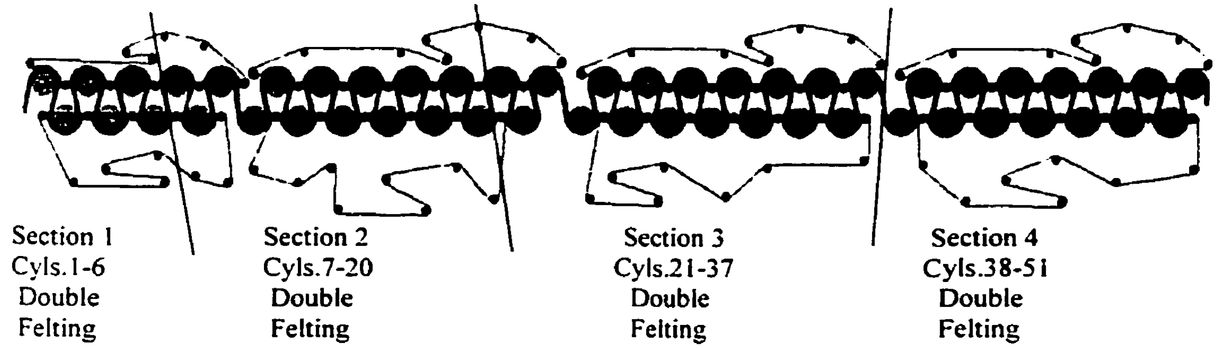

Figure 5-2: Dryer Section: Trenton Corrugated Medium Machine

Table 5-A: Design Specifications: Trenton Corrugated Medium Machine

Variables	S.I. Units	Alternate Units
Cylinder diameter	1.524 m	5 ft
Cylinder shell thickness	30.2 mm	1.2 inch
Machine trim	4.6 m	15.1 ft
Draw length	0.99 m	3.25 ft
Sheet wrap angle	230°	
Felt wrap angle	182°	
Felt thickness	2 mm	0.08 inch
Sheet length in dryer	211.5 m	693.9 ft
Spoiler bars (full-width)	Cylinders 1-51 (all)	

Table 5-B: Current Operating Conditions: Trenton Corrugated Medium Machine

Variable	127 g/m²		161 g/m²	
	S.I. Units	Alternate Units	S.I. Units	Alternate Units
Machine speed	686 m/min	2250 fpm	496 m/min	1627 fpm
Drying time	18.5 s		25.6 s	
Dry sheet caliper	250 microns		300 microns	
Sheet inlet moisture	1.44 kg/kg dry	41% solids	1.44 kg/kg dry	41% solids
Sheet exit moisture	0.08 kg/kg dry	92.6% solids	0.08 kg/kg dry	92.6% solids
Sheet inlet temp.	60°C	140°F	60°C	140°F
Fibre saturation point	0.8 kg/kg dry	55.6 % solids	0.8 kg/kg dry	55.6 % solids
Condensing Steam	S.I. [kPag/°C] and Alternate [psig/°F]			
Section 1 (1-6)	500/159°	72.5/318°	500/159°	72.5/318°
Section 2 (7-20)	550/162°	80/324°	550/162°	80/324°
Section 3 (21-34)	690/170°	100/338°	650/168°	94/334°
Section 4 (35-51)	800/175°	116/348°	700/170°	102/339°

The uncalibrated validations, Table 5-C, show excellent agreement. For the 127 g/m^2 grade, results with the simulation calibrated to the measured exit moisture content and machine speed of Table 5-C are displayed on Figures 5-3 to 5-6.

Table 5-C: Uncalibrated Validation for Trenton Corrugated Medium Machine

	127 g/m^2	161 g/m^2
Exit moisture content		
Validation simulation	8.3 % d.b.	7.2 % d.b.
Measured	8.0 % d.b.	8.0 % d.b.
Machine speed		
Validation simulation	685 m/min	505 m/min
Measured	686 m/min	496 m/min
Difference	-0.01 %	+1.8 %

Large thickness direction moisture gradients develop, Figure 5-3, with local point differences up to 1.0 kg/kg dry between the sheet edge and interior. This extreme gradient demonstrates the necessity of microscale modeling, even with a medium weight sheet under low intensity drying conditions. Interestingly, there is a difference between the 1/3 and 2/3 point moisture contents although the conditions are identical on both tiers. The sheet bottom side contacts the first cylinder and the closest one third point moisture content consequently remains lower throughout drying. Figure 5-4 shows rapid initial sheet heat-up to the wet bulb temperature, then the alternating gradients of up to 15°C from the cylinder contact side changing between the upper and lower tier. The increase in sheet pore air humidity, Figure 5-5, in the early cylinders when there is water in the pores

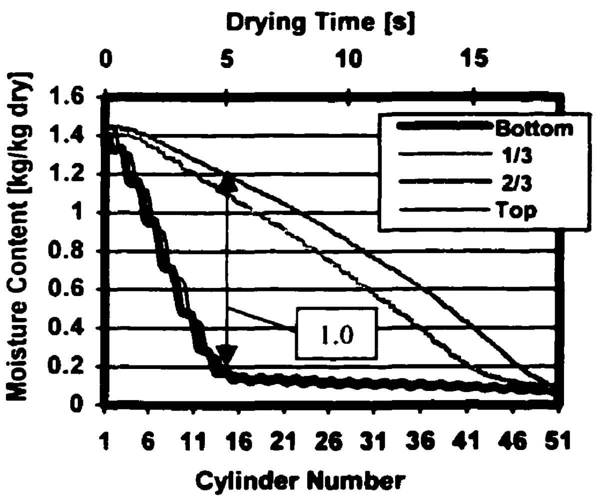

Figure 5-3: Local Moisture Content: Trenton Corrugated Medium Machine-127 g/m^2

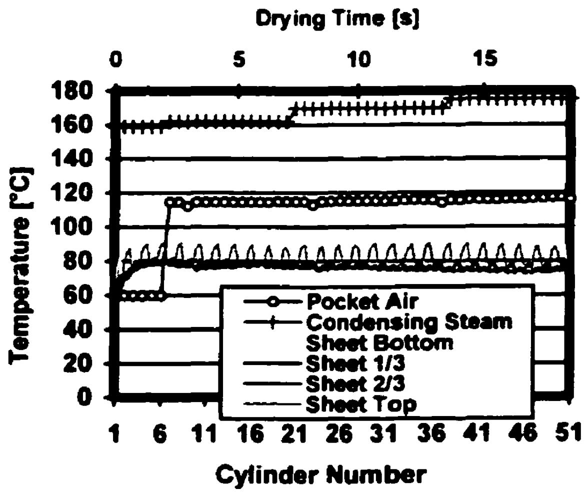

Figure 5-4: Local Temperature Profiles: Trenton Corrugated Medium Machine-127 g/m^2

reflects the increase in sheet temperature, Figure 5-4, while the subsequent decrease in pore humidity reflects the decrease in sheet moisture content, Figure 5-3. Evaporation rates, Figure 5-6, show the normal increasing rate zone over the first few cylinders, then apparently a very short constant rate drying period for the 550 kPag steam pressure in cylinders 6 to 8. The onset of the falling rate period drying occurring at about cylinder 9 corresponds on Figure 5-3 to the surfaces of the sheet reaching a moisture content about 0.7 kg/kg dry, just below the fibre saturation point.

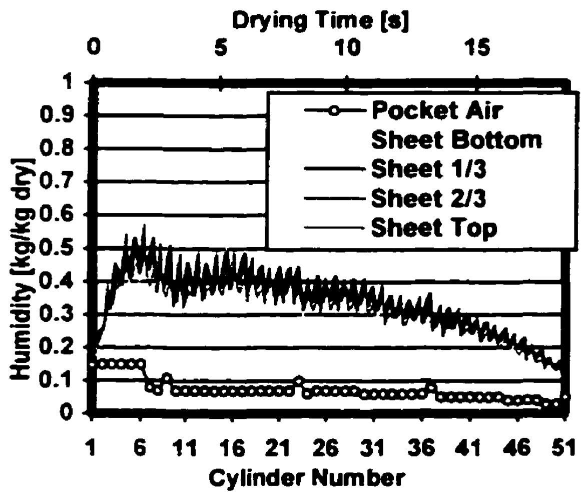

Figure 5-5: Pocket and Local Sheet Pore Air Humidity: Trenton Corrugated Medium Machine-127 g/m^2

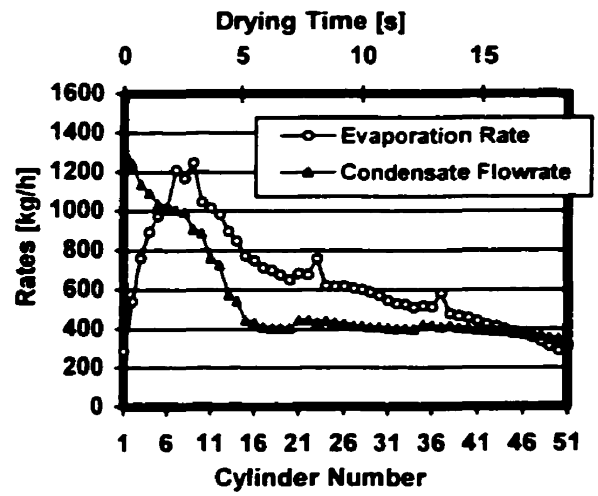

Figure 5-6: Evaporation and Condensate Rate: Trenton Corrugated Medium Machine-127 g/m^2

5.1.2 Machine Modification Simulation

(a) Effect of Cylinder Steam Pressure

With each grade three conditions are run, Table 5-D, the maximum allowable pressure being 1000 kPag. According to mill personnel the highest pressure recommended in the first section based on product quality (picking, linting) and runnability is 700 kPag.

Table 5-D: Operating Conditions: Trenton Corrugated Medium Machine-Variable Steam Pressure

	Steam Pressure and Condensing Temperature [kPag/°C]			
	Cylinders 1-6	Cylinders 7-20	Cylinders 21-34	Cylinders 35-51
A	700/170°	800/175°	900/180°	1000/184°
B	700/170°	1000/184°	1000/184°	1000/184°
C	1000/184°	1000/184°	1000/184°	1000/184°

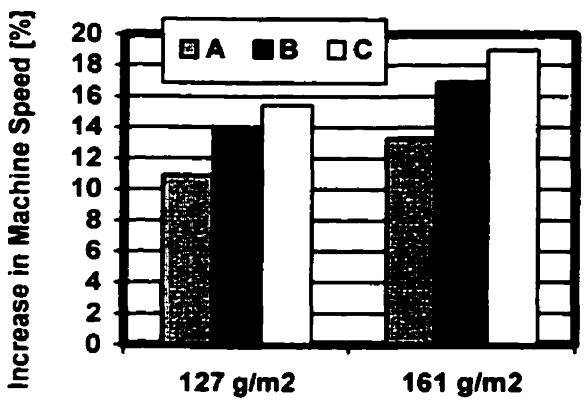

Figure 5-7: Trenton Corrugated Medium Machine: Effect of Steam Pressure

As the predicted speed increases from current operation, Figures 5-7, assuming that the moisture content exiting the press section would not change with machine speed, these increases require discounting for the effect of some increase in the entering moisture content.

During a mill visit personnel stated that two possibilities were modification of the present former or replacement with a C-former, allowing for machine speed to ~750 m/min. With Table 5-D increased steam pressure, the predicted speeds range from 761 to 792 m/min for the 127 g/m^2 grade, 562 to 590 m/min for 161 g/m^2 paper. Thus, for the projected future operation at 750 m/min, the current dryer section at higher steam pressures has the capacity to produce the 127 g/m^2 but not the 161 g/m^2 grade. With full-width spoiler bars and good pocket ventilation already, further modifications would be required to produce heavy grades at the new former speeds. Options include improving the press section to reduce dryer load, adding cylinders or implementing multiple technique drying such as addition of an air impingement convection dryer.

(b) Single Tier Modification

Mill personnel stated that the machine was operating at ~85 % efficiency with 5 to 8 breaks/day, mostly with the weak wet sheet in the first section. With unirun felting, the reduced drying capacity was found unacceptable because the increased steam pressures required causing picking and linting. Another possibility is modification to a single tier section. From Figure 5-2 the first nine cylinders, now covered by one felt on each tier, would be changed to a five cylinder single tier dryer section. For the steam pressures of condition A in Table 5-D, predictions for this layout at Table 5-B speeds show final moisture contents of 7 % and 6 % for the 127 and 161 g/m^2 grades. These predictions show that if linting or picking occurred, steam pressures could be decreased slightly and the desired 8 % exit moisture still obtained. Moreover, machine efficiency would increase substantially, breaks being much reduced with better sheet support.

5.2 *Mississauga Linerboard Machine*

5.2.1 Current Operation

The Mississauga 5-ply machine can produce 125,000 t/y of white and brown top linerboard entirely from recycled fibre. Key grades are 183 and 205 g/m^2. The 55 cylinder dryer section, Figure 5-8 and Tables 5-E, 5-F and 5-G, is double felted except for top felting only on the first 11 cylinders. There are 11, 16, 16 and 10 cylinders in the four pressure sections.

Uncalibrated validations, Table 5-H, show excellent agreement with measured conditions, machine speed predictions being within 1% of actual. All results reported below are from calibrated simulations.

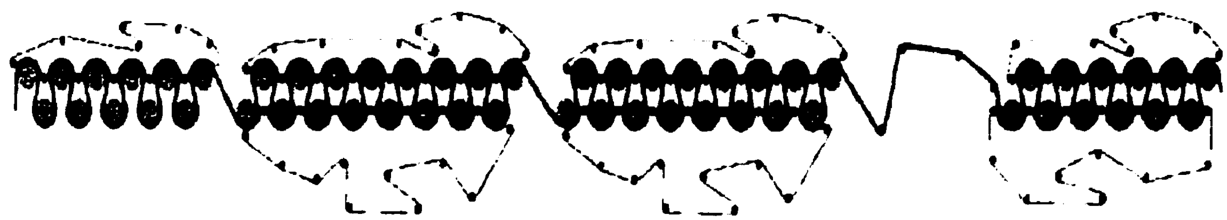

Figure 5-8: Dryer Section: Mississauga Linerboard Machine

Table 5-E: Design Specifications: Mississauga Linerboard Machine

Variables	S.I. Units	Alternate Units
Cylinder diameter	1.524 m	5 ft
Cylinder shell thickness	30.2 mm	1.2 inch
Machine trim	4 m	13.1 ft
Draw length	0.9 m	2.95 ft
Sheet wrap angle	226°	
Felt wrap angle	182°	
Felt thickness	1.8 mm	0.07 inch
Sheet length in dryer	243.3 m	768.7 ft
Spoiler bars	none	

The local moisture content for the surfaces and two interior points of the 205 g/m^2 sheet, Figure 5-9, shows large gradients through most of the drying. The unsymmetrical drying in the first 11 cylinders, top felted only, is reflected in the 2/3 point moisture being higher due to the lack of pressing of the sheet by the felt. This large gradient, up to

Table 5-F: Current Operating Conditions: Mississauga Linerboard Machine

Variable	183 g/m²		205 g/m²	
	S.I. Units	Alternate Units	S.I. Units	Alternate Units
Machine speed	377 m/min	1237 fpm	391 m/min	1283 fpm
Drying time	37.3 s		37 s	
Dry sheet caliper	255 microns		290 microns	
Sheet inlet moisture	1.13 kg/kg dry	47% solids	1.13 kg/kg dry	47% solids
Sheet exit moisture	0.055 kg/kg dry	94.8% solids	0.055 kg/kg dry	94.8% solids
Sheet inlet temp.	40°C	104°F	40°C	104°F
Fibre saturation point	0.8 kg/kg dry	55.6 % solids	0.8 kg/kg dry	55.6 % solids
Condensing Steam	S.I. [kPag/°C] and Alternate [psig/°F]			
Section 1 (1-11)	335/147°	48.6/296°	573/163°	83.1/326°
Section 2 (12-27)	381/150°	55.2/303°	674/169°	97.8/336°
Section 3 (28-43)	405/152°	58.7/306°	496/159°	71.9/318°
Section 4 (44-55)	394/151°	57.1/305°	685/170°	99.4/337°

Table 5-G: Current Operation Pocket Conditions: Mississauga Linerboard Machine

Variable	Temperature		Humidity
	°C	°F	kg/kg dry air
Section 1	50.5	123	0.06
Section 2	53	127	0.07
Section 3	54.4	130	0.06
Section 4	53.3	128	0.06

Table 5-H: Uncalibrated Validation for Mississauga Linerboard Machine

	183 g/m²	205 g/m²
Exit moisture content		
Validation simulation	5.3 % d.b.	5.3 % d.b.
Measured	5.5 % d.b.	5.5 % d.b.
Machine speed		
Validation simulation	381 m/min	394 m/min
Measured	377 m/min	391 m/min
Difference	+1.0 %	+0.7 %

0.2 kg/kg dry between interior 1/3 points and over 1.0 kg/kg dry between the surfaces and interior, is eliminated in the fourth section. The local sheet temperatures, Figure 5-10, develop a 10°C difference between heating on cylinders and evaporative cooling in draws, the latter exaggerated in the three long draws. Figure 5-11 shows large evaporation rates at these draws of 3.9, 3.9 and 13.6 m after cylinders 11, 27 and 43, this rate including the moisture removed in the following long draw. With the evaporative cooling through these long draws, the first subsequent cylinder has lower sheet and

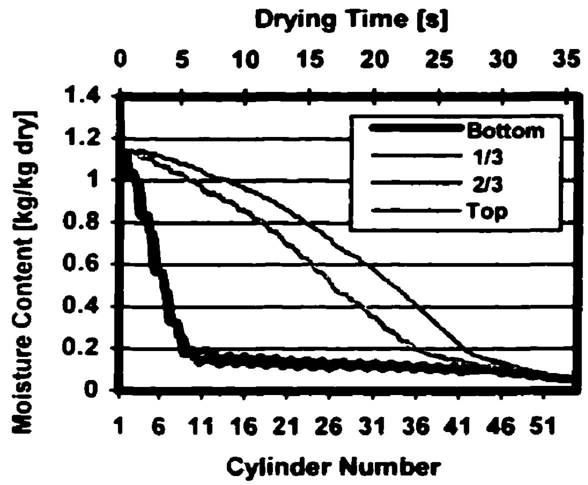

Figure 5-9: Local Moisture Content: Mississauga Linerboard Machine-205 g/m²

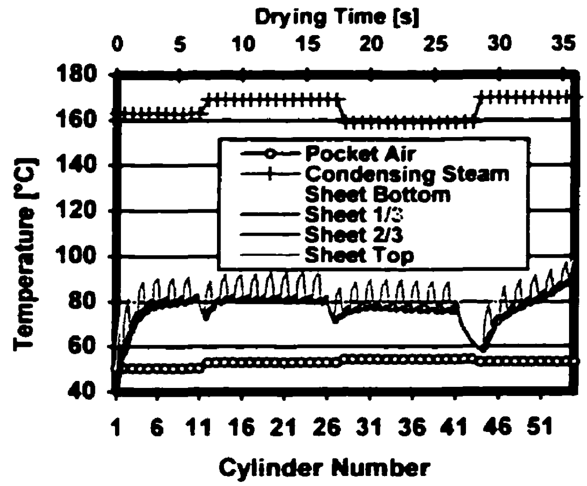

Figure 5-10: Local Temperature Profiles: Mississauga Linerboard Machine -205 g/m²

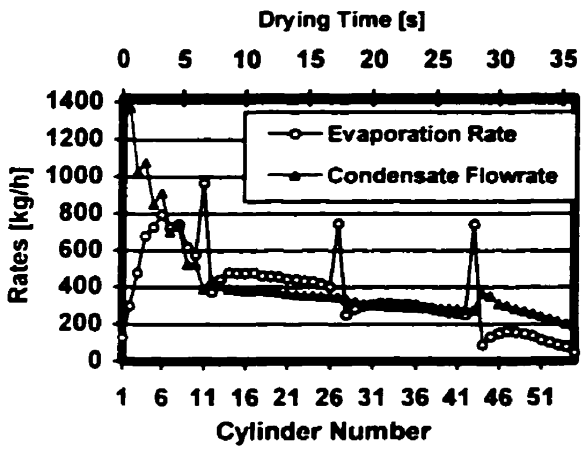

Figure 5-11: Evaporation and Condensate Rate: Mississauga Linerboard Machine-205 g/m²

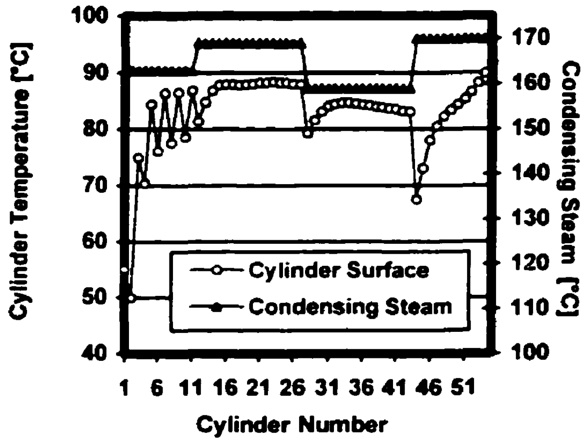

Figure 5-12: Cylinder Surface Temperature: Mississauga Linerboard Machine-205 g/m²

cylinder surface temperatures, hence higher condensation but lower evaporation rates, Figure 5-12. The other distinctive trend is the oscillating condensate flowrate through the first 11 cylinders from the unfelted bottom tier cylinders having lower cylinder surface temperatures than the preceding felted cylinder. As felts depress evaporation and heat transfer with the air, the absence of felting on the bottom cylinders enhances evaporative cooling of the sheet, lowers cylinder surface and sheet temperatures as seen on Figure 5-12, giving the observed higher condensate rates.

With an entirely recycled fibre furnish, day to day operations vary. Mill personnel state that the higher the energy input to refining the pulp, the lower the steam pressure required for drying. As refining increases fibre fibrillation and fines content, these differences seen in dryer performance probably reflect changes also in press section performance. As this mill does not measure the press exit moisture content, they have no data on this aspect. On a production date of lower refining energy, a 205 g/m^2 sheet of 5.5 % moisture content was made at 389 m/min machine speed with steam pressures in the four sections of 601, 725, 748 and 725 kPag. With the assumption that refining conditions changed only the pressing, not the drying characteristics, simulations were run with these conditions to find the dryer inlet moisture content. At the lower refining energy, the predicted press exit moisture was 1.33 kg/kg dry, or 43 % solids compared to 47 % at the higher refining energy. The effect is clearly quite large.

5.2.2 Simulation of Yankee Dryer Modification

To obtain a higher production, use of higher steam pressure is not realistic because the maximum mill steam pressure, 780 kPag, is little higher than that in several dryer sections and varies considerably with mill refining operation. Also, simulations showed that spoiler bars at this low machine speed would have little effect.

Replacing the unused size press occupying 7.6 m between the third and fourth section with a high intensity Yankee dryer, Figure 5-13, could improve printability, the prime objective, while also increasing dryer capacity. For a smoother surface the mill prefers placing the Yankee dryer at ~25 % sheet moisture. For both basis weights, first calibration simulations were run with the cylinder dryers at current steam pressures, Table 5-F, then with addition of the Yankee dryer as specified in Table 5-I, machine speed predictions were run for the desired exit moisture content of 5.5 %.

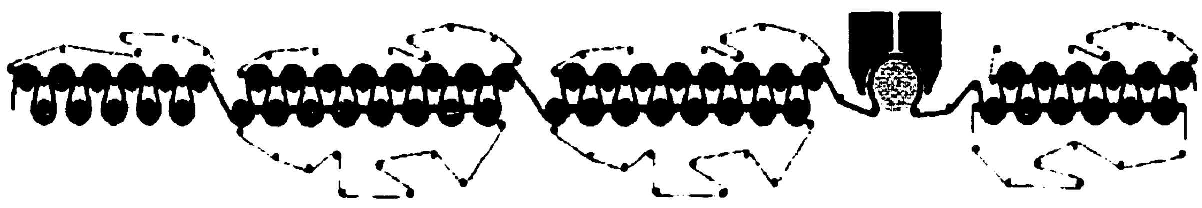

Figure 5-13: Dryer Section: Mississauga Linerboard Machine-Yankee at Size Press Modification

Table 5-I: Yankee Dryer Specifications and Operating Conditions: Mississauga Linerboard Machine-Yankee Dryer

Variables	S.I. Units	Alternate Units
Cylinder diameter	3.66 m	12 ft
Cylinder shell thickness	25 mm	1 inch
Nozzle diameter	5 mm	0.2 inch
Nozzle to web distance	20 mm	0.8 inch
Nozzle spacing/nozzle diameter	4	
Nozzle plate open area ratio	2 %	
Nozzle pattern	equilateral triangle	
Wrap angle before hood	20°	
Wrap angle inside hood	230°	
Wrap angle after hood	20°	
Sheet length in Yankee	8.6 m	28.3 ft
Draw before and after Yankee	0.9 m	2.9 ft
Total sheet length in dryer	232.2 m	761.8 ft
Condensing steam	500 kPag/159°C	72.5 psig/318°F
Jet temperature	300°C	572°F
Jet humidity	0.15 kg/kg dry air	
Jet velocity	75 m/s	14,760 fpm

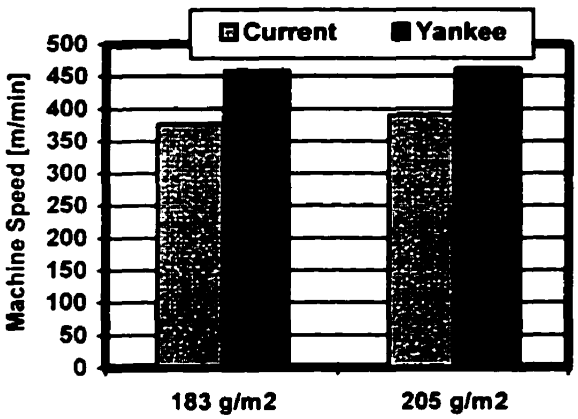

Figure 5-14: Mississauga Linerboard Machine Speed Increase with Yankee Dryer

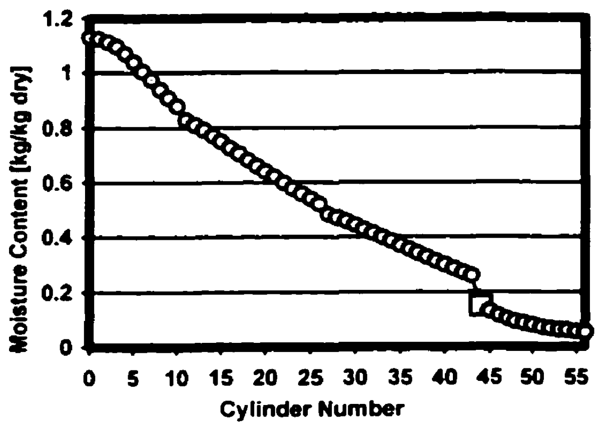

Figure 5-15: Average Moisture Content: Mississauga Linerboard Machine-Yankee Modification for 205 g/m^2

Production increases of about 20 % were predicted, Figure 5-14, with machine speed increases from 377 to 459 m/min for the 183 g/m^2 sheet, from 391 to 462 m/min for the 205 g/m^2 sheet. Figure 5-15, with the large square for the Yankee dryer, shows the moisture content evolution for 205 g/m^2 paper. As the moisture content entering the Yankee dryer is 26 % for the heavier grade, 27 % for 183 g/m^2, very close to the 25 % moisture content of interest to the mill, this case satisfies both mill objectives.

The local moisture profiles, Figure 5-16, provided by microscale modeling are particularly important in multiple technique dryer simulation where the profiles exiting one drying process become the inputs to the next. As the sheet enters the Yankee dryer, the moisture content varies by about 0.35 kg/kg dry between the sheet top and adjacent third point. With this entering profile, the Yankee dryer reduces the average moisture content from 0.26 to 0.159 kg/kg dry with an average drying rate on the Yankee of 66.8 kg/m^{2}h. For the same inlet moisture but no moisture gradient, the identical Yankee dryer conditions would have dried the sheet to 0.142 kg/kg dry. Thus without using the actual moisture gradient, drying in the Yankee would have been overpredicted by 17 %. The

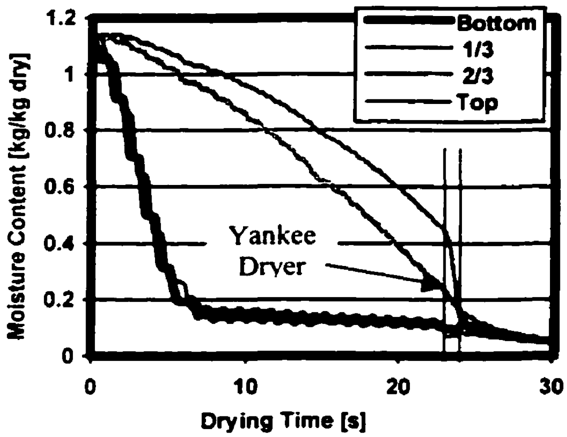

Figure 5-16: Local Moisture Content: Mississauga Linerboard Machine-Yankee Modification for 205 g/m^2

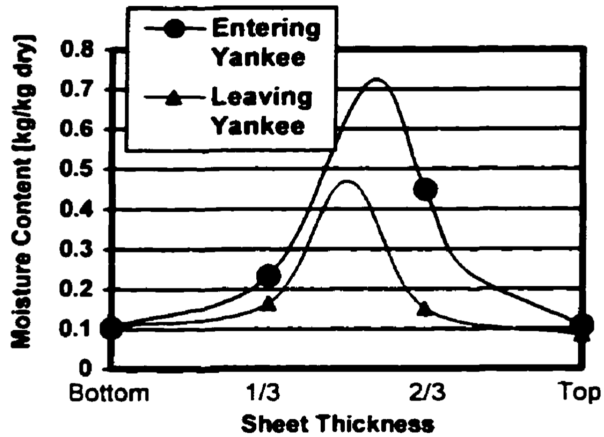

Figure 5-17: Moisture Content Thickness Profile: Mississauga Linerboard -Yankee Modification for 205 g/m^2

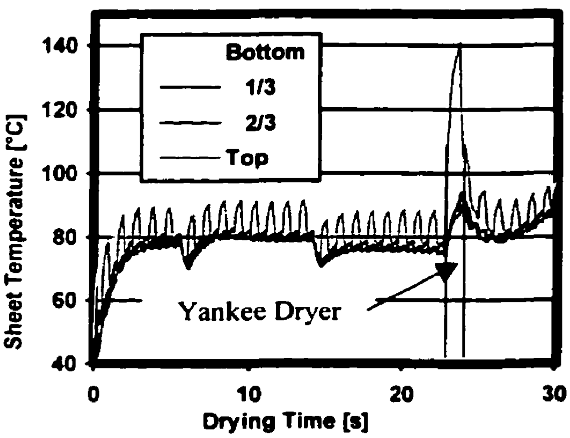

Figure 5-18: Local Sheet Temperature: Mississauga Linerboard Machine-Yankee Modification for 205 g/m^2

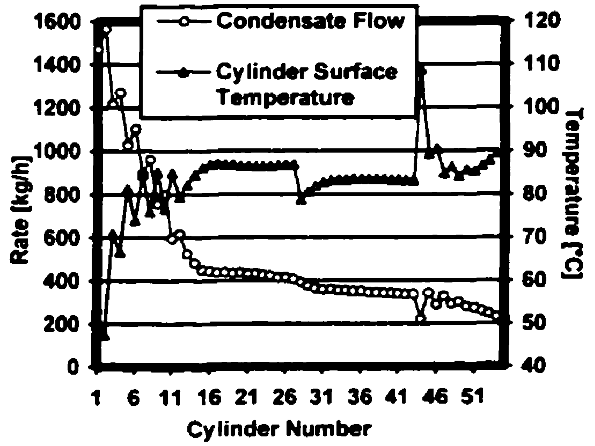

Figure 5-19: Condensate Rate and Cylinder Surface Temperature: Mississauga Linerboard - Yankee Modification for 205 g/m^2

moisture content thickness direction profiles, Figure 5-17, show the Yankee preferentially dries the part of the sheet contacting the hot impinging air and eliminates the asymmetry.

As important as moisture content, the evolution of local temperature is shown in Figure 5-18. The 1.1 s of Yankee dryer heating from impinging jets gives a surface temperature spike of about 60°C, about a 20°C rise at the cylinder contact side. The resulting softening of the sheet surface at a sufficiently high moisture content at the surface contributes the desired improved printability. The heating of the sheet also has the advantage of reducing the condensate rates, Figure 5-19, in the cylinders following. Figure 5-13 shows that the air impingement side of the sheet in the Yankee dryer becomes the cylinder contact side in cylinders 44 and 46 which follow. Two effects of this high temperature side of the sheet, Figure 5-18, are seen on Figure 5-19. First, the cylinder surface temperatures of cylinders 44 and 46, 110° and 90°C, are unusually high, and second, the condensate rate in cylinders 44 and 46 is reduced by 33 % and 14 %. This example illustrates the utility of the *Drying Doctor* simulator for questions of paper properties as well as for design and process engineering. As this machine has a moisture profiler situated before the fourth section, the Yankee dryer could replace it for cross directional moisture gradient profiling, providing yet another benefit from this multiple technique drying layout.

5.3 Red Rock Linerboard Machine #1

5.3.1 Current Operation

The two machines of this mill are together capable of producing 450,000 t/y. Papermachine #1 was converted from newsprint to linerboard in 1992 and uses a furnish of 80% kraft pulp and 20% OCC. The 48 cylinder dryer section, Figure 5-20, Tables 5-J

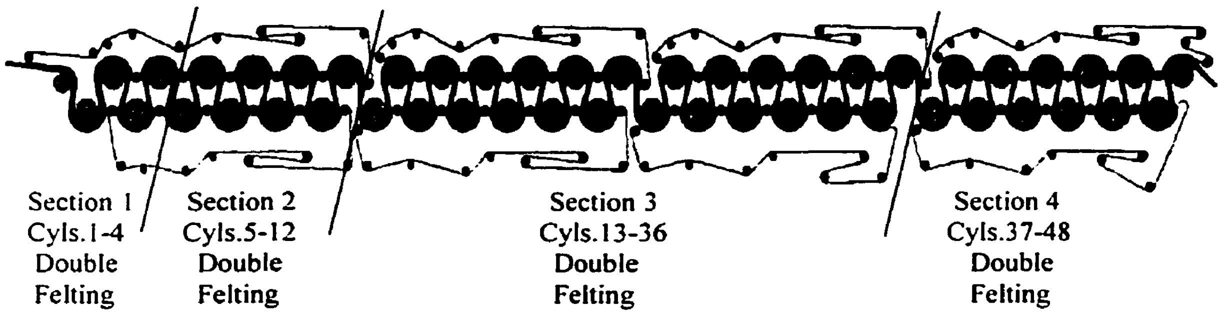

Figure 5-20: Dryer Section: Red Rock Linerboard Machine #1

Table 5-J: Design Specifications: Red Rock Linerboard Machine #1

Variables	S.I. Units	Alternate Units
Cylinder diameter	1.524 m	5 ft
Cylinder shell thickness (Cyl.1-12/13-48)	27/30 mm	1.1/1.2 inch
Machine trim	5.64 m	18.5 ft
Draw length	1.6 m	5.2 ft
Sheet wrap angle	220°	
Felt wrap angle	182°	
Felt thickness	1.8 mm	0.07 inch
Sheet length in dryer	217 m	712 ft
Spoiler bars	none	

Table 5-K: Current Operating Conditions: Red Rock Linerboard Machine #1

Variable	127 g/m²		161 g/m²	
	S.I. Units	Alt. Units	S.I. Units	Alt. Units
Machine speed	497 m/min	1631 fpm	358 m/min	1175 fpm
Drying time	26.2 s		36.4 s	
Dry sheet caliper	215 microns		271 microns	
Sheet inlet moisture	1.94 kg/kg dry	34 % solids	1.94 kg/kg dry	34 % solids
Sheet exit moisture	0.07 kg/kg dry	93.5 % solids	0.07 kg/kg dry	93.5 % solids
Sheet inlet temperature	45°C	113°F	45°C	113°F
Fibre saturation point	0.8 kg/kg dry	55.6 % solids	0.8 kg/kg dry	55.6 % solids
Condensing Steam	S.I. [kPag/°C] and Alternate [psig/°F]			
Section 1 (1-4)	150/128°	22/262°	150/128°	22/262°
Section 2 (5-12)	200/134°	29/273°	200/134°	29/273°
Section 3 (13-36)	900/180°	131/356°	900/180°	131/356°
Section 4 (37-48)	1000/184°	145/363°	1000/184°	145/363°

Table 5-L: Current Operation Pocket Conditions: Red Rock Linerboard Machine #1

Variable	Temperature		Humidity
	°C	°F	kg/kg dry air
Cylinder 1	**60**	**140**	**0.1**
Cylinders 2-12	**60**	**140**	**0.15**
Cylinders 13-48	**68**	**155**	**0.2**

Table 5-M: Uncalibrated Validation for Red Rock Linerboard Machine #1

	127 g/m²	161 g/m²
Exit moisture content		
Validation simulation	8.6 % d.b.	5.8 % d.b.
Measured	7.0 % d.b.	7.0 % d.b.
Machine speed		
Validation simulation	479 m/min	381 m/min
Measured	497 m/min	358 m/min
Difference	-3.6 %	+6.4 %

and 5-K, has pocket ventilation on cylinders 13-48 in pressure sections 3 and 4. As the ventilation supply air rate and temperature were neither measured nor controlled, typical values at this mill for air temperature and humidity in the pockets, Table 5-L, were entered in *Drying Doctor*, giving uncalibrated validation speed predictions, Table 5-M, within about +/- 5% of actual.

Using calibrated simulations, the effects of the 200 to 900 kPag steam pressure (134° to 180°C condensing temperature) increase from cylinder 13 are seen on Figures 5-21 to 5-24. For example, from cylinder 12 to 13 the moisture at the sheet surfaces, Figure 5-21, begins to drop dramatically and the temperature difference across the sheet, Figure 5-22, increases from about 10° to 15°C. Figures 5-23 and 5-24 show the condensate rate is very low for the first cylinder, which contacts the felt not the sheet, then jumps

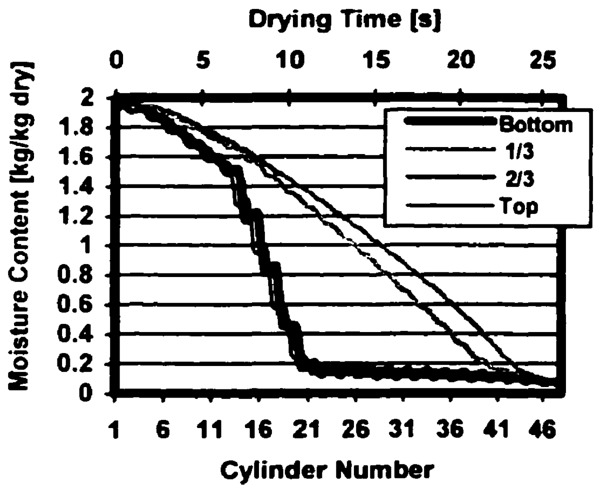

Figure 5-21: Local Moisture Content: Red Rock Linerboard Machine #1-127 g/m^2

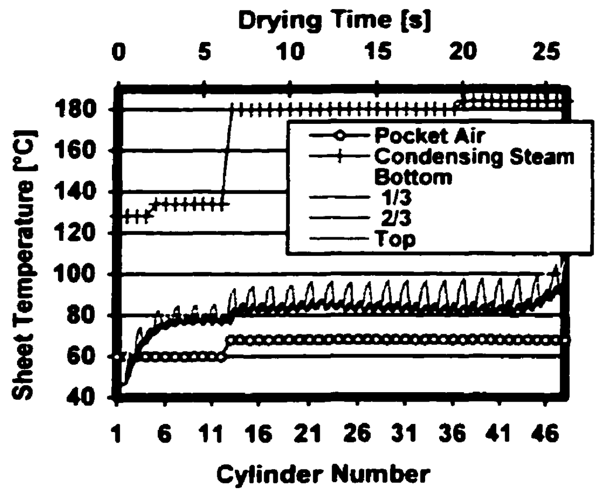

Figure 5-22: Local Temperature Profiles: Red Rock Linerboard Machine #1-127 g/m^2

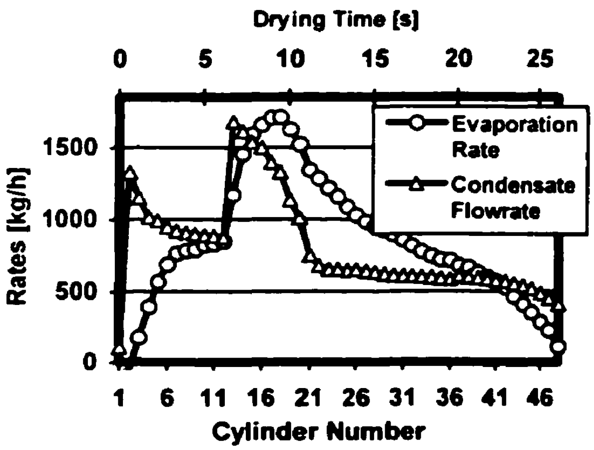

Figure 5-23: Evaporation and Condensate Rate: Red Rock Linerboard Machine #1-127 g/m^2

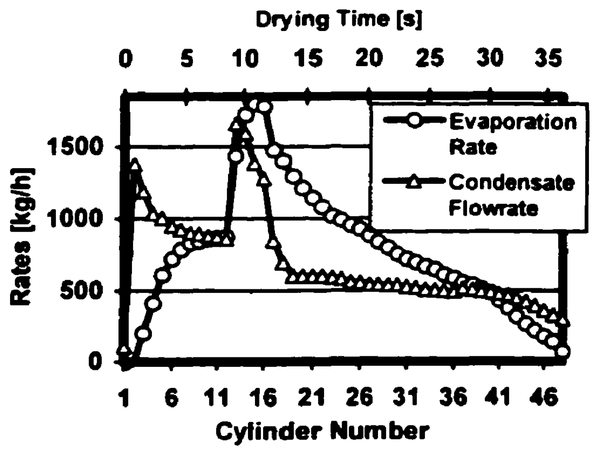

Figure 5-24: Evaporation and Condensate Rate: Red Rock Linerboard Machine #1-161 g/m^2

dramatically when the second cylinder contacts the cool sheet. The condensate rate decreases in the succeeding cylinders as the sheet warms, Figure 5-22, and the sheet surfaces begin to dry, Figure 5-21. The leveling of condensate rate at cylinder 21 coincides with the surfaces of the 127 g/m^2 sheet reaching near dryness, Figure 5-21, an effect seen also in evaporation rate. A notable difference between Figures 5-23 and 5-24 is that, after the large steam pressure increase at cylinder 13, the rates decrease faster for the heavier sheet. In the thicker paper, the greater resistance to heat and mass transfer produces larger thickness direction differences, hence dryer fibres near the sheet surfaces. The corresponding lower moisture diffusivity and thermal conductivity of these drier surface regions lowers drying rate more quickly for heavier paper.

Table 5-N: Operating Conditions: Red Rock Machine #1: Sack Paper -February 1997

Variable	**118 g/m^2**	
	S.I. Units	**Alternate Units**
Machine speed	365 m/min	1196 fpm
Drying time	35.6 s	
Dry sheet caliper	200 microns	
Sheet inlet moisture	1.85 kg/kg dry	35 % solids
Sheet exit moisture	0.072 kg/kg dry	93.3 % solids
Sheet inlet temperature	45°C	113°F
Fibre saturation point	0.8 kg/kg dry	55.6 % solids
Condensing Steam	S.I. [kPag/°C] and Alternate [psig/°F]	
Section 1	131/125°	19/257°
Section 2	172/130°	25/267°
Section 3	427/154°	62/309°
Section 4	400/152°	58/305°

Table 5-O: Uncalibrated Validation of Red Rock Machine #1: Sack Paper -February 1997

Exit moisture content	
Validation simulation	5.8 % d.b.
Measured	7.2 % d.b.
Machine speed	
Validation simulation	392 m/min
Measured	365 m/min
Difference	+7.3 %

Conditions for an earlier dryer survey by Hill Drying Systems during production of 118 g/m^2 sack paper are given in Table 5-N. Three cylinders (1, 35 and 36) were shut off and a water spray moisture profiler was sometimes used between cylinders 35 and 36. The uncalibrated validation, Table 5-O, predicts a machine speed 7 % too high. Over-prediction of drying is expected as the moisture profiler in operation at this time, being of unknown characteristics, adds an unknown amount of water and cannot be simulated.

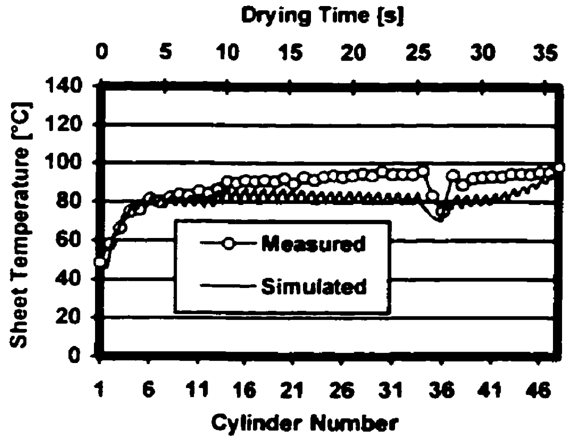

Figure 5-25: Average Sheet Temperature Comparison: Red Rock Machine #1: Sack Paper-February 1997

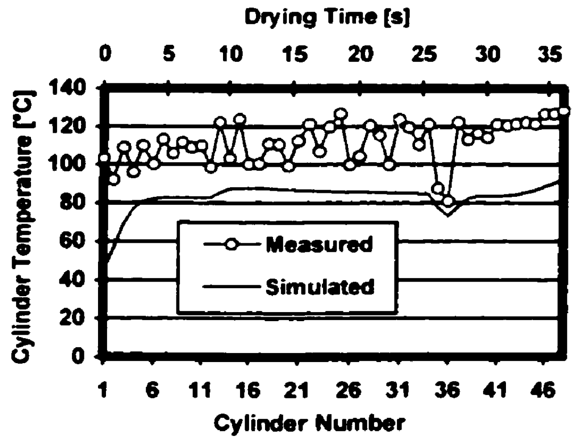

Figure 5-26: Cylinder Surface Temperature Comparison: Red Rock Machine #1: Sack Paper -February 1997

Although the predicted sheet and cylinder surface temperatures, Figure 5-25 and 5-26, are generally somewhat low, the dryer survey noted a problem from some cylinders having excessive cross direction temperature profiles of up to 15°C.

5.3.2 Machine Modification Simulation

(a) Pocket Ventilation Modification

Simulations with full pocket ventilation of all cylinders using the default conditions of a supply of 120°C pocket air at 14 m^3/min-m width, Table 5-P, show that a significant speed increase could be obtained by installing ventilation air in the first two sections and increasing the supply temperature and flowrate to all pockets. These significant increases reflect the very poor current pocket ventilation. For example, the 0.2 kg/kg dry air at 68°C in dryer sections 3 and 4, Table 5-L, indicates the sheet was being contacted by air of 86 % relative humidity and 65°C wet bulb temperature.

Table 5-P: Machine Speed: Red Rock Linerboard Machine #1-Full Pocket Ventilation Modification

	127 g/m^2	161 g/m^2
Machine speed		
Original	497 m/min	358 m/min
Full Pocket Ventilation	536 m/min	385 m/min
Speed Increase	7.8 %	7.5 %

(b) Spoiler Bar Modifications

Simulations were run initially with full width bars installed on the first 24 cylinders, an option under consideration by the mill, then with spoiler bars installed on all cylinders. Figures 5-23 and 5-24 show the former to be a good choice as it includes the cylinders of highest condensate production and hence with the greatest potential for improvement by spoiler bars. Table 5-Q shows that installing spoiler bars would enable machine speed increases of over 3 % for the light grade, by 1.6 % for heavier. The capacity increase is small because machine speed is low and spoiler bars are more effective as turbulence promoters with the thicker condensate layers maintained by higher centrifugal force. The higher speed increase is of course for the lighter grade, produced at over 100 m/min faster.

Table 5-Q: Machine Speed: Red Rock Linerboard Machine #1-Spoiler Bar Modification

	127 g/m^2	161 g/m^2
Machine speed		
Original	497 m/min	358 m/min
Spoiler Bars (Cyl.1-24)	502 m/min	361 m/min
Speed Increase	1.0 %	0.8 %
Spoiler Bars (Cyl.1-48)	513 m/min	364 m/min
Speed Increase	3.3 %	1.6 %

(c) Yankee Dryer Modification

For addition of a high-intensity Yankee dryer, Table 5-R, the five options were:

- Modification 1: Yankee dryer before cylinder 1 (48 cylinders)
- Modification 2: Yankee dryer after cylinder 48 (48 cylinders)
- Modification 3: Yankee dryer replaces cylinders 1-8 (40 cylinders)
- Modification 4: Yankee dryer replaces cylinders 25-32 (40 cylinders)
- Modification 5: Yankee dryer replaces cylinders 41-48 (40 cylinders)

with the additional parameter of Yankee cylinder steam pressure from 200 to 1000 kPag. All other conditions were maintained as in Section 5.3.1. The machine room layout allows moving the winder and reel to make space for the Yankee dryer allowing Modification 2. The replacement of 8 cylinders is derived from the floor space required for the 3.7 m Yankee cylinder and its peripherals. Sheet length in the dryer was 227 m and 191 m for the 48 and 40 cylinder modifications, respectively.

Table 5-R: Dryer Specifications and Operating Conditions: Red Rock Linerboard Machine #1-Yankee Dryer Modification

Variables	S.I. Units	Alternate Units
Cylinder diameter	3.66 m	12 ft
Cylinder shell thickness	25 mm	1 inch
Nozzle diameter	5 mm	0.2 inch
Nozzle to web distance	20 mm	0.8 inch
Nozzle spacing/nozzle diameter	4	
Nozzle plate open area ratio	2 %	
Nozzle pattern	equilateral triangle	
Wrap angle before hood	20°	
Wrap angle inside hood	230°	
Wrap angle after hood	20°	
Sheet length in Yankee	8.6 m	28.3 ft
Jet temperature	350°C	662 °F
Jet humidity	0.15 kg/kg dry air	
Jet velocity	100 m/s	20,000 fpm

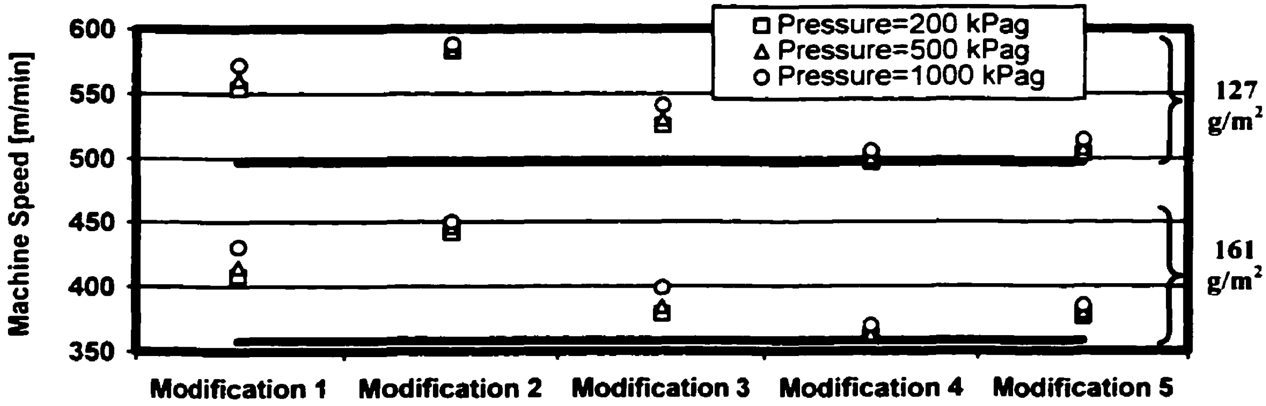

Figure 5-27: Machine Speed Predictions: Red Rock Machine #1-Yankee Modification

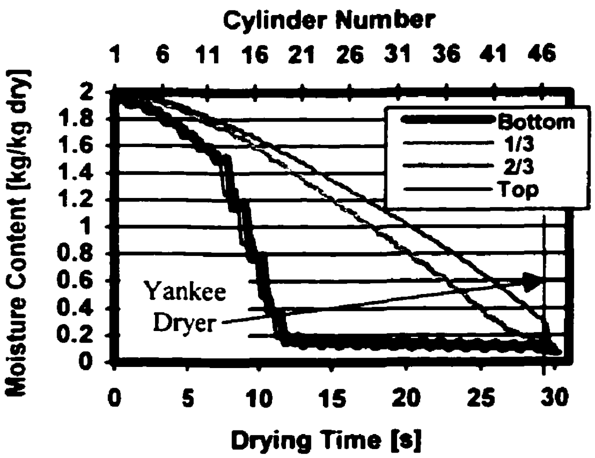

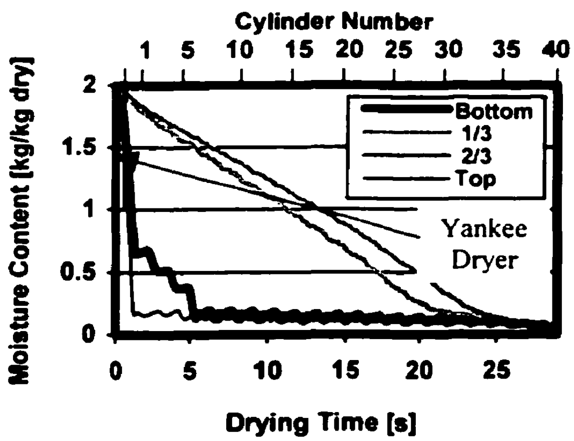

Figure 5-28: Local Moisture Content: Red Rock Machine #1-Yankee Modification 2-161 g/m²

Figure 5-29: Local Moisture Content: Red Rock Machine #1-Yankee Modification 3-161 g/m²

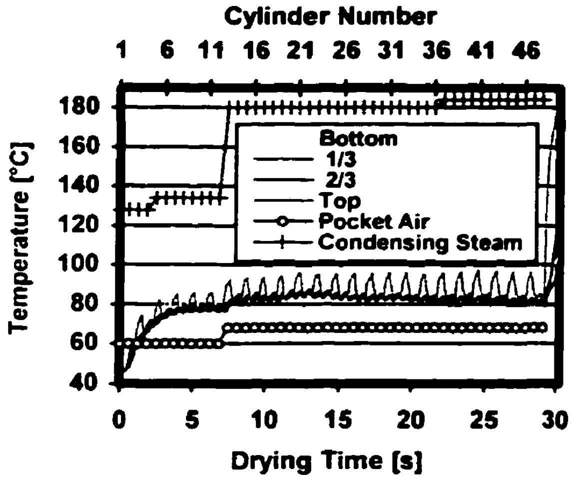

Figure 5-30: Local Temperature Profiles: Red Rock Machine #1-Yankee Modification 2-161 g/m^2

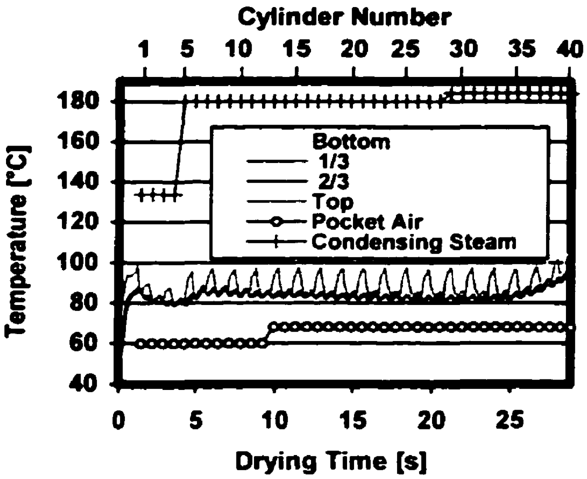

Figure 5-31: Local Temperature Profiles: Red Rock Machine #1-Yankee Modification 3-161 g/m^2

The Figure 5-27 predictions show that Yankee cylinder steam pressure has limited effect, consistent with the demonstration in Chapter 4 that in a Yankee the air impingement drying dominates over that by hot surface heat conduction. The sheet moisture and temperature drying history for Modifications 2 and 3 with 1000 kPag steam pressure are shown in Figures 5-28 to 5-31. Modifications 1 and 2 both use 48 cylinders, however Modification 2 leads to a higher machine speed and as the winder and reel may be moved, this modification is examined. Modification 3 is shown as it leads to the greatest increase for the 40 cylinder modifications. The drying time on Figures 5-28 and 5-29 is almost the same because of compensating effects of dryer length and drying rate. These graphs show that the Yankee dryer for Modification 2 dries the moisture remaining in the center of the sheet at the dry end while for Modification 3 it dries the edges of the wet sheet, thereby moving earlier the region of large moisture gradients. Figures 5-30 and 5-31 show the sheet temperature boost at the dry and wet ends for the Yankee in these positions.

When simply adding a Yankee dryer, several factors explain why it is more effective when placed at the dry end, Modification 2. At the wet end, Modification 1, drying is pure heat transfer controlled prior to the onset of falling rate drying, hence the high impingement flow convection heat transfer coefficients might be considered to make this the favored location, which it is clearly not. When added at the wet end the 161 g/m^2 sheet leaves the Yankee dryer at 86-101°C, then traverses 12 relatively cool cylinders with 150-200 kPag steam condensing at 128-134°C. These cylinders, no longer serving as a "heat-up" zone for the sheet entering at 45°C, should now be operated at higher steam pressure. A central factor in the greater effectiveness of the Yankee at the dry than the wet end is the effect of sheet temperature on drying rate. Near the end of the falling rate period the remaining water is as bound moisture within the fibres. Leaving cylinder 48 and entering the Yankee, the 161 g/m^2 sheet average moisture and temperature are 0.20 kg/kg dry and 85°C. The high convection heat transfer to the sheet in the Yankee brings sheet temperature to 180, 120, 102 and 104°C at the four points from top to bottom. These substantial temperature increases greatly facilitate removal of the bound moisture and explain the higher effectiveness of the Yankee at the dry end. For Modification 2, Figure 5-32, the potential for this benefit is greater the thicker the sheet, so the larger percent increase in machine speed for the heavier grade, Table 5-S, is anticipated. As for the high paper temperature leaving the Yankee with a 76°C difference across the sheet, the 3.66 m diameter Yankee dryer would be followed by a calendar stack of about the same height. If there were a 6 m open draw from the sheet leaving the bottom of the Yankee cylinder and entering the top of the calendar stack, then in the 0.8 s transfer time for the 161 g/m^2 sheet, simulation shows that this temperature difference in the thickness direction would be reduced to about 5°C, the range experienced from cylinder dryers.

If 8 cylinders are replaced the best option is replacing the wet end cylinders, Modification 3. Replacing cylinders at the dry end, Modification 5, is next best while replacing cylinders in the middle of the machine is worst. Replacing wet end cylinders is best only because these cylinders operate at very low pressure, 150-200 kPag. In the case of Modifications 4 and 5 where the replaced cylinders all operate in the 900-1000 kPag range, the replacement of dry end cylinders is advantageous over those earlier because of the sheet heating effect already described for Modification 2. In Modification 4, the sheet average moisture content entering the Yankee is still sufficiently high, 0.65 kg/kg dry, that the water is not yet bound to the fibres and therefore the effect of heating the sheet is of less importance. In Modifications 1 and 3 the sheet temperature, Figure 5-31, rises to the wet bulb temperature very quickly compared to Modification 2, Figure 5-30, and remains there. As most breaks occur at the wet end, in terms of runnability Modifications

1 and 3 have the advantage that the sheet will be much drier, hence stronger when experiencing its first open draw. Thus the machine speed advantage of Modification 2 over Modification 1 must be balanced by an estimate of the greater loss of operating time due to sheet breaks with Modification 2.

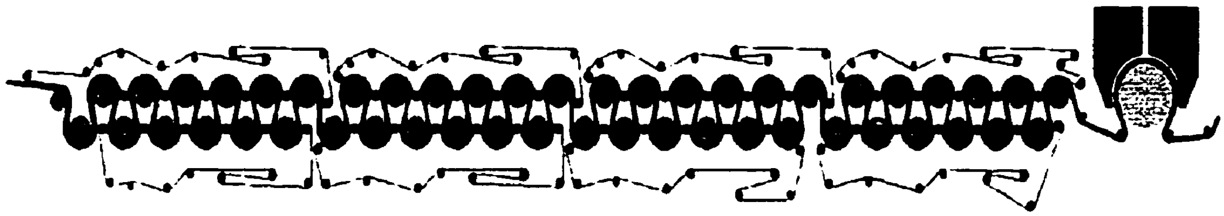

Figure 5-32: Dryer Section: Red Rock Machine #1-Yankee Modification 2

Table 5-S: Machine Speed: Red Rock Machine #1- Yankee Modification 2

	127 g/m^2	161 g/m^2
Machine speed		
Original	497 m/min	358 m/min
Yankee Dryer Modification 2	588 m/min	450 m/min
Speed Increase	18.3 %	25.7 %

(d) Yankee Modification 2 plus Spoiler Bars

As section (b) showed, addition of spoiler bars to the original machine provides little increased drying capacity as speeds are too low for the bars to be effective. Table 5-T shows the case for full-width spoiler bars in all cylinders and the Yankee dryer. With the 161 g/m^2 sheet, the increase in speed attributable to the spoiler bars is 1.6 % with the original machine, 2.4 % with the Yankee dryer. For the 127 g/m^2 sheet the relative increase is larger, 3.3 % to 6.6 %. The actual speed increase from spoiler bars with a Yankee is more than double that without (39 vs. 16 m/min) because of the higher base speed with the Yankee.

In total, by modifying the machine layout, adding a Yankee dryer after the existing 48 cylinders and installing full-width spoiler bars in all cylinders, linerboard production can be increased an impressive 26-29 %. The machine speed increases with Yankee dryer Modification 2 plus spoiler bars are larger than the two summed individual contributions because of the increased effectiveness of spoiler bars at the higher machine speed with the Yankee dryer.

Table 5-T: Machine Speed: Red Rock Machine #1-Yankee Modification 2 plus Spoiler Bars

	127 g/m^2	161 g/m^2
Machine speed		
Original	497 m/min	358 m/min
Original plus Full Spoilers	513 m/min	364 m/min
Speed Increase from Original	3.3 %	1.6 %
Yankee Dryer Modification 2	588 m/min	450 m/min
Speed Increase from Original	18.3 %	25.7 %
Yankee Dryer Modification 2 plus Full Spoilers	627 m/min	461 m/min
Speed Increase from Original	26.2 %	28.8 %
Speed Increase from Original plus Full Spoilers	22.2 %	26.6 %
Speed Increase from Yankee Dryer	6.6 %	2.4 %

5.4 Red Rock Linerboard Machine #2

5.4.1 Current Operation

Figure 5-33 and Tables 5-U, 5-V and 5-W specify this machine producing 183, 205 and 337 g/m^2 linerboard from the same furnish as Machine #1. To this 85 cylinder dryer section, notably with 36 unfelted cylinders, the most recent modification was a new press and addition of the fifth dryer section. There is pocket ventilation in the first two sections only, with the air temperature and humidity obtained from mill data.

Table 5-U: Design Specifications: Red Rock Machine #2

Variables	S.I. Units	Alternate Units
Cylinder diameter	1.524 m	5 ft
Cylinder shell thickness (Cyl.1-71)	27 mm	1.1 inch
Cylinder shell thickness (Cyl.72-85)	30 mm	1.2 inch
Machine trim	5.73 m	19 ft
Draw length	1.35 m	4.4 ft
Sheet wrap angle	220°	
Felt wrap angle	180°	
Felt thickness	1.8 mm	0.07 inch
Sheet length in dryer	343 m	1125 ft
Spoiler bars	none	

Section 1 Cyls.1-6 Double Felting

Section 2 Cyls.7-18 Double Felting

Section 3 Cyls.19-38 Top Felting

Section 4 Cyls.39-71 Top Felting (39-54) No Felting (55-71)

Section 5 Cyls.72-85 Double Felting

Figure 5-33: Dryer Section: Red Rock Machine #2

Section 1 Cyls.1-6 Double Felting

Section 2 Cyls.7-18 Double Felting

Section 3 Cyls.19-38 Double Felting

Section 4 Cyls.39-71 Double Felting

Section 5 Cyls.72-85 Double Felting

Figure 5-34: Dryer Section: Red Rock Machine #2-Felting Modification

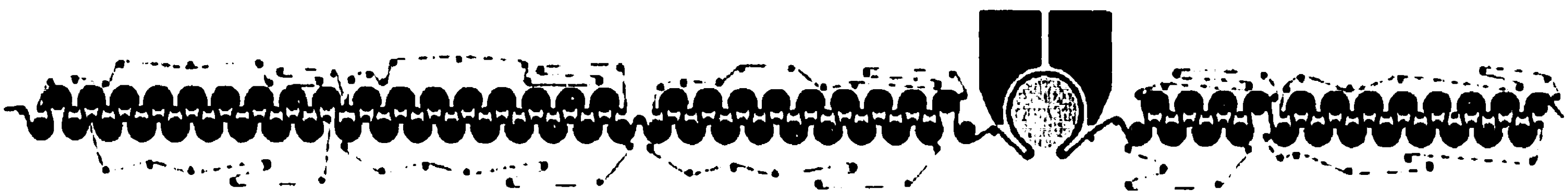

Section 1 Cyls.1-6 Double Felting

Section 2 Cyls.7-18 Double Felting

Section 3 Cyls.19-38 Double Felting

Section 4a Cyls.39-54 Double Felting

Yankee Dryer

Section4b Cyls.64-71 Double Felting

Section 5 Cyls.72-85 Double Felting

Figure 5-35: Dryer Section: Red Rock Linerboard #2-Yankee Modification 4

Table 5-V: Current Operating Conditions: Red Rock Machine #2

Variable	183 g/m^2		205 g/m^2		337 g/m^2	
	S.I. Units	Alternate	S.I. Units	Alternate	S.I. Units	Alternate
Machine speed	564 m/min	1850 fpm	558 m/min	1830 fpm	372 m/min	1220 fpm
Drying time	36.5 s		36.9 s		55.3 s	
Dry sheet caliper	258 microns		295 microns		475 microns	
Sheet inlet moisture	1.22 kg/kg dry	45 % solids	1.22 kg/kg dry	45 % solids	1.22 kg/kg dry	45 % solids
Sheet exit moisture	0.06 kg/kg dry	94.3 % solids	0.065 kg/kg dry	93.9 % solids	0.07 kg/kg dry	93.5 % solids
Sheet inlet temperature	45°C	113°F	45°C	113°F	45°C	113°F
Fibre satn. point	0.8 kg/kg dry	55.6 % solids	0.8 kg/kg dry	55.6 % solids	0.8 kg/kg dry	55.6 % solids
Condensing Steam	S.I. [kPag/°C] and Alternate [psig/°F]					
Section 1	550/162°	80/324°	662/168°	96/335°	758/173°	110/344°
Section 2	650/168°	94/334°	738/172°	107/342°	758/173°	110/344°
Section 3	700/170°	101/339°	814/176°	118/349°	814/176°	118/349°
Section 4	725/172°	105/341°	750 /173°	109/343°	786/174°	114/345°
Section 5	800/175°	116/348°	800/175°	116/348°	800/175°	116/348°

Table 5-W: Current Operation Pocket Conditions: Red Rock Machine #2

Variable	Temperature		Humidity	Relative Humidity	Wet Bulb Temperature
	°C	°F	kg/kg dry air	%	°C
Cylinders 1-18	55	130	0.11	97	54
Cylinders 19-85	38	100	0.04	92	37

Uncalibrated validation simulations, Table 5-X, show good agreement for the heaviest linerboard, but significant over-drying for the two lighter grades. As this machine has 85 cylinders, any errors seen in a typical machine (ca. 40-50 cylinders) simulation are doubled with twice as many cylinders.

Table 5-X: Uncalibrated Validation for Red Rock Machine #2: Current Operations

	183 g/m^2	205 g/m^2	337 g/m^2
Exit moisture content			
Validation simulation	3.3 % d.b.	4.4 % d.b.	7.8 % d.b.
Measured	6.0 % d.b.	6.5 % d.b.	7.0 % d.b.
Machine speed			
Validation simulation	657 m/min	609 m/min	366 m/min
Measured	564 m/min	558 m/min	372 m/min
Difference	+ 16.4 %	+ 9.1 %	- 1.6 %

From the drying history for simulations calibrated to current operating conditions, Figures 5-36 to 5-41, the development and decline of the moisture content difference in the thickness direction across the top third of the sheet is seen to reach a maxima of 0.85 kg/kg dry (cylinder #17) for 183 g/m^2 sheet, 1.1 kg/kg dry (cylinder #11) for the 337 g/m^2 grade. For thick linerboard even under the low intensity cylinder drying, such thickness direction gradients, to more than 75 % of the entering moisture content, are especially important when considering rebuilds to add a high intensity technique such as a Yankee dryer or a gas heated conduction cylinder dryer. Pilot dryer tests done using paper at a uniform inlet moisture content, as is unavoidable, will show drying rates substantially in excess of those that would be achieved in a dryer section at the same sheet average inlet moisture content but with an entering thickness direction profile of the magnitude shown on Figures 5-36 and 5-37. The substantial size of this error was shown for the case of the Mississauga linerboard machine, section 5.2.2. As such pilot plant dryer tests are thereby incapable of providing valid drying rate measurements, use of a simulator based on a microscale model, the *Drying Doctor* simulator, is necessary.

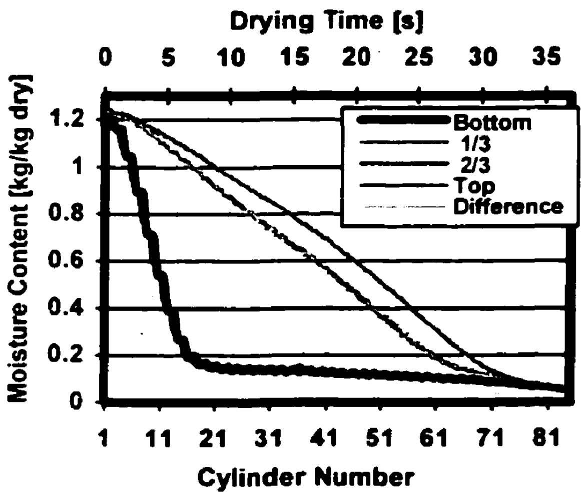

Figure 5-36: Local Moisture Content: Red Rock Machine #2-183 g/m^2

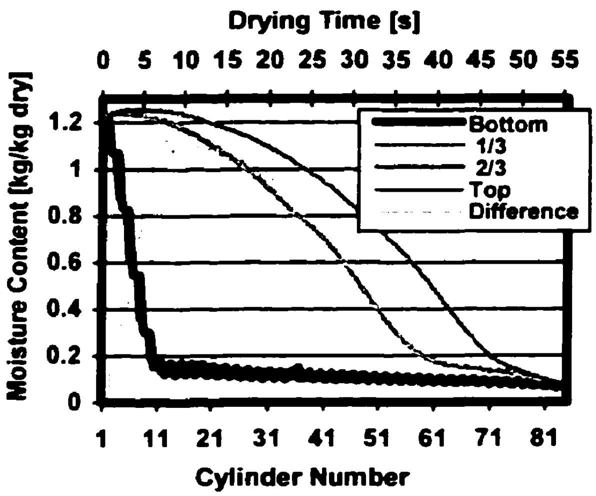

Figure 5-37: Local Moisture Content: Red Rock Machine #2-337 g/m^2

The sheet temperature evolution, Figures 5-38 and 5-39, shows the short heat-up zone, a long constant rate period at the wet bulb temperature, and the rise during the falling rate drying period. With the heavier sheet there is naturally, for the same drying conditions, a longer heat up zone and a larger temperature difference across the sheet, to about 15°C instead of 10°C from the center to surface. During the falling rate period of increasing sheet temperature, the combination of significant ΔT across the sheet with negligible moisture difference, Figures 5-36 and 5-37, shows that mass transfer has ceased to be a factor, with drying now essentially heat transfer controlled.

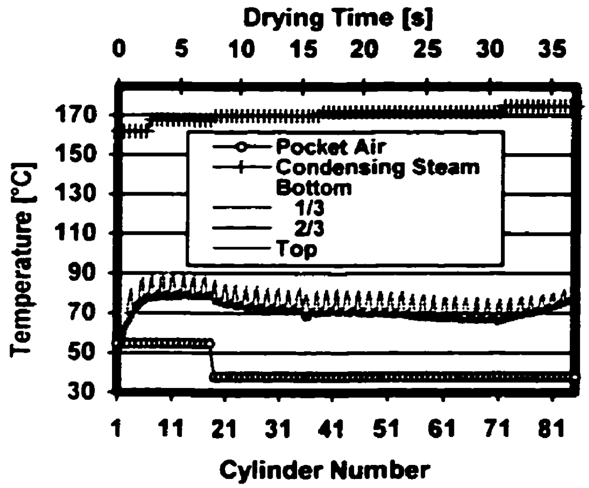

Figure 5-38: Local Temperature Profiles: Red Rock Linerboard Machine #2-183 g/m²

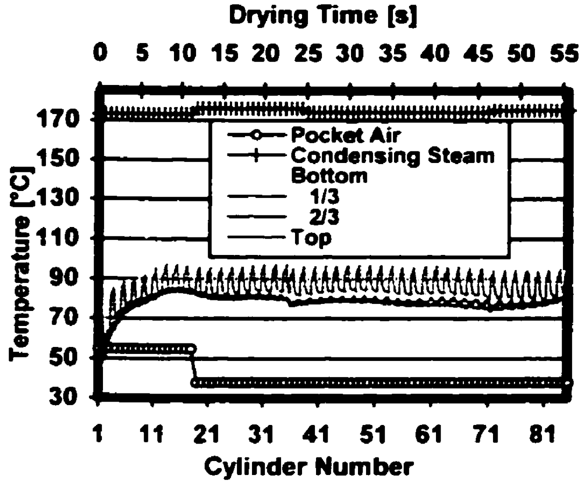

Figure 5-39: Local Temperature Profiles: Red Rock Linerboard Machine #2-337 g/m²

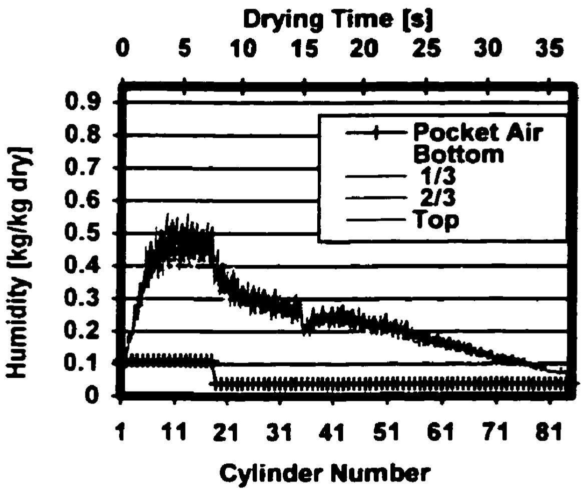

Figure 5-40: Pocket and Local Sheet Pore Air Humidity: Red Rock Machine #2-183 g/m²

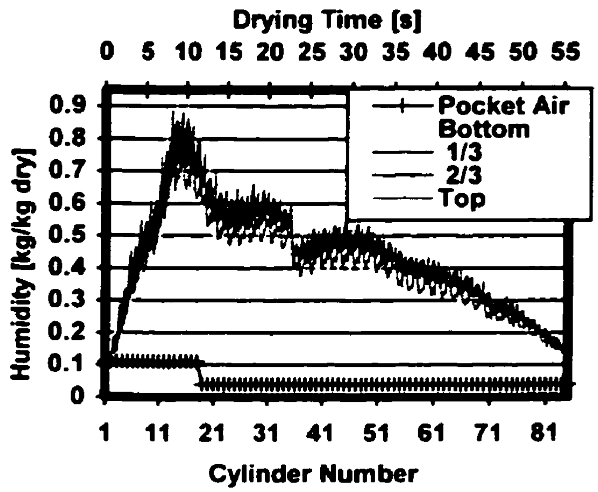

Figure 5-41: Pocket and Local Sheet Pore Air Humidity: Red Rock Machine #2-337 g/m²

Figures 5-40 and 5-41 show the final component of mass transport in the sheet, the local air humidity in the sheet. The thicker sheet has a higher humidity throughout the dryer, expected with the higher temperature of the thicker sheet, Figure 5-38 and 5-39.

5.4.2 Machine Modification Simulation

Modifications of interest to mill staff were felting the unfelted cylinders, spoiler bars, pocket ventilation upgrade and addition of a Yankee dryer.

(a) Felting Modification

Double felting was achieved with felting on the lower tier for 36 cylinders (19-54) and double felting the 17 remaining cylinders (55-71) of the fourth section, Figure 5-34. Calibrated machine speed predictions for this layout showed negligible change. The large thickness direction moisture and temperature gradients, Figures 5-36 to 5-39, show that internal transport resistance controls drying rate, hence addition of felting should not much affect dryer performance, as the simulator confirms.

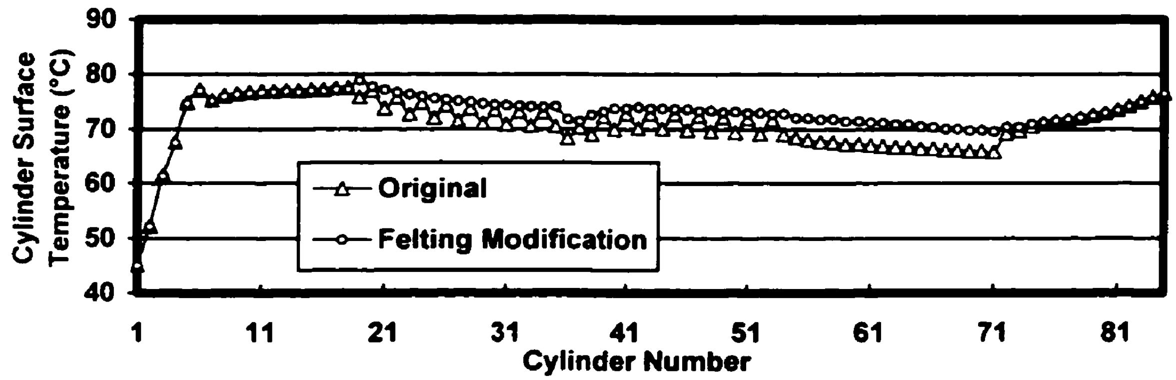

Figure 5-42: Cylinder Surface Temperature: Red Rock Machine #2-Felting Modification-183 g/m^2

In the third and fourth dryer sections, the addition of double felting marginally increases cylinder surface temperature, Figure 5-42, for the 183 g/m^2 grade. With the addition of felting to the lower tier through cylinders 19-50, these cylinders assume the temperature of the original upper cylinders as felting reduces heat loss. The saw-tooth pattern in the original cylinder surface temperature occurred also in the evaporation and condensate flow rate predictions for the cylinders which are top felted only. Addition of the felt eliminates the saw-tooth alternation and, because of the higher sheet temperature, reduces the total condensate rate, Table 5-Y, and therefore the ratio of condensate to water removed. Thus double felting reduces steam consumption with negligible effect on drying rate or machine speed.

Table 5-Y: Condensate Flow Rate: Red Rock Machine #2-Felting Modification

	183 g/m^2		205 g/m^2		337 g/m^2	
	Condensate Flow kg/h	Ratio	Condensate Flow kg/hr	Ratio	Condensate Flow kg/h	Ratio
Original	47,886	1.16	51,543	1.14	54,382	1.10
Felting Modification	47,587	1.15	51,114	1.12	53,640	1.08
% change	-0.6 %	-0.9%	-0.8 %	-1.8%	-1.4 %	-1.8%

(b) Spoiler Bar Modification

With the mill interest in spoiler bars, the effect of full-width spoiler bars to all cylinders was simulated, Table 5-Z. Machine speed increase is naturally more pronounced for the lighter grades as spoiler bar effectiveness in counteracting condensate rimming is proportional to speed.

Table 5-Z: Machine Speed: Red Rock Machine #2-Spoiler Bar Modification

	183 g/m^2	205 g/m^2	337 g/m^2
Machine speed			
Original	564 m/min	558 m/min	372 m/min
Spoiler Bar Modification	583 m/min	573 m/min	375 m/min
% change	+ 3.4 %	+ 2.7 %	+ 0.8 %

(c) Pocket Ventilation Modification

Another option of interest at the mill concerned pocket ventilation. Modification to supply 120°C air to all pockets at 14 m^3/min-m width, the default conditions of *Drying Doctor*, showed a significant increase in machine speed, Table 5-AA, even for the heaviest sheet with greatest internal resistance, with the effect becoming more important as sheet thickness decreases. Such significant increases are not surprising because the ineffective ventilation currently in use, Table 5-W, indicates that the cool pocket air is almost saturated.

Table 5-AA: Machine Speed: Red Rock Machine #2-Pocket Ventilation Modification

	183 g/m^2	205 g/m^2	337 g/m^2
Machine speed			
Original	564 m/min	558 m/min	372 m/min
Pocket Ventilation Modification	651 m/min	625 m/min	400 m/min
% change	+15.4 %	+12.0 %	+7.5 %

The effects of sheet thickness are seen also in cylinder surface temperature, Figure 5-43, the saw-tooth pattern of Figure 5-42 being seen again due to the felting. As sheet thickness and hence, internal transport resistance increases, ΔT across the sheet increases and cylinder surface temperature increases correspondingly. Thus sheet and cylinder surface temperature move together. Comparison of Figures 5-45 and 5-38 shows the expected result that the increased evaporation in the dryer pockets produces cooler sheet temperatures, while Figure 5-46 shows sheet air pore and pocket air humidities correspondingly much lower than Figure 5-40. A cooler sheet from more

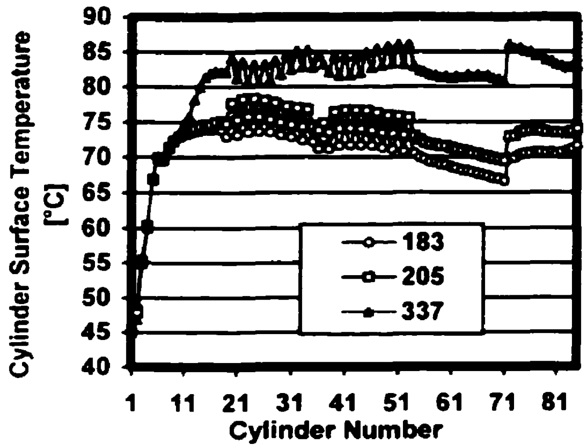

Figure 5-43: Cylinder Surface Temperature: Red Rock Machine #2- PV Modification

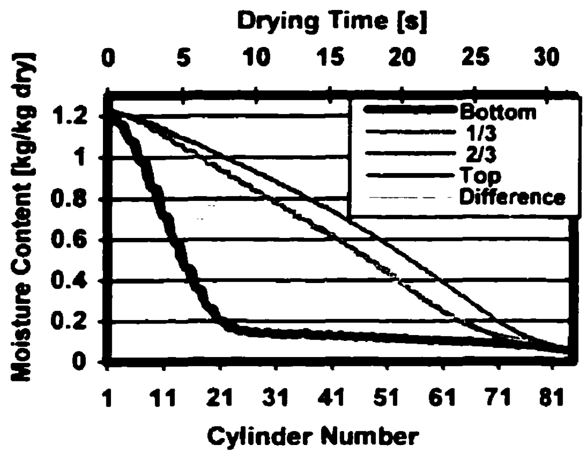

Figure 5-44: Local Moisture Content: Red Rock Machine #2- PV Modification-183 g/m^2

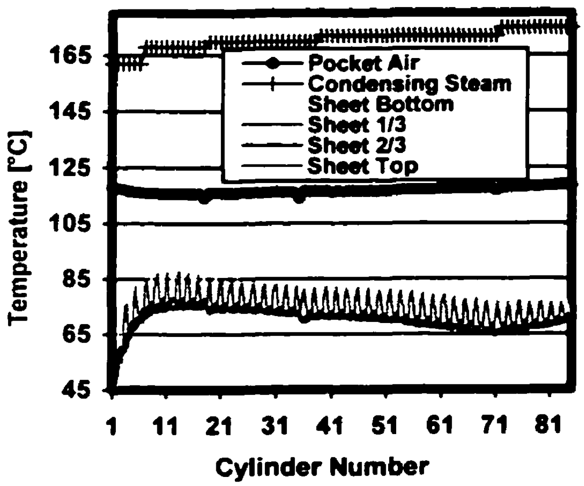

Figure 5-45: Local Temperature Profiles: Red Rock Machine #2- PV Modification-183 g/m^2

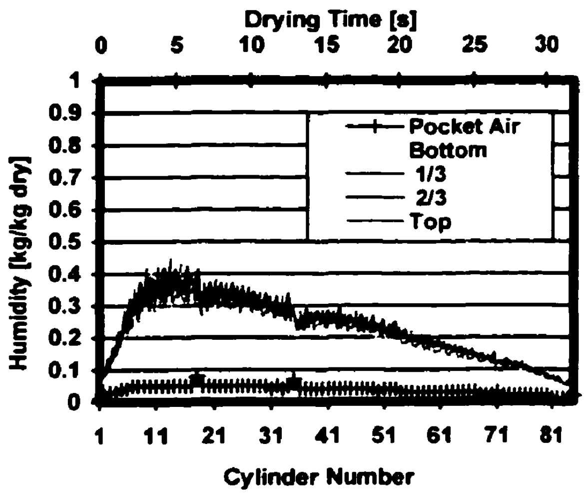

Figure 5-46: Pocket and Local Sheet Pore Air Humidity: Red Rock Machine #2- PV Modification-183 g/m^2

drying in the pockets also provides a higher ΔT for heat conduction from the dryer cylinders and the higher drying and condensation rates reflected in Tables 5-AA and 5-BB. Although improved pocket ventilation also improves the cylinder drying component, comparison of Tables 5-AA and 5-BB show that the increase in machine speed and hence in average drying rate is several times the increase in condensate rate. Thus most of the improvement is from drying in the pockets. Table 5-BB shows that as the sheet gets thicker, improved pocket ventilation becomes less effective, leading to a smaller reduction in condensate to water removal ratio. Therefore the lower the basis weight, the more effective the pocket ventilation, the greater the amount of air convection drying in the pockets, hence the larger the reduction in the ratio of steam required to water removed. An important practical consequence is that the *Drying Doctor* simulator enables searching for the economic optimum in water removal by the compensating processes of conduction drying over steam heated cylinders and convection drying in dryer pockets.

Table 5-BB: Condensate Flow Rate: Red Rock Machine #2-PV Modification

	183 g/m^2		205 g/m^2		337 g/m^2	
	Condensate Flow kg/h	Ratio	Condensate Flow kg/hr	Ratio	Condensate Flow kg/h	Ratio
Original	47,886	1.16	51,543	1.14	54,382	1.10
PV Modification	49,423	1.04	52,114	1.02	54,552	1.02
% change	+3.2 %	-10.3 %	+1.1 %	-10.5 %	+0.3 %	-7.2 %

(d) Pocket Ventilation and Spoiler Bar Modification

Table 5-CC gives the machine speed predictions for the combination of the three previous modifications: addition of double felting to the third and fourth sections, installation of spoiler bars in all cylinders, and supply to all pockets of 120°C air at 14 m^3/min-m width. The increases predicted with all modifications for the two lighter grades have an increase in machine speed greater than the sum of individual contributions. This compounding is due to the increased effectiveness of spoiler bars at the higher speed resulting from the pocket ventilation modification. The machine speeds predicted for all modifications combined, ranging from 9 % for the heaviest sheet, to a 21 % increase for the 183 g/m^2 sheet, are examined below.

Table 5-CC: Machine Speed: Red Rock Machine #2-PV and Spoiler Bar Modification

	183 g/m^2	205 g/m^2	337 g/m^2
Machine speed			
Original	564 m/min	558 m/min	372 m/min
PV Modification			
% change	+15.4 %	+12.0 %	+7.5 %
Spoiler Bar Modification			
% change	+3.4 %	+2.7 %	+0.8 %
All Modifications	681 m/min	654 m/min	405 m/min
% change	+ 20.7 %	+17.2 %	+8.8 %

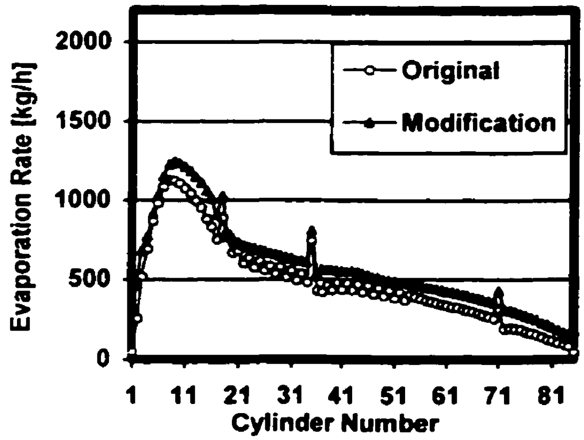

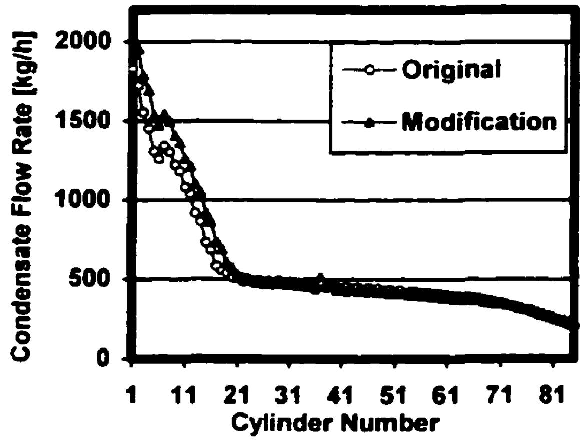

Figure 5-47: Evaporation Rate -Red Rock Machine #2-PV and Spoiler Bar Modification-183 g/m^2

Figure 5-48: Condensate Flow Rate -Red Rock Machine #2-PV and Spoiler Bar Modification-183 g/m^2

Table 5-DD: Condensate Flow Rate: Red Rock Machine #2-Felting, PV and Spoiler Bar Modification

	183 g/m^2		205 g/m^2		337 g/m^2	
	Condensate Flow kg/h	Ratio	Condensate Flow kg/h	Ratio	Condensate Flow kg/h	Ratio
Original	47,886	1.16	51,543	1.14	54,382	1.10
Modification	51,092	1.03	53,810	1.01	54,625	1.01
% change	+6.7 %	-11.2 %	+4.4 %	-11.4 %	+0.5%	-8.2%

As Table 5-CC makes clear, the drying rate enhancement of Figure 5-47 comes mostly from improved pocket ventilation and only secondarily from spoiler bars. As the latter effect directly increases steam condensation it might be expected that the increase in condensate flow, Figure 5-48, would be relatively much less significant than for the evaporation rate, Figure 5-47. Table 5-DD shows that the increase in condensate rate is indeed less than that for drying rate, Figure 5-47 and Table 5-CC, but is still substantial. As the Figure 5-45/38 comparison showed, better pocket ventilation can produce cooler sheets, a cause of the higher condensation rates recorded on Figure 5-48, the other cause being the spoiler bars. As Table 5-DD shows, although the condensate rate increases, by 0.5 to 6.7 %, the ratio condensate to evaporation decreases around 10% for all grades, reflecting the greater proportion of water removal by air convection drying in the pockets.

(e) Yankee Modifications

As this machine has had a fifth dryer section added, space limitations require removal of 9 cylinder dryers to provide the 7.6 m to accommodate the Yankee dryer, Table 5-EE. Machine layout and operation of the remaining steam-heated cylinder dryers are the original conditions for each grade. Five Yankee dryer locations were considered:

- Modification 1: Yankee dryer replaces cylinders 1-9
- Modification 2: Yankee dryer replaces cylinders 19-27
- Modification 3: Yankee dryer replaces cylinders 36-44
- Modification 4: Yankee dryer replaces cylinders 55-63
- Modification 5: Yankee dryer replaces cylinders 77-85

Table 5-EE: Dryer Specifications and Operating Conditions: Red Rock Machine #2-Yankee Dryer Modification of Original Machine

Variables	S.I. Units	Alternate Units
Cylinder diameter	3.66 m	12 ft
Cylinder shell thickness	25 mm	1 inch
Condensing steam	700 kPag/170°C	101 psig/339°F
Nozzle diameter	5 mm	0.2 inch
Nozzle to web distance	20 mm	0.8 inch
Nozzle spacing/nozzle diameter	4	
Nozzle plate open area ratio	2 %	
Nozzle pattern	equilateral triangle	
Wrap angle before hood	20°	
Wrap angle inside hood	230°	
Wrap angle inside hood	20°	
Sheet length in Yankee	8.6 m	28.3 ft
Draw before and after Yankee	1.2 m	3.9 ft
Total sheet length in dryer	317.7 m	1042 ft
Jet temperature	350°C	662 °F
Jet humidity	0.15 kg/kg dry air	
Jet velocity	100 m/s	20,000 fpm

The *Drying Doctor* simulator predictions, Table 5-FF and Figure 5-49, show that the Yankee dryer position plays an important role. For the 337 g/m^2 product, the

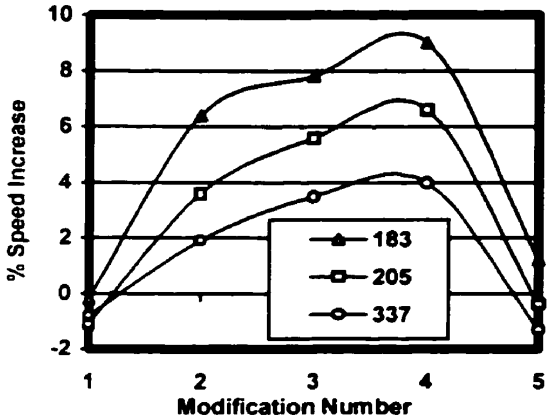

Figure 5-49: Machine Speed Increase from Original: Red Rock Machine #2- Yankee Dryer Modifications

production increases with this modification are small, a maximum of 4.0 % with Modification 4. The lower speed increases of Modification 1 (Yankee at wet end) reflect the increase in drying rate from impinging jets being insufficient to compensate for the loss in drying from the 9 cylinders replaced. The low speed increases of Modification 5 (Yankee at dry end) are a result of insufficient time after the Yankee dryer to allow the high sheet temperature to aid in desorption of bound moisture from the sheet. For all other modifications the increase in machine speed from the Yankee dryer is greater for lighter grades, with 6.6 % and 9.0 % increases for 205 and 183 g/m^2 linerboard for Modification 4. The most effective technique for increasing machine speed of those examined in the preceding sections (a)-(d), was the pocket ventilation change, section (c), recorded in Table 5-AA. Those increases from improved pocket ventilation, ranging from 7 to 15 % depending on the grade, are substantially larger than can be obtained by addition of a Yankee dryer which, for the best location, are in the 4 to 9 % range.

Table 5-FF: Machine Speed: Red Rock Machine #2-Yankee Dryer Modification of Original Machine

	Original	Modification (Cylinders replaced)				
		1 (1-9)	2 (19-27)	3 (36-44)	4 (55-63)	5 (77-85)
183 g/m^2	564 m/min change	563 m/min -0.2 %	600 m/min +6.4 %	608 m/min +7.8 %	615 m/min +9.0 %	571 m/min +1.2 %
205 g/m^2	558 m/min change	552 m/min -1.1 %	578 m/min +3.6 %	589 m/min +5.6 %	595 m/min +6.6 %	556 m/min -0.4 %
337 g/m^2	372 m/min change	369 m/min -0.8 %	379 m/min +1.9 %	385 m/min +3.5 %	387 m/min +4.0 %	367 m/min -1.3 %

For Modification 4 the local moisture and temperature drying histories for the lightest and heaviest grades, Figures 5-50 to 5-53, show the development and decline of very large thickness direction moisture gradients and the sharp increase in sheet temperature in the Yankee dryer. In the 183 g/m^2 grade the Yankee dryer eliminates the difference in moisture gradient between the impingement surface and the 2/3 position, Figure 5-50, and greatly reduces the even larger moisture difference over this region of

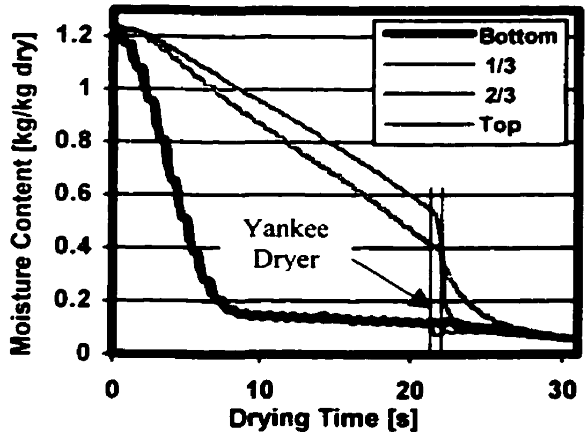

Figure 5-50: Local Moisture Content: Red Rock Machine #2- Yankee Dryer Modification 4 of Original Machine-183 g/m^2

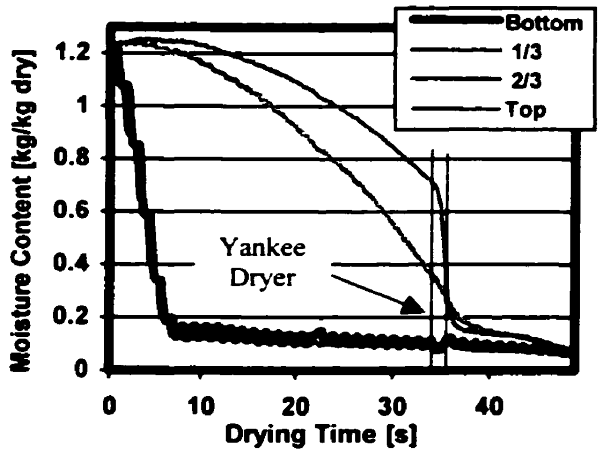

Figure 5-51: Local Moisture Content: Red Rock Machine #2- Yankee Dryer Modification 4 of Original Machine-337 g/m^2

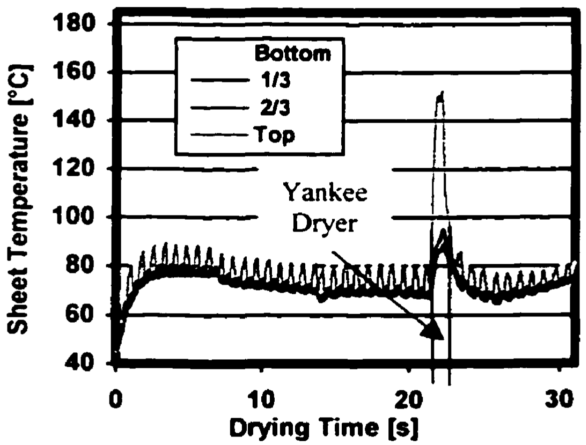

Figure 5-52: Local Sheet Temperature: Red Rock Machine #2- Yankee Dryer Modification 4 of Original Machine-183 g/m^2

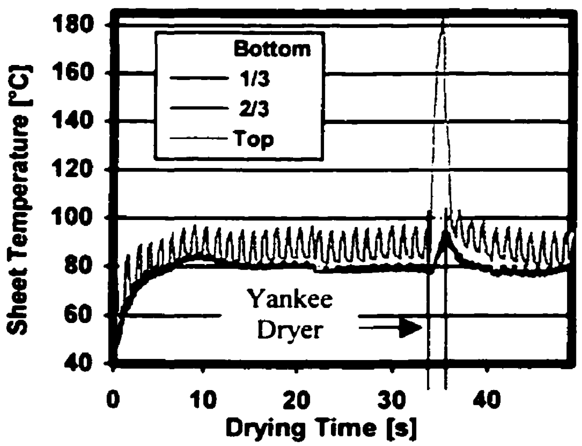

Figure 5-53: Local Sheet Temperature: Red Rock Machine #2- Yankee Dryer Modification 4 of Original Machine-337 g/m^2

the 337 g/m^2 sheet. As discussed in connection with Figures 5-28 and 5-30, the Yankee dryer impinging jets strongly increase the temperature of low moisture content sheets, aiding desorption of water from fibres in the latter part of the falling rate drying period. For the 337 g/m^2 grade, the top side of the sheet is heated momentarily to 185°C in the Yankee dryer, 20°C more than with the lightest sheet because of the slower machine speed.

Combination of the previous modifications is now examined, i.e. Yankee dryer added the dryer section upgraded with full-width spoiler bars and a good ventilation air

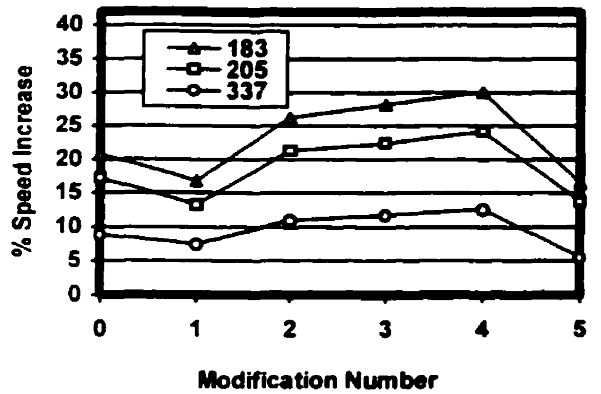

Figure 5-54: Machine Speed: Red Rock Machine #2- Yankee Dryer Modifications with PV and Spoiler Bars

supply, Figure 5-35. The simulation results are shown in Table 5-GG and Figure 5-54. The machine speed increases are relative to the modifications of section (d) with improved pocket ventilation and spoiler bars, denoted as Modification 0 in Table 5-GG. The trend of low speeds for Modifications 1 and 5 is similar to that of the Figure 5-49 modifications.

Table 5-GG: Machine Speed: Red Rock Machine #2-Yankee Dryer Modification with PV and Spoiler Bars

	Section (d) Mod. 0	Modification (Cylinders replaced) 1 (1-9)	2 (19-27)	3 (36-44)	4 (55-63)	5 (77-85)
183 g/m^2	681 m/min % change	659 m/min -3.2 %	712 m/min +4.6 %	723 m/min +6.2 %	734 m/min +7.8 %	657 m/min -3.5 %
205 g/m^2	654 m/min % change	632 m/min -3.4 %	677 m/min +3.5 %	683 m/min +4.4 %	693 m/min +6.0 %	635 m/min -2.9 %
337 g/m^2	405 m/min % change	400 m/min -1.2 %	413 m/min +2.0 %	416 m/min +2.7 %	419 m/min +3.5 %	393 m/min -3.0 %

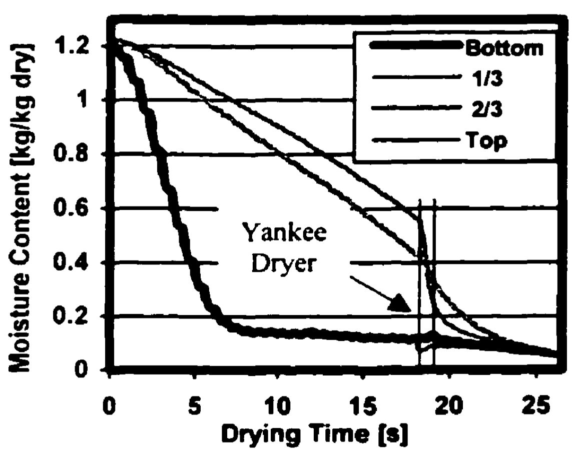

Figure 5-55: Local Moisture Content: Red Rock Machine #2- Yankee Dryer Modification 4 of with PV and Spoiler Bars-183 g/m^2

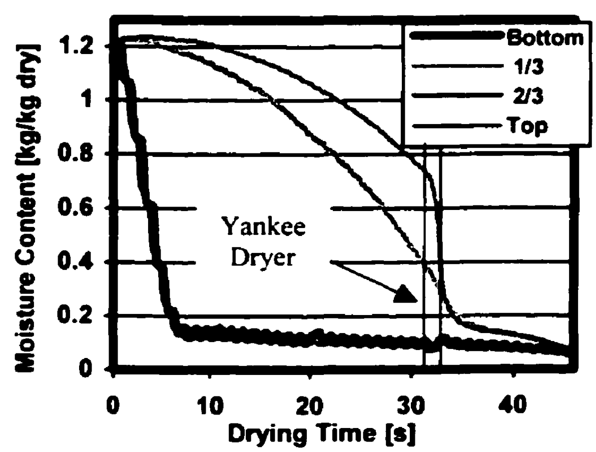

Figure 5-56: Local Moisture Content: Red Rock Machine #2- Yankee Dryer Modification 4 with PV and Spoiler Bars-337 g/m^2

For the best alternative including a Yankee, i.e. Modification 4, Figures 5-55 and 5-56 record the local moisture predictions. Comparison with Figures 5-50 and 5-51, (no pocket ventilation or spoiler bar changes) shows little difference with the increased machine speed possible.

(f) Summary

Table 5-HH summarizes these *Drying Doctor* predictions. Upgrading the pocket ventilation provides by far the largest single improvement, 7 to 15 % machine speed increases, depending on the grade. The second largest single increase is by replacement of 9 cylinders by a Yankee dryer, giving 4 to 9 % speed increase, followed by 1 to 3 % increase from spoiler bars. The combined modifications exceed the sum of the individual contributions for the two lighter grades because of a compounding effect at higher machine speeds. With the large speed increases from the pocket ventilation and Yankee modifications, the additional effect of adding spoiler bars is much larger than with only spoiler bar addition.

Table 5-HH: Machine Speed: All Red Rock Machine #2 Modifications

	183 g/m^2	205 g/m^2	337 g/m^2
Current Operation	564 m/min	558 m/min	372 m/min
MODIFICATIONS	% Speed Increase Predicted		
Double Felting	0 %	0 %	0 %
Spoiler Bars	3.4 %	2.7 %	0.8 %
Yankee Modification 4 with Current Operations	9.0 %	6.6 %	4.0 %
Pocket Ventilation	15.4 %	12.0 %	7.5 %
Felting, PV and Spoiler Bars	20.7 %	17.2 %	8.8 %
Yankee Modification 4 with Felting, PV and Spoiler Bars	30.1 %	24.2 %	12.6 %

The demonstration with the *Drying Doctor* simulator that improved pocket ventilation offers the largest single way of improving dryer performance indicates the strong incentive for thorough exploration of alternate pocket ventilation systems.

Although only one specification of pocket ventilation was demonstrated, the detailed analysis of moisture content, temperature and humidity with the microscale model of the *Drying Doctor* simulator is shown to provide an understanding of the interaction between these variables and dryer performance. This knowledge may be put to good use, for example, in examining alternate pocket ventilation system specifications in order to determine an economic optimum in water removal by the complimentary processes of conduction drying over steam heated cylinders and air convection drying in dryer pockets.

6 CONCLUSIONS

6.1 *Paper Drying Model Structures*

The paper drying process is complex through the involvement of several mechanisms for transport of moisture, water vapor and heat within and adjacent to the sheet and the high sensitivity of the rate of these transport processes to the local moisture content and temperature of the sheet. A comparison of model structures showed that for a simulation to satisfactorily predict the sheet drying history, it must include the following:

- Modeling of both the sheet and the external systems
- Microscale modeling of the three transport processes within the sheet without simplifying assumptions
- Machine speed prediction capability without intervention of the user
- Robust graphical user interface
- Multiple technique drying capabilities

The *Drying Doctor* simulator is the only known package that includes all of these requirements.

6.2 *Industrial Validation*

The *Drying Doctor* simulator underwent substantial further development from experience gained during extensive validation and testing using industrial data. The simulator was shown capable of reliable prediction for grades varying from 19 g/m^2 tissue to 430 g/m^2 containerboard. Through use of the microscale model the papermachines simulated included traditional steam heated conduction cylinder dryers, Yankee air impingement dryers and the combination of them for multiple technique dryer sections. The necessity of a microscale model was demonstrated for the most demanding cases of light weight grades dried under high intensity drying processes and heavy sheets dried under low intensity drying conditions.

With 31 validation simulations, the average error of predicted machine speed relative to actual speed was +0.6 %, indicating a small systemic error in the simulation leading to slight over-prediction of drying. For these 31 validations, the standard deviation of the absolute value of the difference between actual and predicted machine speed is 3.6 %. Only three simulations had a difference significantly larger than 5 %, the limit set for acceptable validation. Thus this dryer simulator may now be considered successfully validated for the drying techniques for which it has been tested.

6.3 Industrial Application to Domtar Containerboard Machines

In the Trenton corrugated medium machine, the dryer section was shown to be operating near full capacity. With increased steam pressure to all dryer cylinders, production increases would be limited to around 10%. For a projected future machine rebuild, this simulation indicated that the current machine would be capable of drying only the lighter weight grades at the desired speed increase. Thus the rebuild must include significant modifications to the press or dryer section.

The linerboard machine in Mississauga currently has an unused size press between the third and fourth dryer sections. With the simulator the effect of adding a Yankee air impingement dryer at this point for increased profitability was evaluated. This configuration would produce a speed increase of 20%. If the actual thickness direction moisture gradients in the sheet as it exits the third dryer section into the Yankee dryer had not been used, as in dryer pilot plant tests or with a dryer simulator not using a microscale model, drying would be over predicted by 17%. Thus the reality of large internal gradients in the sheet, important for paper quality, are demonstrated to be important for process engineering considerations as well.

Several options were examined for papermachine #1 in Red Rock. The simulator was used to investigate the preferred location for adding an air impingement Yankee dryer. For the optimum location, machine speed increases of 18-26% were found, depending on basis weight. This entire potential speed increase could be lost by not choosing the optimum location as determined with the simulator. The effectiveness of spoiler bars was demonstrated to be minimal if installed in the current configuration, but if added along with an air impingement dryer, spoiler bars would increase machine speed by up to an additional 6%.

For papermachine #2 at Red Rock, the modification giving the largest speed increase would be improvement of the pocket air ventilation system to supply a higher flow rate of warmer air. Just this modification would increase machine speed by 7.5% for the heaviest 337 g/m^2 sheet, by an impressive 15% for the lightest grade of 183 g/m^2. Spoiler bars alone would increase speed by only 1 to 3% due to the current low machine speed but this increase could be more than doubled if carried out in conjunction with improved pocket ventilation. The multiple technique capability of the simulator was again used to optimize the location for adding an air impingement Yankee dryer. This modification, when implemented with the pocket ventilation system improvement and installation of spoiler bars as well, would enable an impressive increase in machine speed by up to 30% for 183 g/m^2 linerboard.

6.4 Recommendations for Future Work

- Improve cylinder report to include Yankee air impingement dryers as well as all other drying processes simulated
- Improve cylinder report to include sheet average temperature, often measured in dryer surveys
- Include plot for water vapor flux as a function of time for the four points displayed
- Investigate and improve the predictions of sheet and cylinder surface temperatures (present study includes diagnosis of the cause of low cylinder surface predictions)
- Improve simulation for unirun felting cylinders to include effects from the felt-cylinder contact and to account for this in condensate calculations
- Improve Yankee air impingement simulation to update boundary conditions at each time step
- Allow specification of dryer pocket ventilation air supply humidity
- Improve calibration mode to allow specification of moisture contents throughout the dryer section and to use a different calibration parameter for air impingement drying
- Improve default dryer pocket conditions to appropriate levels, including use of an appropriate profile through the dryer section
- Increase output resolution of pore air humidity in graphs
- Allow access to calculated data at every node used in the simulation

7 REFERENCES

Abbott, R.D., Edwards, L.L., Fischer, F.B. and Dimond, P.M., 1984, Linerboard Drying: Model Development and Heat Transfer Coefficient Determination, *Proc. Tappi Engineering Conference*, pp.241-252

Asensio, M.C. and Seyed-Yagoobi, J., 1992, Further Analysis of Heat and Mass Transfer in a Paper Sheet During Drying, *HTD, Vol. 193,* ASME National Heat Transfer Conference, San Diego

Asensio, M.C. and Seyed-Yagoobi, J., 1992, Theoretical Drying Study of Single-tier vs. Two-tiered Dryer Configurations, *Tappi Journal* 75(10), pp.203-211

Asensio, M.C., Seyed-Yagoobi, J., Lehtinen, J.A., Karlsson, M.A., Timofeev, O.N. and Kuppi, K., 1994, Comparison of Several Multi-Cylinder Paper Drying Simulation Models, *Drying '94*, Hemisphere Publishing Corporation, pp. 1171-1178

Bell, D.O., Seyed-Yagoobi, J. and Fletcher, L.S., 1990, Recent Developments in Paper Drying, *Advances in Drying Vol.5*, Hemisphere Publishing Corporation, pp. 203-261

Bond, J.F., Gomes, V.G. and Douglas, W.J.M., 1996, Computer Simulation of Drying Paper by Multiple Techniques, *Pulp & Paper Canada* 97(12), pp.110-112

Bond, J.F., 1991, Drying Paper by Impinging Jets of Superheated Steam: Drying Rates and Thermodynamic Cycles, *Ph.D. Thesis*, McGill University, Montreal, 175pp

Bond, J.F., Crotigino, M.H. and Douglas, W.J.M., 1992, An Experimental Study of the Falling Rate Period of Super Heated Steam Impingement Drying of Paper, *Drying Technology* 10(4), pp.961-977

Bond, J.F., and Douglas, W.J.M., 1997, Drying of Heavy Paper Products by Impinging Jets of Air or Superheated Steam, Part I: Experimental Results

Bond, J.F., 1998, Personal Communication

CPPA, 1996, Reference Tables

Depoy, J.A., 1972, Analog Computer Simulation of Paper Drying: A Workable Model, *Pulp and Paper Magazine of Canada* 73(5), pp. 67-74

Donner, B.C. and Renk, F.J., 1982, Evaluation and Improvement of Individual Dryer Performance, *Proc. Tappi Papermakers Conference*, pp. 227-236

Eskelinen, P.J., 1985, How to Improve the Paper Machine Performance by Combining Dryer Section Survey and Computer Simulation, *Drying Technology* 3(2), pp.255-269

Farell, M., Dragu, J., Pannersleven, M., Bond, J.F., Douglas, W.J.M. and Kerr, R.B., Accepted for publication in CPPA January, 1999, Integrated Pressing and Drying Simulation of PM7, Domtar, Windsor

Fralic, G., Guertin, D. and Glendenning, S., Computer-Aided Optimization of Company-Wide Drying Operations, *Pulp and Paper Design Project*, McGill University, April 1996

Fralic, G., Glendenning, S., Guertin, D., Kerr, R.B., Bond, J.F. and Douglas, W.J.M., 1997, Computer Aided Engineering of Paper Machine Dryer Sections at Kruger's Bromptonville Mill, TAPPI Conference

Hartley, F.T. and Richards, R.J., 1974, Hot Surface Drying of Paper - The Development of a Diffusion Model, *Tappi* 57(3), pp. 157-160

Heikkilä, P. and Karlsson, M., 1988, Experience Gained from Dryer Section Surveys, *Paperi ja Puu* 70(8), pp.684-687

Hinds, J.A. and Neogi, A.N., 1983, The Dynamic Computer Simulation of a Paper Machine Dryer, *Tappi Journal* 66(6), pp. 79-82

Iida, K., 1985, The Computer Simulation of Web Drying in a Paper Machine Dryer Section, *Preprints Japanese Tappi/CPPA Pulp and Paper Technology Conference*, Tokyo, pp. 115-127

Karlsson, K. and Paltakari, J., 1992, A Simulation Model for Paper Machine Dryer Section, *Drying '92*, Elsivier Science Publishers, pp.913-923

Karlsson, K. and Soininen, M., 1982, The Influence of the Hygroscopic Properties of Paper on the Transient Phenomena During Contact Drying of Paper Webs, *Proc. 3rd International Drying Syposium, Vol.1*, pp.494-503

Kiiskinen, H. and Retulainen, E., 1995, Simulation of Papermaking Processes, *Technical Research Centre of Finland*

Kirk, L.A., 1980, Digital Simulation of the Effect of Operating and Design Variables on the Dryer Section of a Paper Machine, *Paper Technology and Industry* 21(2), pp.61-71

Kirk, L.A., 1984, A Literature Review of Computer Simulation of Paper Drying, *Advances in Drying Vol.3*, Hemisphere Publishing Corporation, New York, pp.1-37

Knight, R.L.C and Kirk, L.A., 1975, Simulation of the Papermachine Drying Section, *Proc. International Water Removal Symposium*, London, pp. 276-278

Kuhasalo, A., 1995, *Challenges Set by High Speed On Dryer Section*, PaperAge, December, pp.16-19

Lampinen, M.J. and Toivonen, K., 1984, Application of a Thermodynamic Theory to Determine Capillary Pressure and other Fundamental Material Properties Affecting the Drying Process, *Drying '84*, Hemisphere Publishing Corporation, pp. 228-244

Lee, P.F. and Hinds, J.A., 1980, Measurement of Heat and Mass Transport within a Sheet of Papermaking Fibers During Drying, *Drying '80*, Hemisphere Publishing Corporation, pp. 523-528

Lee, P.F. and Hinds, J.A., 1981, Modeling Heat and Mass Transfer Within a Moist Sheet of Paper or Board, *Tappi* 64(12), pp.39-44

Lehtikoski, O.I., 1970, A Mathematical Model of the Dryer Section, *Paperi ja Puu* 52(2), pp.63-72

Lemaitre, A., Veyre, J., Lebeau, B. and Foulard, C., 1980, Case Study: Method for Systemic Analysis of Paper Machine Multicylinder Drying Section, *Preprints 4th IFAC Instrumentation and Automation Conference*, Ghent, Belgium, pp.261-270

Lin, S.H., 1991, Moisture Adsorption in Cellulosic Materials, *Ind. Eng. Chem. Res*, 30, pp.1833-1836

Martin, H., 1977, Heat and Mass Transfer Between Impinging Gas Jets and Surfaces, *Adv. Heat Transfer*, vol. 13, Academic Press, pp.1-80

Nault, G. and Maltais, D., 1997, Application of an on-line expert system to optimize dryers and press sections at Domtar Windsor, *Pulp and Paper Canada* , pp.111-113

Navarri. S., 1992, *Mechanisms of Moisture Diffusion in Porous Media*, Journal of Colloid and Interface Science, 154(2), pp.305-315

Niemenmaa, A., Lappalainen, J., Juslin, K. and Laukkanen, I., 1996, Dynamic Modelling and Simulation of Paper Machine Drying Section, *Drying '96 Vol. B*, Hemisphere Publishing Corporation, pp.1157-1164

Nissan, A.H. and Kaye, W.G., 1955, An Analytical Approach to the Problem of Drying of Thin Fibrous Sheets on Multicylinder Machines, *Tappi* 38(7), pp. 385-398

Nissan, A.H. and Hansen, D., 1960, Heat and Mass Transfer Transients in Cylinder Drying: Part I. Unfelted Cylinders, *AIChE Journal* 6(4), pp.606-611

Nissan, A.H. and George, H.H., 1961, Heat and Mass Transfer Transients in Cylinder Drying: Part II. Felted Cylinders, *AIChE Journal* 7(4), pp.635-641

Pearson, D.R., 1986, Modeling Paper Machine Drying on a Microcomputer, *Tappi Journal* 69(9), pp.194-495

Persson, H. and Stenström, S., 1996, Possibilities for Capacity Increase in Dryer Limited Paperboard Machines, *International Dryer Symposium 1996*, Krakow. Poland

Powell, T. and Strong, A.B., 1974, An Analysis of Drying on Conventional Paper Machines, *Pulp and Paper Magazine of Canada* 75(3), pp.71-78

Ramaswamy, S., 1990, Analysis of Heat and Mass Transfer During Drying of Paper/Board Under Conventional and High-intensity Conditions, Ph.D. Thesis, State University of New York, Syracuse, 201pp

Reese, R., 1988, Revised TAPPI Drying-Rate Curves, *Tappi* Dec. 1988, pp. 231-233

Rhodius, D. and Göttsching, L., 1979, Der Trocknungsverlauf von Papier und Pappe in Abhängigkeit von trocknungstechnischen und papiertechnologischen Parametern. Teil IV: Trocknung in der Mehrzylinder-Trockenpartie, *Das Papier* 33(1), pp. 1-9

Robinson, G.W.F., and Baker, C.D., 1989, Understanding and Troubleshooting Papermachine Dryer Sections, *CPPA Publication*, pp.1.13-1.24

Snow, R.H., 1980, Computer Modeling of Drying in Paperboard Machines, *Proceedings of the Tappi Annual Meeting, Atlanta*, pp.243-258

Stenstrom, S., 1997, Mathematical Modeling and Numerical Techniques for Multi-Cylinder Paper Dryers, *Mathematical Modeling and Numerical Techniques in Drying Technology*, Marcel Dekker Inc., pp.613-661

Stenstrom, S., Wilhelmsson, B., Nilsson, L., Krook, R. and Wimmerstedt, R., 1994, Measurement of Reference Experimental Data for the Multi-Cylinder Paper Dryer, *Drying '94*, Hemisphere Publishing Corporation, pp. 1179-1186

Wilhelmsson, B., Nilsson, L., Stenstrom, S. and Wimmerstedt, R., 1993, Simulation Models of Multi-Cylinder Paper Drying, *Drying Technology* 11(6), pp.1177-1203

Wilhelmsson, B., Stenstrom, S., Nilsson, L., Krook, R., Persson, H. and Wimmerstedt, R., 1996, Modeling Multicylinder Paper Drying-Validation of a New Simulation Program, *Tappi Journal* 79(4), pp. 157-167

NET1-1994, Paper Drying Expert System, http://ai.iit.nrc.ca/IR_publc/pma/pdes_desc.html

NET2-1997, APROS/APMS-Advanced PROcess Simulator/Advanced Paper Mill Simulator, VTT, http://www.vtt.fi/aut/tau/ala/apros.htm

NET3-1997, APMS-A Multi-Purpose Tool for Dynamic Simulation of Paper and Board Mills, VTT Automation, http://www.vtt.fi/aut/tau/ala/apms.htm

A *DRYING DOCTOR* FORMS

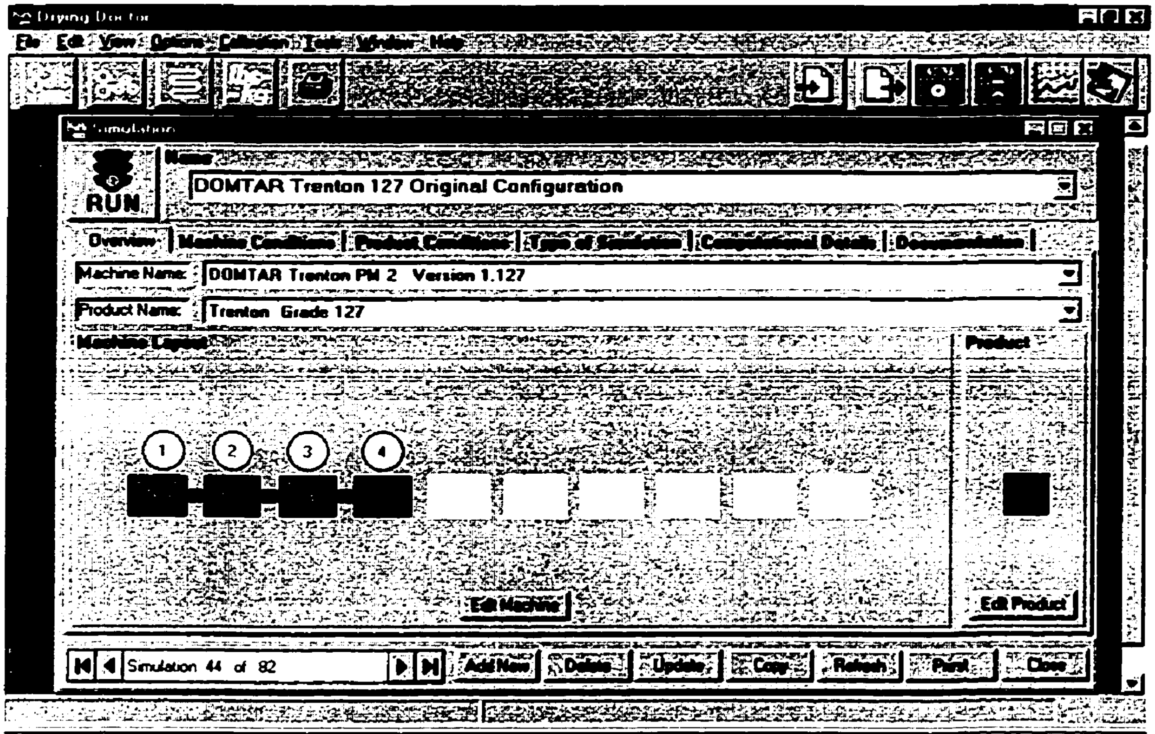

Figure A-1: Current Simulation Form-Overview Tab

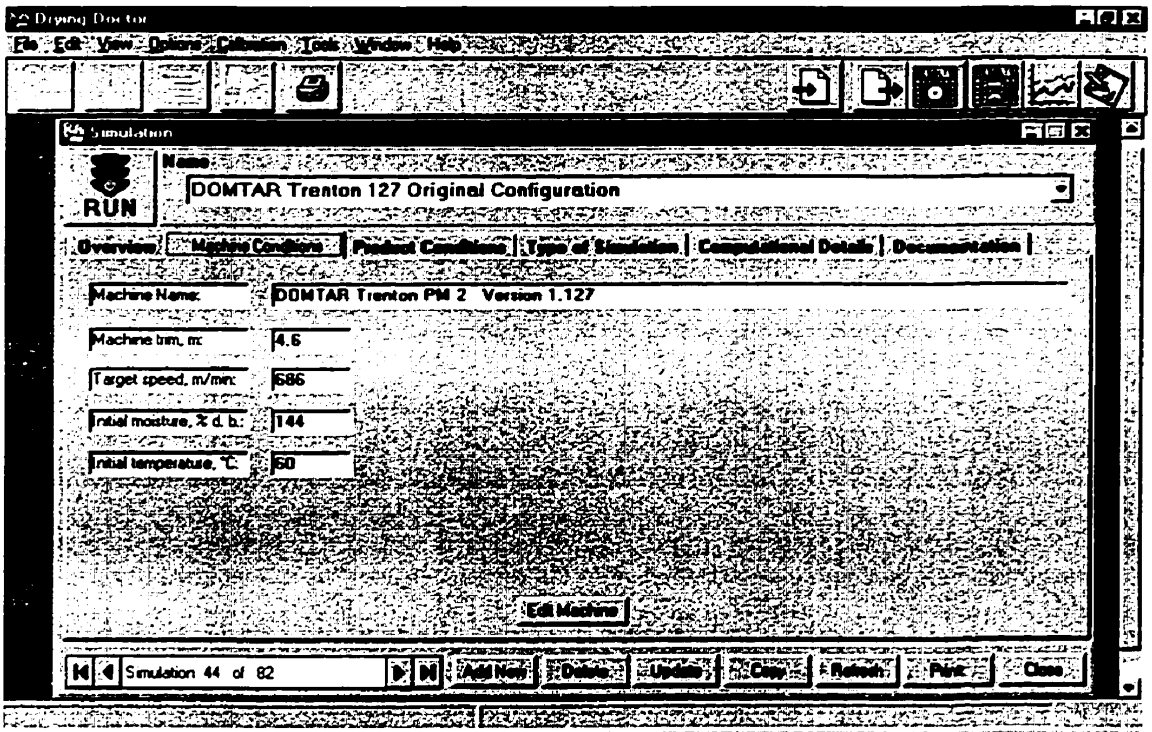

Figure A-2: Current Simulation Form-Machine Conditions Tab

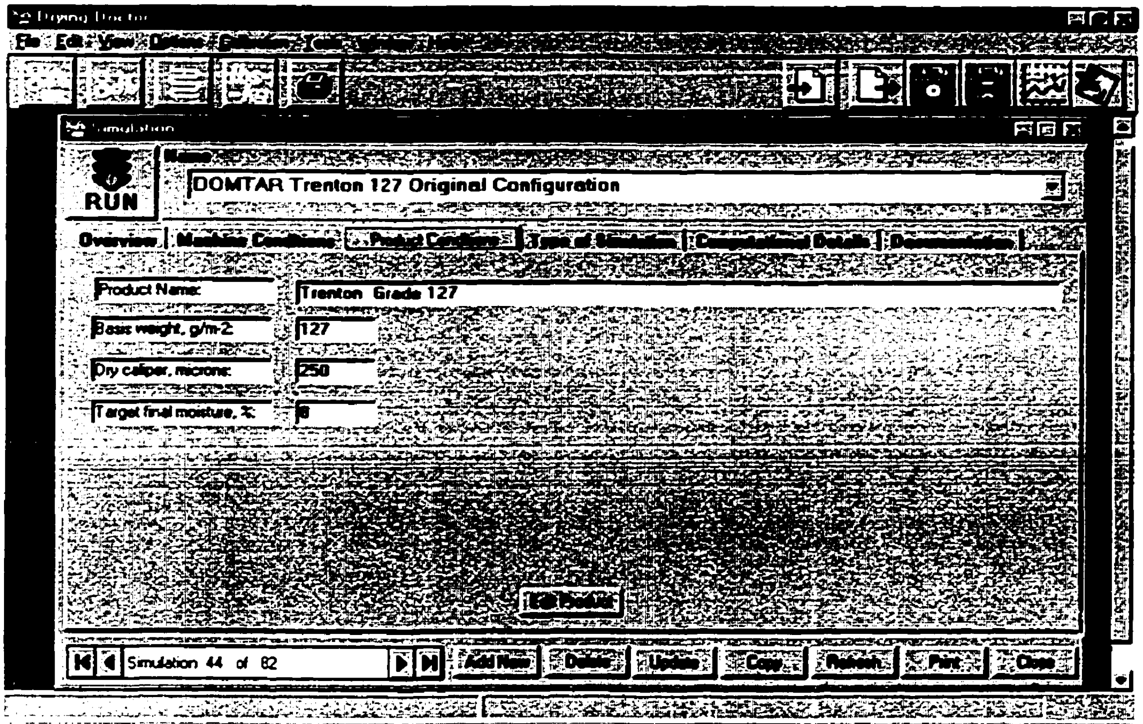

Figure A-3: Current Simulation Form-Product Conditions Tab

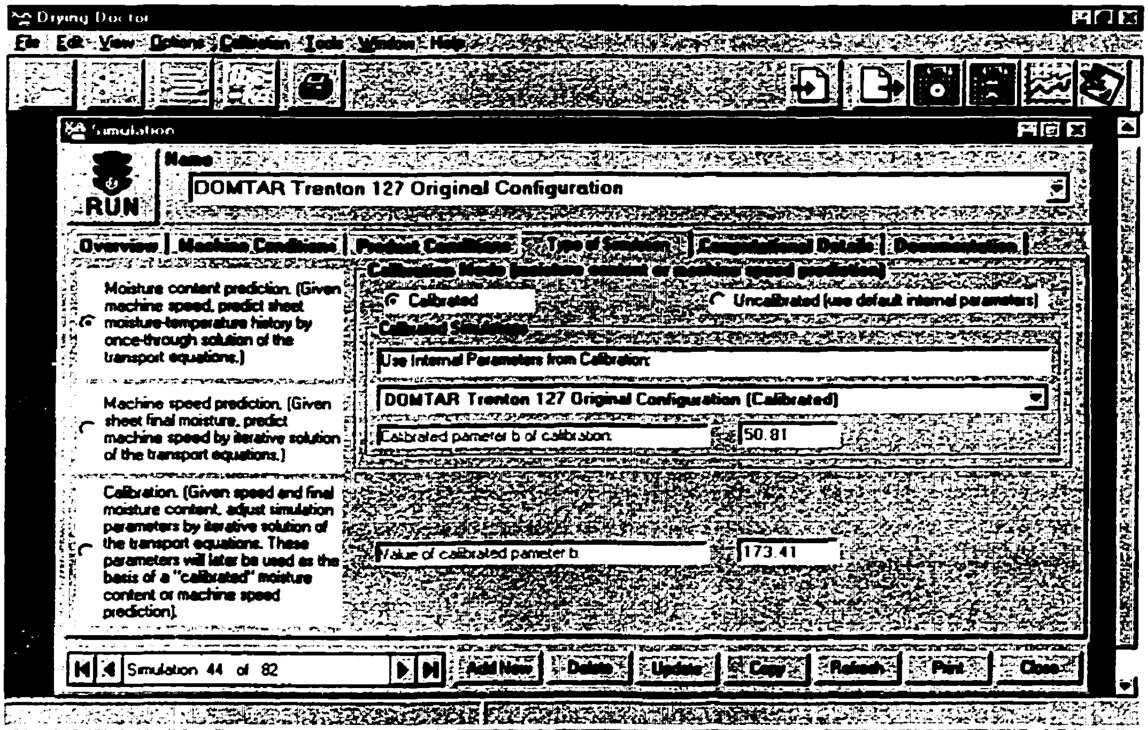

Figure A-4: Current Simulation Form-Type of Simulation Tab

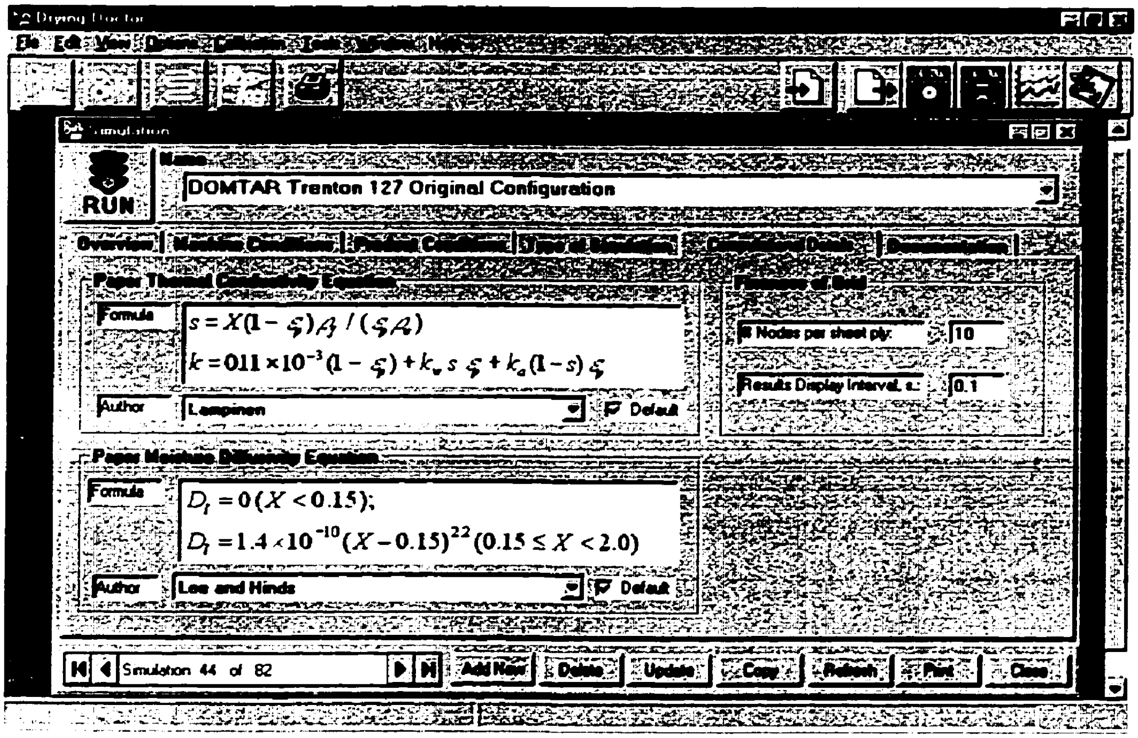

Figure A-5: Current Simulation Form-Computational Details Tab

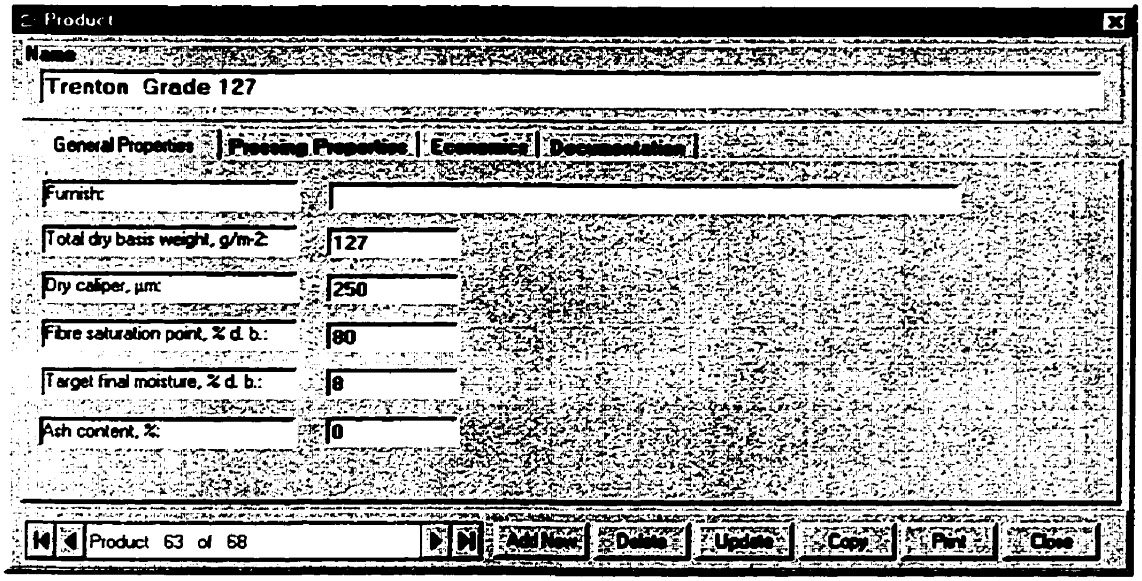

Figure A-6: Product Form-General Properties Tab

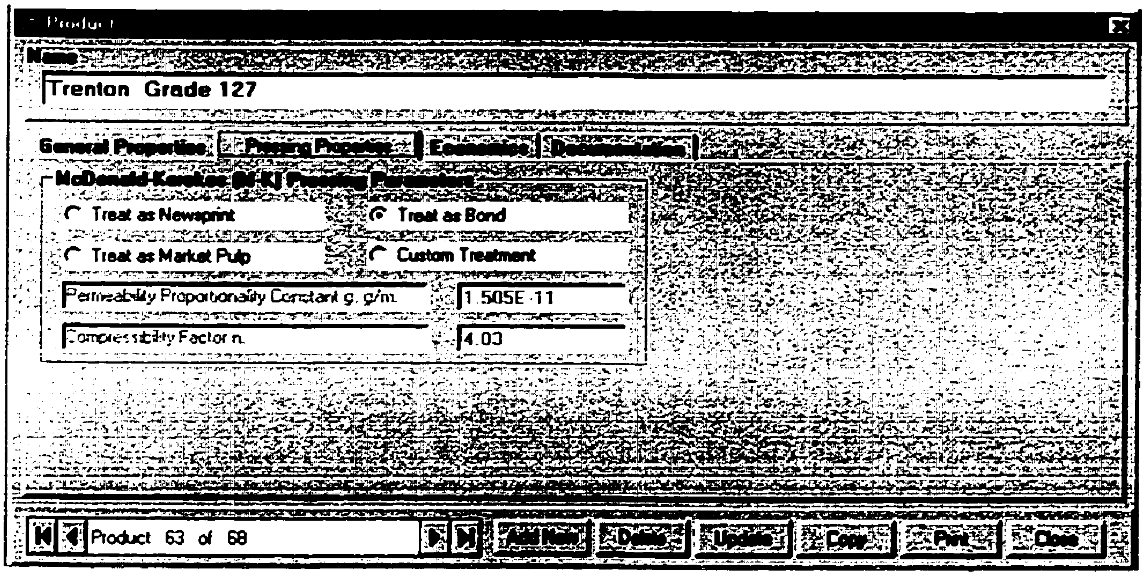

Figure A-7: Product Form-Pressing Properties Tab

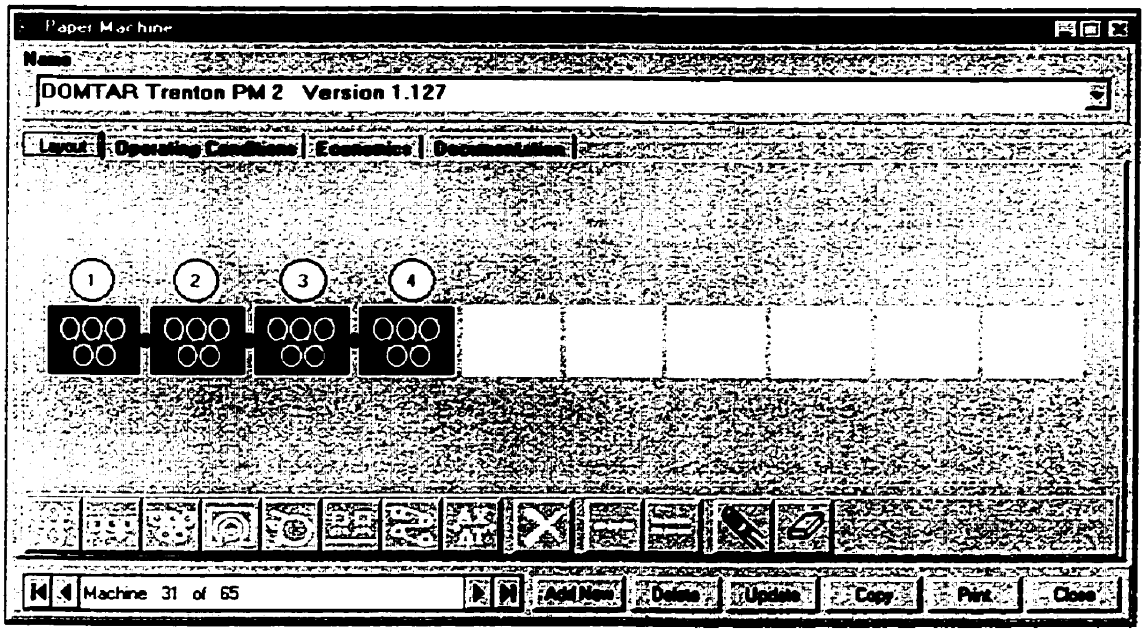

Figure A-8: Paper Machine Form-Layout Tab

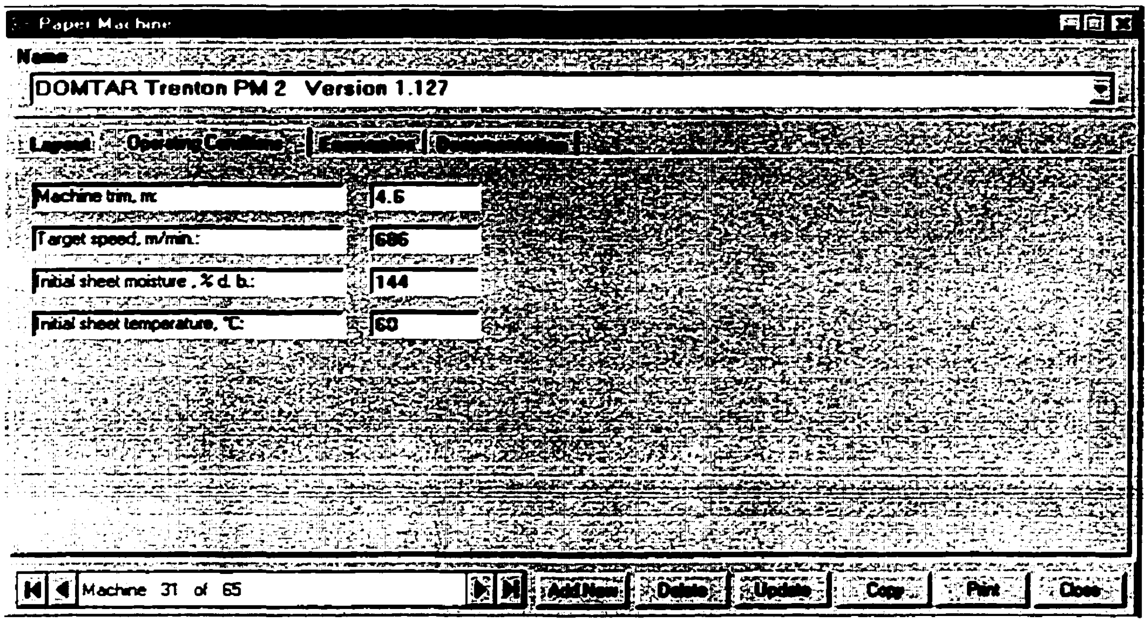

Figure A-9: Paper Machine Form-Operating Conditions Tab

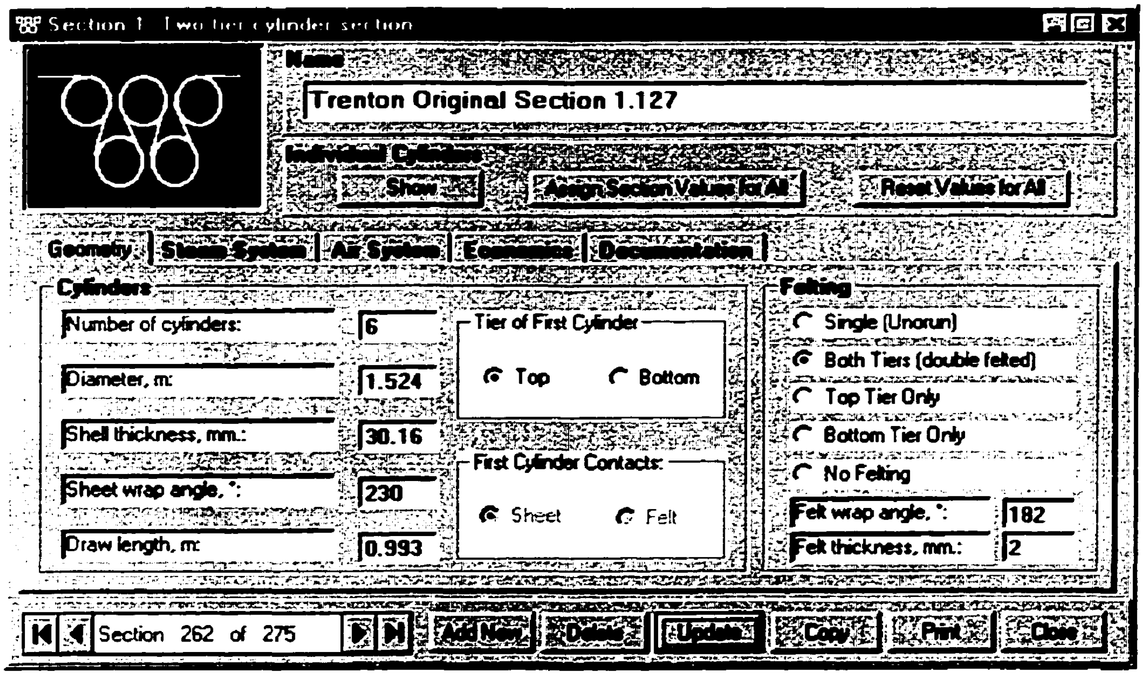

Figure A-10: Two-Tier Cylinder Section Form-Geometry Tab

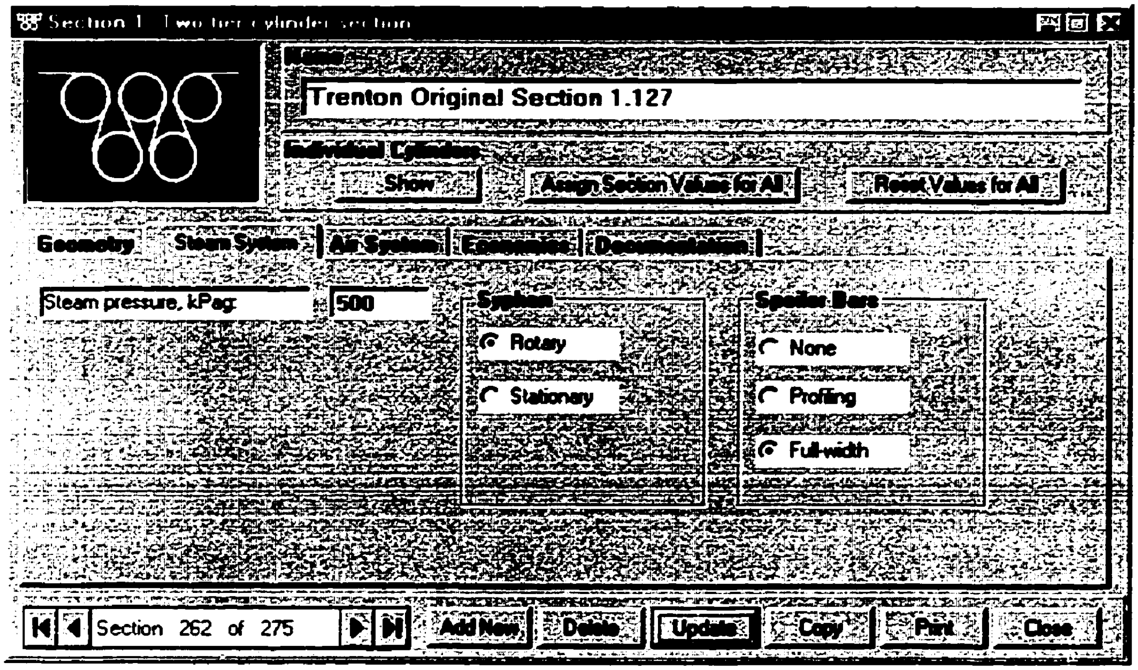

Figure A-11: Two-Tier Cylinder Section Form-Steam System Tab

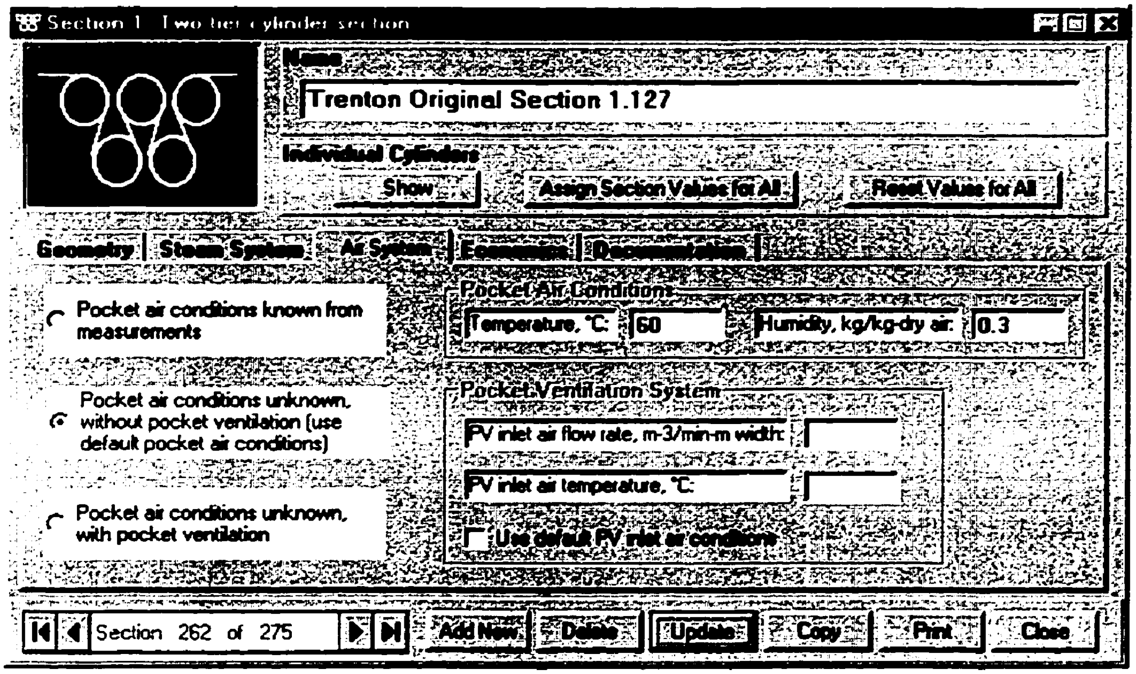

Figure A-12: Two-Tier Cylinder Section Form-Air System Tab

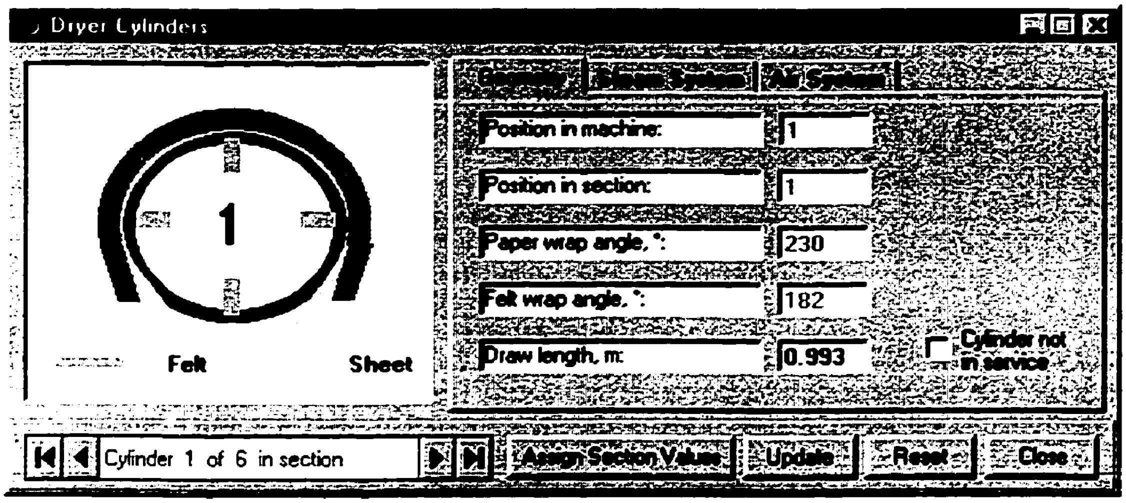

Figure A-13: Individual Dryer Cylinder Form-Geometry Tab

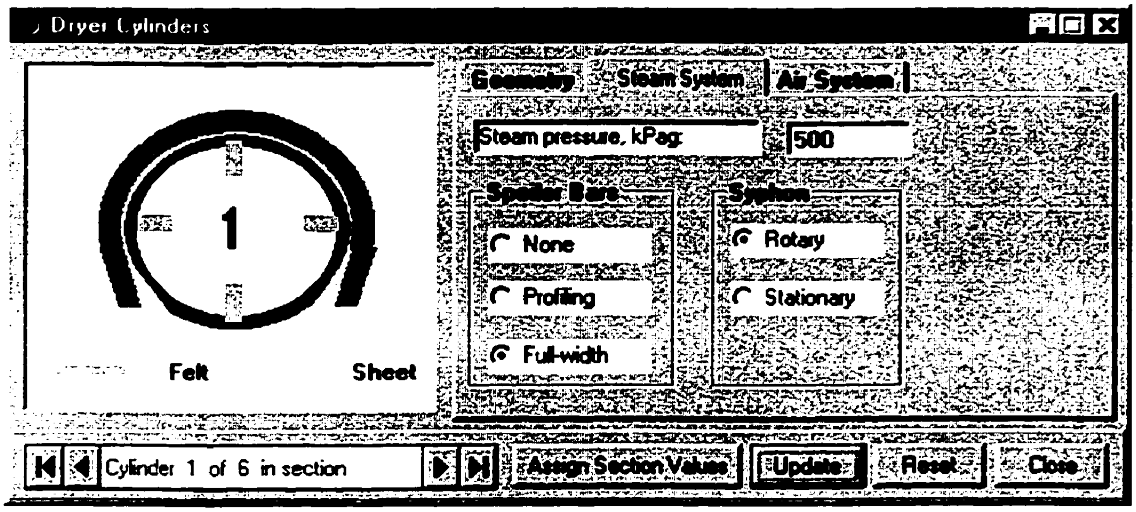

Figure A-14: Individual Dryer Cylinder Form-Steam System Tab

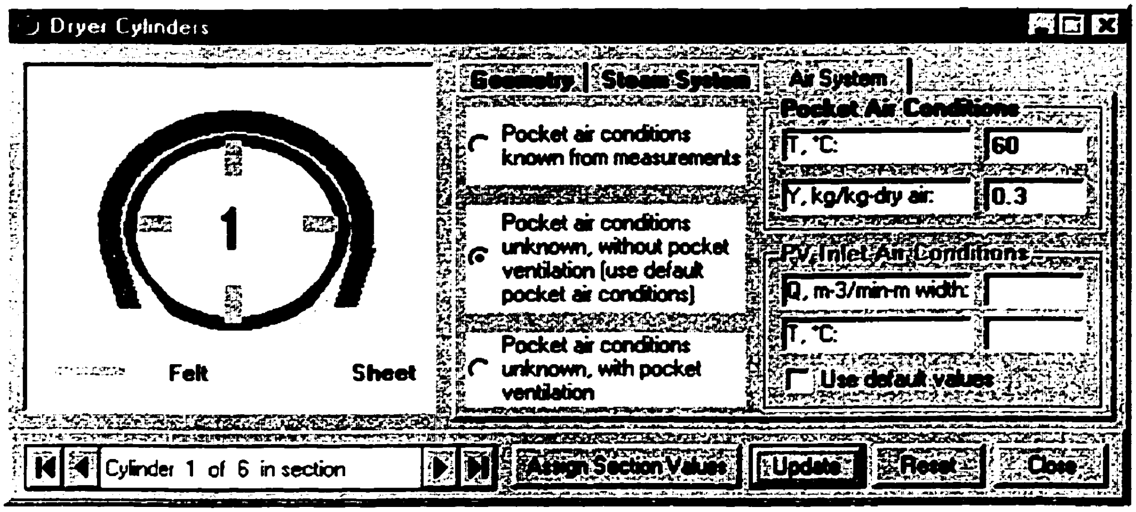

Figure A-15: Individual Dryer Cylinder Form-Air System Tab

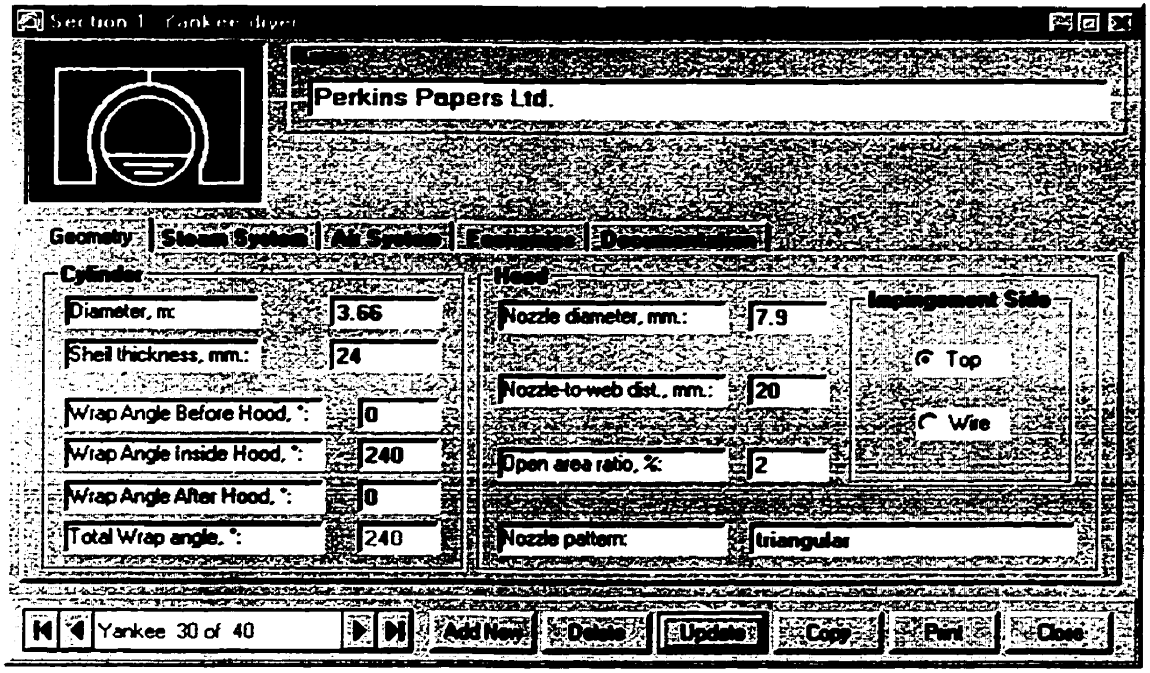

Figure A-16: Yankee Dryer Form: Geometry Tab

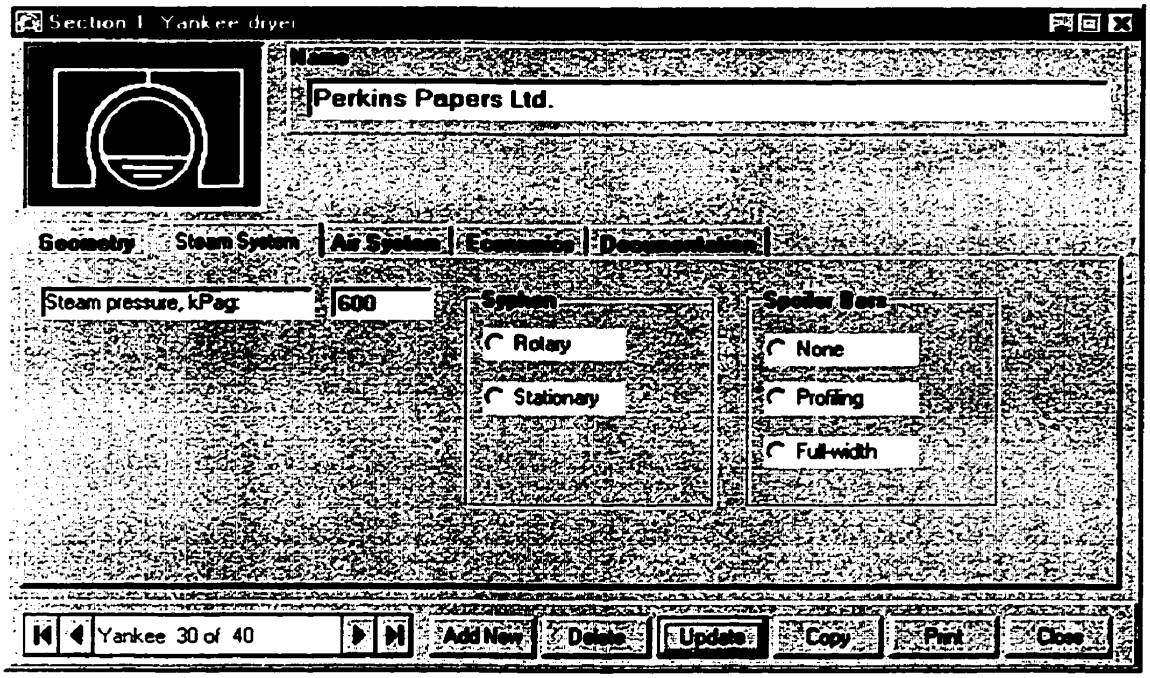

Figure A-17: Yankee Dryer Form: Steam System Tab

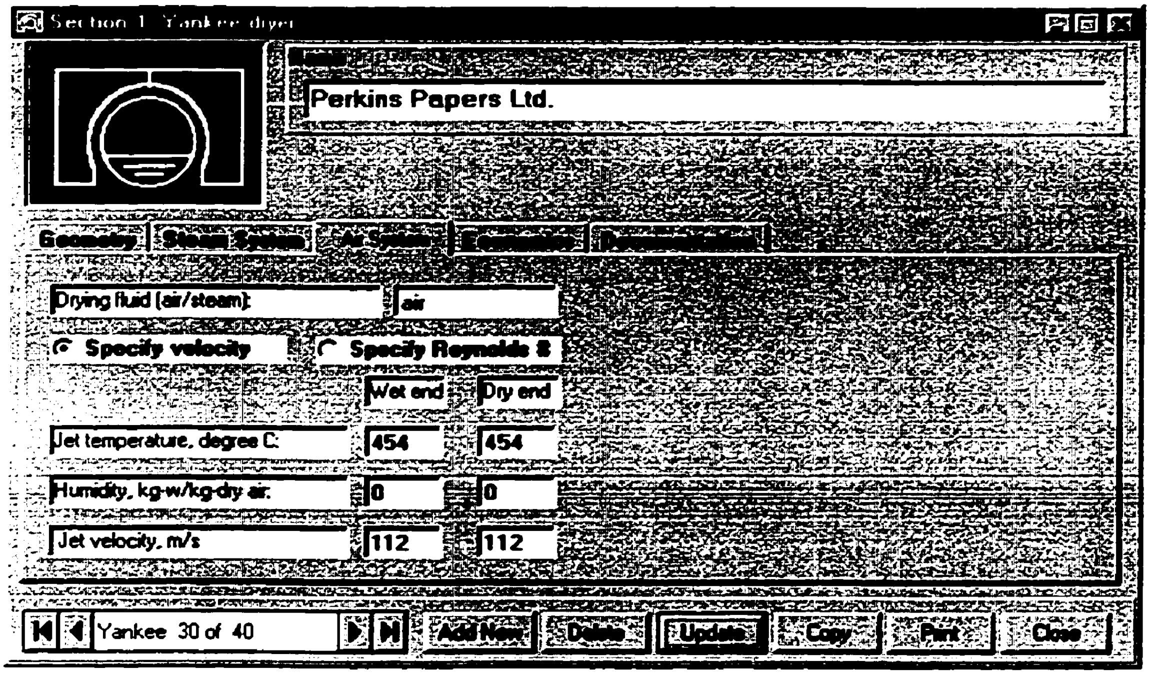

Figure A-18: Yankee Dryer Form: Air System Tab

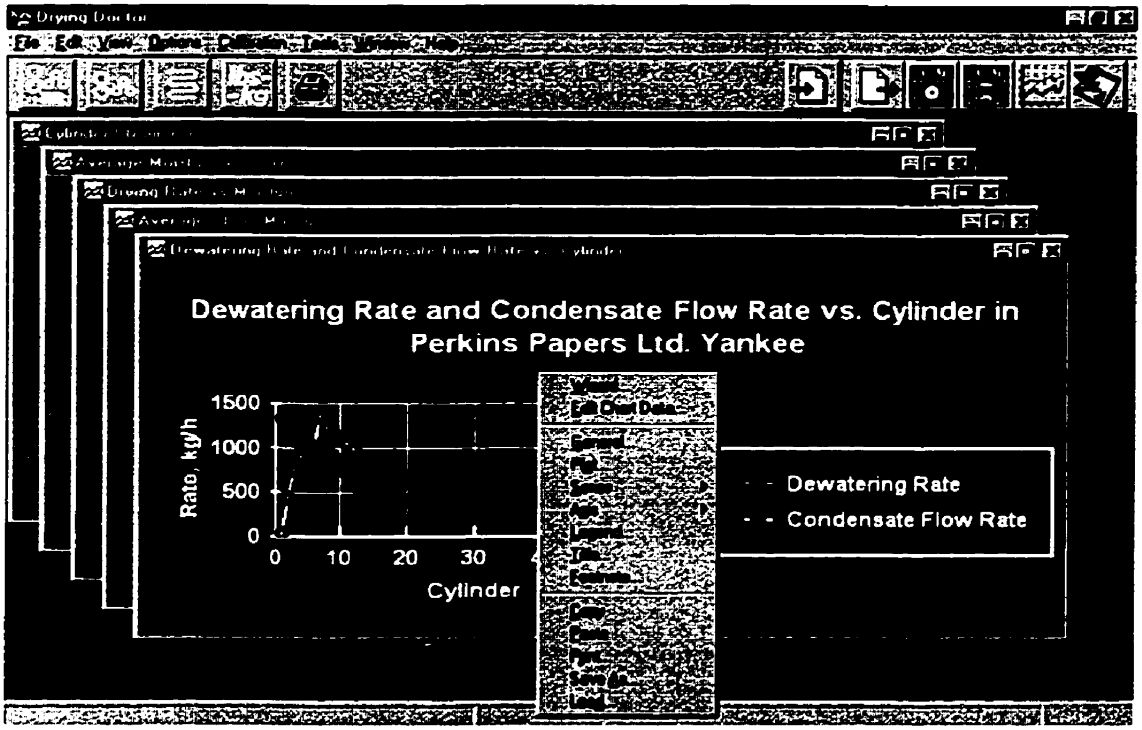

Figure A-19: *Drying Doctor* Graphical Results

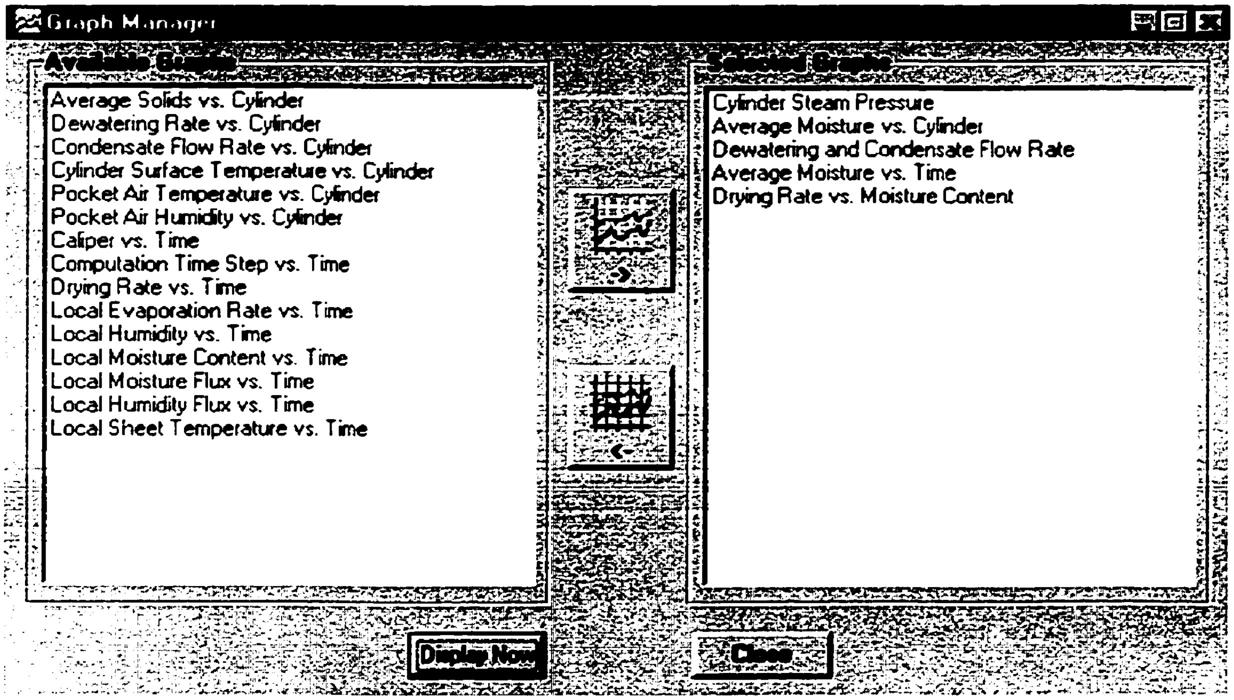

Figure A-20: Graph Manager

B *DRYING DOCTOR* MODEL EQUATIONS

Heat Transfer Equations:

1) Within sheet $\frac{B}{l} c_p \frac{\partial T}{\partial t} = k \frac{\partial^2 T}{\partial z^2} + E_v \, \Delta h_v$

2) At top of sheet $Q_n = h_n \left(T_{top} - T_n \right)$

3) At bottom of sheet $Q_o = h_o \left(T_{bottom} - T_o \right)$

Liquid Mass Transfer Equation:

4) Within sheet $\frac{B}{l} \frac{\partial X}{\partial t} = \rho_w \, D_l \frac{\partial^2 X}{\partial z^2} - E_v$

Vapor Mass Transfer Equations:

5) Within sheet $\rho_g \, \varepsilon \frac{\partial Y}{\partial t} = \rho_g \, D_v \frac{\partial^2 Y}{\partial z^2} + E_v$

6) At top of sheet $G_n = K_n \left(Y_{top} - Y_n \right)$

7) At bottom of sheet $G_n = K_o \left(Y_{bottom} - Y_o \right)$

8) Within the sheet E_l-Local Evaporation Term

C *DRYING DOCTOR* AIR IMPINGEMENT CONVECTION DRYING CORRELATIONS

$$K_{HDF} = \left[1 + \left(\frac{H/D}{0.6/\sqrt{F}}\right)^6\right]^{-0.05}$$

$$G = K_{HDF} \cdot \sqrt{F} \cdot \frac{1 - 2.2\sqrt{F}}{1 + 0.2(H/D - 6)\sqrt{F}} \cdot \mathrm{Re}^{\frac{2}{3}}$$

$$\left(\frac{\overline{Sh}}{Sc^{0.42}}\right) = \left(\frac{\overline{Nu}}{\mathrm{Pr}^{0.42}}\right) = G$$

$$2000 \leq \mathrm{Re} \leq 100{,}000$$

$$0.004 \leq F \leq 004$$

$$2 \leq H/D \leq 12$$

$$\overline{Sh} = \frac{\beta \cdot D}{\delta} \quad \overline{Nu} = \frac{\alpha \cdot D}{k} \quad \mathrm{Pr} = \frac{C_P \cdot \mu}{k} \quad Sc = \frac{\mu}{\rho \cdot \delta} \quad \mathrm{Re} = \frac{D \cdot V_{JET} \cdot \rho}{\mu}$$

Nomenclature:

Sh	Sherwood number	
Nu	Nusselt number	
Pr	Prandtl number	
Sc	Schmidt number	
Re	Reynold number	
H	Nozzle to web distance	[m]
D	Nozzle diameter	[m]
F	Nozzle plate open area ratio/100	
α	Heat transfer coefficient	[W/m^2K]
β	Mass transfer coefficient	[m/s]
δ	Diffusivity of air	[m^2/s]
k	Thermal conductivity of air	[W/m K]
C_P	Heat capacity of air	[J/kg K]
μ	Viscosity of air	[kg/ms]
ρ	Density of air	[kg/m^3]
V_{JET}	Jet exit velocity	[m/s]